Adsorptive systems for post-combustion CO_2 capture

Design, experimental validation and evaluation of a supported amine based process

Rens Veneman

ADSORPTIVE SYSTEMS FOR POST-COMBUSTION CO_2 CAPTURE

Design, experimental validation and evaluation of a supported amine based process

Promotion Committee:
Vervangend Voorzitter: prof.dr.ir. J.F. Dijksman

VOORZITTER: *(Chairman)*	prof.dr.ir. J.W.M. Hilgenkamp	Universiteit Twente, TNW
SECRETARIS: *(Secretary)*	prof.dr.ir. J.W.M. Hilgenkamp	Universiteit Twente, TNW
PROMOTOR: *(Supervisor)*	prof.dr. S.R.A. Kersten	Universiteit Twente, TNW
CO-PROMOTOR: *(Co-Supervisor)*	dr.ir. D.W.F. Brilman	Universiteit Twente, TNW
REFERENT: *(Referee)*	dr.ir. E. Goetheer	TNO
LEDEN: *(Members)*	prof.dr.ir. H. van den Berg	Universiteit Twente, TNW
	prof.dr.ir. D.C. Nijmeijer	Universiteit Twente, TNW
	dr. Z. Li	Tsinghua University
	prof.dr.ir. M. van Sint Annaland	Technische Universiteit Eindhoven

This research has been carried out in the context of the CATO-2-program. CATO-2 is the Dutch national research program on CO_2 Capture and Storage technology (CCS). The program is financially supported by the Dutch government (Ministry of Economic Affairs) and the CATO-2 consortium partners.

Thesis design:
Laura Bouhuys, http://www.laurabouhuys.nl

Adsorptive systems for post-combustion CO_2 capture
Design, experimental validation and evaluation of a supported amine based process
ISBN: 978-90-365-3926-5
DOI: 10.3990/1.9789036539265
URL: http://dx.doi.org/10.3990/1.9789036539265
Printed by Ipskamp Drukkers BV, Enschede, The Netherlands

ADSORPTIVE SYSTEMS FOR POST-COMBUSTION CO_2 CAPTURE

Design, experimental validation and evaluation of a supported amine based process

PROEFSCHRIFT

ter verkrijging van
de graad van doctor aan de Universiteit Twente,
op gezag van de rector magnificus,
Prof. dr. H. Brinksma,
volgens besluit van het College voor Promoties
in het openbaar te verdedigen
op vrijdag 18 september 2015 om 16:45 uur

door

Rens Veneman
geboren op 21 maart 1986
te Haaksbergen, Nederland

This thesis has been approved by:

Prof. dr. S.R.A. Kersten (Promotor)

Dr. ir. D.W.F. Brilman (Assistant promotor)

Aan
Lammigje Veneman-Van Munster
Pietje Jantje Comello-Aukema
Jan Hendrik Veneman
Willem Comello

Contents

4.

5.

6.

7.

Chapter 01

Cutting the cost of carbon capture

Abstract

This thesis deals with the development of a new supported amine based CO_2 capture process in order to reduce the costs for CO_2 capture at power plants. This chapter serves as a general introduction to carbon capture and storage, the conventional solvent based capture process and the novel sorbent based capture process we aim to develop and evaluate in this thesis. This general introduction is followed by a discussion on the potential of adsorption based CO_2 capture as an alternative to the conventional solvent technology, and a summary of the status of the research on supported amines. Lastly, the scope and outline of this thesis are explained.

The author would like to note that this chapter does not solely contain literature references. It also contains references to work presented in other chapters of this thesis. This will be explicitly mentioned in the text and the reader will be referred to the specific chapter for further details. Moreover, a list of all abbreviations used is provided at the end of this chapter.

1.0

Carbon Capture, Transportation and Storage

The atmospheric CO_2 concentration has increased rapidly in the last decades from around 315 ppm in 1958 to nearly 400 ppm in 2014 [1]. A large part of this increase is related to the enormous amount of fossil energy consumed in today's society. And since the global energy consumption is only expected to increase further in the coming decades, the CO_2 concentration is projected to increase further as well. There are major concerns about how this increase in the atmospheric CO_2 concentration would impact the climate on earth on the long term, and hence efforts are made to reduce anthropogenic CO_2 emissions.

Carbon capture and storage (CCS) at fossil fuel burning plants is, among other alternatives, a technically feasible method to significantly reduce the global anthropogenic emission of CO_2. CCS focusses on purification, transportation and storage of CO_2. Storage will prevent CO_2 from entering to the atmosphere and so from contributing to the greenhouse effect. Almost 35% of the anthropogenic CO_2 is emitted by the energy sector and because most of this CO_2 is emitted at relatively high concentrations by large point sources, it is possible to build centralized plants that capture large amounts of CO_2 at a relatively low cost.

Post-combustion capture, in particular, aims to capture the CO_2 produced by existing coal-fired or gas-fired power plants. Here, CO_2 is emitted in a dilute mix of gasses referred to as flue gas. Flue gas contains the combustion products CO_2 and H_2O and, since air is often used to combust the fuel, a large amount of N_2 and some unreacted O_2. The composition of the flue gas depends on the type of fuel used but typical CO_2 levels in a flue gas range, from 4 vol% to 15 vol%. At present, flue gas is emitted to the atmosphere after being cleaned of particulate matters and pollutants like H_2S, SO_x and NO^x. However, in a power plant equipped with a CCS system, the flue gas passes through a CO_2 capture facility that purifies the CO_2 i.e. separates the CO_2 from the other gasses before venting these flue gasses to the atmosphere. The near pure CO_2 product gas is liquefied prior to transportation by compressing it to around 74 bar and slight cooling. Liquefaction of the CO_2 product stream is required for its cost-effective transportation and storage. This way of CO_2 capture can be retrofitted to exist-

ing power plants which is its main advantage over other capture systems like pre-combustion capture. The installation of a post-combustion capture system does not require changes to the layout of the power plant and can be seen as an end-of-pipe capture technology.

Commercial carbon capture and storage projects already exist. The post-combustion capture plant at the Boundary Dam (Canada) power station is the first and largest commercial scale capture project [2]. The plant is owned by SASK Power and is designed to capture 1 Mt of CO_2 per year. Sleipner was the first commercial CO_2 storage project and has injected and stored more than 10 Mt of CO_2 since the start of operation in 1996 [3]. The CO_2 storage site is located in the North Sea and is operated by Statoil.

2.0

CO_2 purification

The current benchmark technology for the separation of CO_2 from dilute gas streams utilizes a mixture of amine molecules, typically monoethanolamine (MEA) and water, to selectively absorb CO_2 from flue gases. Already at low temperatures, CO_2 dissolves in this absorption liquid (or solvent). By contacting the CO_2 containing gas with this solvent in an absorber column, the absorption liquid 'captures' the CO_2. Subsequently, the liquid with the dissolved CO_2 is transported to a second column, the desorber. Here, the liquid is heated, which causes the solvent to release the CO_2. This supplies a stream of pure CO_2, which is compressed and stored, while the regenerated solvent is pumped back to the adsorber column to capture more CO_2. This process has been widely applied in chemical industry for many years for gas sweeting and numerous studies have been focusing on the development of more efficient solvents and improving the process layout to cut down the cost associated with the capture of CO_2 using this technology.

Still, post-combustion CCS is currently considered too costly for large scale deployment. The cost of capture accounts for around 80% of the total costs of CCS. Installation of a capture facility at a power plant could double the cost of the electricity produced (see Table 1) which is mainly due to the high cost of carbon capture using the above described solvent technology. This process suffers from several drawbacks of which its high thermal energy demand is the most important one. The costs associated with the heat demand of the process account for 30% of the total CO_2 capture cost making it its main cost driver.

The installation of a capture facility at a power plant results in a decrease in the gross power output of the power plant as steam is extracted from the steam cycle for solvent regeneration. The main part of this heat is required for heating of the aqueous amine solution from the absorption temperature to the desorption temperature and another important part is associated with the evaporation of solvent in the desorber column. A MEA based capture plant requires between 3-4 GJ of heat per ton of CO_2 captured. To capture 90% of the CO_2 emitted by a 500 MWe coal fired power plant, a MEA based capture plant requires between 345–460 MW of heat for solvent regeneration. In addition, part of the produced electricity is required to operate electrical equipment like the flue gas blower and the CO_2 compressor

in the capture plant, causing the net power output of the power plant to decrease further. Installation of an amine based capture facility at a coal-fired power plant would reduce the electricity output with almost 40%, which is the main reason for the large increase in the cost of electricity (COE). This large increase in COE is a major hurdle in deployment, and therefore the development of a more cost effective capture technology is a main objective in CO_2 capture research.

Table 1: Performance of a coal-fired power plant with and without CO_2 capture [4].

Plant data	No capture	MEA
Gross power (MWe)	500	354
Net power (MWe)	453	282
Power plant auxiliaries (MWe)	47	47
Power output reduction due to capture (MWe)	-	171
Relative power output reduction (over ref. plant)	-	38%
Capture plant capital requirement ($/t$CO_2$)	-	15.1
CO_2 emitted (Mt/yr)	3428	343
CO_2 captured (Mt/yr)	-	3085
Emission rate (tCO_2/MWh)	1.02	0.16
CO_2 capture energy requirement (GJe/tCO_2)	-	1.49
Cost of CO_2 avoided ($/t$CO_2$)	-	59.3
Cost of electricity ($/MWh)	**33.6**	**84.1**

3.0

An alternative capture technology

Applying supported amine sorbents (SAS) may offer a low-cost alternative to the MEA based process described in section 2. These supported amine sorbents consist of a porous support material with amine functional groups immobilized on or grafted to its surface [5]. In this novel 'dry' sorbent based process, H_2O is thus replaced by a porous support material and hence the process can be thought of as a "solid analogue" of the absorption processes [6].

As mentioned, the main cost driver in the MEA based process is its large energy demand, mainly associated with heating of the aqueous amine solution from the absorption temperature to the desorption temperature and with the evaporation of solvent in the desorber column. The aqueous amine solution is heated from the absorption temperature (40-60˚C) to the desorption temperature (110-130˚C) in order to release CO_2 again. Due to the large heat capacity of water (4.2 kJ/kg/K), the heat required for heating the solvent is large as well; around 5-6 GJ/t. Although a large part of this heat can be saved by exchanging heat between the hot solvent leaving the stripper and the cool solvent leaving the scrubber, the net sensible heat penalty is still considerable; 0.5-1.2 GJ/t.

Since the desorption temperature is above the boiling point of the solvent, a significant amount of the solvent is evaporated in the stripper. The molar ratio of H_2O/CO_2 in the gas leaving the stripper at the top is around 1.3 [4]. The solvent is condensed and send back to the stripper. The evaporation of the solvent requires around 1.4 GJ/t [4]. This number is however dependent on the temperature and pressure in the stripper as well as on the configuration of the stripper column.

In addition to the sensible heat and the evaporation heat, reaction heat is required to break the chemical bond between MEA and CO_2. This requires around 2.0 GJ/t when MEA is used as a solvent [4].
Switching to a sorbent based process could greatly reduce the energy required for CO_2 capture as; (1) the evaporation of water can be inhibited and (2) the energy required for heating the sorbent up to the desorption temperature is lower due to the lower heat capacity of solid amine sorbents (1.5 kJ/kg/K [7]) compared to water.

In addition to the envisioned savings in energy, the use of supported amine adsorbents offer other advantages over the solvent based process. Choi et al. [6] advocate it as follows: "Unlike amine solutions, degradation due to evaporation can be less of an issue for supported amines. Also, because solid-solid contact between silica particles and other solid surfaces is poor, vessel corrosion is less problematic than for an aqueous amine configuration". At present, these corrosion issues limit the concentration of amine in the solvent solution which limits the working capacity in the amine process and results in high maintenance costs and expensive equipment [8].

In an attempt to quantify the envisioned savings in the energy demand, we present a preliminary energy analysis of the sorbent based process in Figure 1. Here the thermal energy requirement of the process is plotted as a function of the sorbent operating capacity [9]. The sorbent working capacity plays an important role in achieving these envisioned savings in energy. The working capacity of the solid material is defined as the difference between the capacity of the sorbent particles before and after the adsorption step. The working capacity determines the amount of solid material that is required to capture a certain amount of CO_2 and thus also the amount of solids that needs to be heated to the regeneration temperature to capture the same amount of CO_2. In other words, the higher the working capacity the lower the sensible heat energy penalty of the process. In these calculations, the heat capacity of the sorbent material was assumed to be 1.5 kJ/kg/K and the temperature difference between the adsorption column and the desorber column was assumed to be 70˚C.

Whereas the benchmark process requires 3-4 GJ/t, switching to a supported amine based process could reduce this energy demand to around 1.8-2 GJ/t of CO_2. These values are 30% lower than the values reported for MEA-based systems with advanced stripper configurations and 20% lower than values reported for the KS-1 [10] solvents by Mitsubishi Heavy Industries (MHI). A working capacity of at least 1.5 mol/kg sorbent is required for the SAS based process to be significantly more energy efficient than the MEA benchmark. At working capacities higher than 3 mol/kg the reaction heat will dominate the thermal energy demand of the SAS-based capture facility. Hence, increasing the operating capacity much further will not result in a substantial further decrease in the thermal energy requirement of the SAS-capture system.

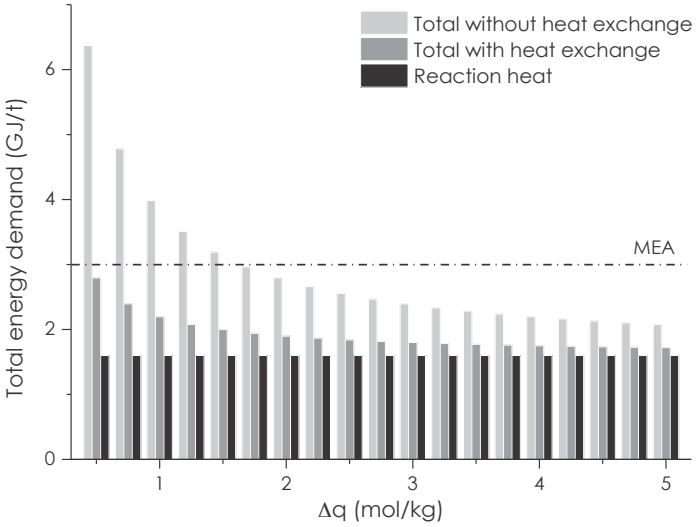

Figure 1: Plot of the estimated heat demand of the SAS based process. In these calculations it was assumed that 75% of the sensible heat required for heating the sorbent material can be recovered in a solid-solid heat exchanger. The MEA thermal energy demand is also shown.

4.0

Supported amine sorbents

Supported amine materials were first considered for the removal of CO_2 from air in space shuttles and submarines in research done by the NASA in the early 80's. The idea to apply these materials in post-combustion capture came up in the early 90's. Choi et al. [6] stated that: "Silica supported amines were first used for CO_2 capture by Tsuda in 1992. Amorphous silica gels were created by co-condensation of various amine-containing silanes and used for CO_2 capture under dry conditions. Leal reported the first use of amine-functionalized mesoporous silicas for CO_2 adsorption in 1995".

The reactions between amine molecules and CO_2 in aqueous solutions have been widely studied. The reaction mechanism was originally proposed by Caplow [11] and reintroduced by Danckwerts [12]. It is the generally accepted mechanism for the reaction of primary and secondary amines, and CO_2 [13]. It involves two steps. In the first step, CO_2 reacts directly with an amine molecule under the formation of a zwitterion molecule after which, in a second step, a free base, either water or another amine group, deprotonates the zwitterion, forming carbamate [6]. Under dry conditions two amine groups are required to bind one molecule of CO_2. The reaction pathway for the reaction between CO_2 and primary and secondary amines under dry conditions is given below.

$$RNH_2+CO_2 \leftrightarrow RNH_2{}^{+}COO^{-} \quad (1)$$

$$RNH_2{}^{+}COO^{-}+RNH_2 \leftrightarrow [RNHCOO^{-}][RNH_3^{+}] \quad (2)$$

Tertiary amines react differently with CO_2. Choi et al. [6] described this as follows: "Tertiary amines, instead of reacting directly with CO_2, catalyze the formation of bicarbonate. Primary and secondary amines can also react with H_2O and CO_2 in this manner. However, while the activation energy for this pathway is lower than for the formation of carbamates, the rate constant is actually smaller. It has been observed for humid CO_2 capture with solid-tethered amines that carbamates form initially and then are converted to carbonates and bicarbonates".
The reaction between amines and CO_2 is exothermic. MEA, which is a primary amine, reacts with CO_2 releasing around 88.9 kJ/mol of heat [14]. Diethanolamine (DEA), a secondary amine, and triethanolamine (TEA), a tertiary amine, release 70.4 and 44.7 kJ/mol respectively [14]. A similar

amount of energy is required to release the bonded CO_2 again. The heats of adsorption of supported amines typically fall into the range of 40 to 90 kJ/mol depending on the type of amine used [15].

In general, primary amines have a higher heat of adsorption compared to secondary and tertiary amines while tertiary amines show slower reaction kinetics. Hence, secondary amine are mainly considered for CO_2 capture applications since they combine good uptake kinetics with a relatively low regeneration heat [8].

There are two main types of supported amine sorbents. One class of sorbents for which the support-amine interaction is only physical (Impregnated sorbent materials, Class 1 sorbents), and sorbents that have amine groups covalently bonded to their internal surface (Class 2 and Class 3 sorbents).

Impregnated amine sorbents are mostly prepared by wet impregnation. Here, the amine, dissolved in a volatile solvent, is impregnated into the support, after which the solvent is evaporated, leaving the amine molecules dispersed inside pores of the support. The amine loading is controlled by controlling the amine concentration in the amine-solvent solution. Amines commonly used for impregnation of support materials include polyethylenimine (PEI) [16], tetraethylenepentamine (TEPA) [17] and diethanolamine [18]. The most important criteria for amine selection include (1) the number of nitrogen atoms per amine molecule, (2) the adsorption heat and (3) the sorption kinetics.

Regarding the support material, porous carbons [19], zeolites [20], polymers such as poly(methyl methacrylate) [21] and polystyrene [22], and silica's [23-25] have all been considered as support candidates. A porous support will provide an open, accessible backbone resulting in a large contact area for the contact between amine and CO_2. Work has been done on optimization of impregnated sorbent particles by tuning the support type and its structural characteristics, the amine type and the amine loading [26-31] (this thesis, Chapter 2). For impregnated sorbents, the interaction between the amine and the support material is relatively weak and these type of amine sorbents are often subject to amine loss due to evaporation at temperatures above 100°C. Although low molecular weight amines are more easy to impregnate into the support pore space, amines with longer chains tend to suffer less from evaporation losses upon regeneration [32, 33] (this thesis, Chapter 2).

The second class of supported amine sorbents have amine groups chemically bonded to their internal surface. These adsorbents have a clear advantage over amine-impregnated sorbent materials in that they have a better thermal stability due to the strong amine support interaction. This allows for

deeper regeneration of the sorbent particles.
The most applied method for synthesizing these type of materials is by reacting amino-silane molecules to the surface of silica, often called grafting (Class 2 sorbents). The adsorption of CO_2 by these sorbent materials was first researched by Leal et al. [34] who grafted 3-aminopropyltriethoxysilane (APTES) on silica gel. Amines commonly used for functionalization of a silica support include 3-aminopropyltrimethoxysilane (APTS), 3-aminopropyltriethoxysilane (APTES) and N-[3-(trimethoxysilyl)propyl]-ethylenediamine (AEAPTS). The degree of functionalization of the silica surface depends on factors like support surface area, pore volume and the silanol concentration on the silica surface [35, 36]. The N-content of these sorbents is more difficult to control than for impregnated sorbent materials. Another method to covalently bind amines to a silica support is via a surface polymerization reaction of aziridine inside the SBA-15 pore space (Class 3). This method was pioneered by Jones and his research group [15, 37]. These so-called hyperbranched aminosilicas (HAS) materials have a considerably higher nitrogen content than the above mentioned grafted amine sorbents.
The main advantages of supported amine sorbents include: high CO_2 capacities, high CO_2/N_2 selectivities, fast CO_2 uptake rates, a low heat of adsorption and relatively mild regeneration conditions compared to other chemical sorbents. It is because of these characteristics that supported amines are seen as promising sorbent candidates. High CO_2 capacities could translate into high sorbent working capacities which will lower the energy demand of the process as was shown in section 3. Also a low heat of adsorption and a low regeneration temperature will help to lower the energy demand of the process. High selectivity towards the adsorption of CO_2 will allow for high product gas purities, essential for transportation and storage of the captured CO_2, and fast uptake rates will allow for a more compact absorber design, lowering investment costs.
In the following sections, these aspects will be discussed in more detail.

4.1 | CO_2 sorption capacity

Supported amine sorbents typically possess CO_2 capacities in the range of 2-4 mol/kg at CO_2 partial pressures relevant for post combustion CO_2 capture (typically 0.04 to 0.15 bar). To the best of our knowledge, the highest capacity reported is 14 mol/kg [21]. This was measured for a TEPA impregnated polymer at 343 K and in 0.15 bar CO_2.
The capacities measured for supported amine sorbents are higher than that of most physical sorbents in the above mentioned CO_2 pressure and these sorbents possess an excellent CO_2/N_2 selectivity [38].

The most obvious way to increase the CO_2 capacity of supported amine sorbents is by increasing the nitrogen content of the support material; the more active sites on the support the more CO_2 the sorbent can potentially bind. There are however physical limitations to the amount of amine that can be loaded onto the support material. For Class 1 sorbents, theoretically, the maximum amount of amine that can be impregnated into the support material is limited by the pore volume of the support. However, even far below this maximum, impregnated sorbent materials suffer from pore blocking and filling effects at high amine loadings reducing the accessibility of the amine active sites. For high amine loadings the adsorption capacity is not so much determined by the amount of active site but rather by the amount of accessible active sites and hence several researchers found that for impregnated sorbent materials there is an optimum in the loading of amine into the support material [16, 26, 27, 39]. A higher loading than this optimum will only reduce the accessibility of amine groups and thus lower the capacity. Ways to increase the accessibility of the amine active sites and consequently the CO_2 capacity include tuning the amine loading and increasing the pore size of the support material to prevent blocking of pores [39] (This thesis, Chapter 2).

Other ways to improve the sorbent capacity are to focus on finding the most suitable amine type and modifying the amine molecules to improve their reactivity. Low molecular weight amines like TEPA or low molecular weight PEI's adsorb more CO_2 when impregnated into a support material than long chain, bulky amine molecules [33, 40]. Moreover, it was demonstrated that secondary amines offer better CO_2 capacities than primary amines [8]. Filburn et al. [8, 21] reacted acrylonitrile to TEPA before impregnating it into a Poly(methyl acrylate) (PMMA) polymer support. This converted the primary amine groups in TEPA into secondary amines which resulted in an enhanced CO_2 uptake of 14 mol/kg.

For grafted amine sorbents (Class 2), the maximum amine loading is limited by the amount of available silanol groups on the surface of the silica support. Moreover, as mentioned in the previous paragraph controlling the amine loading in the grafting process is not as straight forward as in the impregnation process. The degree of functionalization of the silica surface depends on factors like support surface area, pore volume and the silanol concentration on the silica surface [35, 36].
Figure 2 shows adsorption capacities reported for both impregnated sorbent materials as well as grafted sorbents. Typically, the N-content is lower

for grafted amine sorbents than for impregnated amine sorbents and consequently, also the capacity of these sorbent materials is lower than that of the impregnated sorbents. However, optimization of grafting conditions and the use of high surface area silicas improves the amine contents of these sorbents. At the moment of writing, the highest CO_2 capacities observed for Class 2 sorbents is 2.65 mol/kg [41] measured in 5 vol% of CO_2 and at 25°C.

For Class 3 supported amines, similar to the impregnated sorbents, the pore volume will set an upper limit to the amount of N molecules that can be loaded onto the support material. HAS have a considerably higher nitrogen content than the above mentions grafted amine sorbents. Here amines are bonded to a silica support via a surface polymerization reaction of aziridine inside the SBA-15 pore space. Aziridine does not only bind to the surface of the support but also to aziridine molecules already attached to the surface. Hence, the amine loading is not limited to the amount of available active sites on the support which is often the case for grafted amine sorbents. The amine loading and capacity of these sorbent materials is higher than that of grafted sorbents [15, 37]. The highest capacity observed for a HAS sorbent developed by Jones et al. [15] had an amine content as high as 9.78 mol/kg and was capable of adsorbing 5.5 mol/kg (10% CO_2 , 90% Ar, saturated with water at 25°C).

In summary, all three classes of supported amine sorbents possess useful CO_2 capacities i.e. >1.5 mol/kg. Currently there is not a clear winner. Class 1 sorbents are easy to prepare and show the highest CO_2 capacities. Class 2 and Class 3 sorbents show good capacities as well as they are in general more stable than Class 1 sorbents.
The main challenge here is however not solely to create a sorbent with a useful capacity. It should also be possible to effectively utilize this capacity under process conditions. This seems trivial but this implies that (1) the sorbent can be regenerated while producing a high purity CO_2 gas, (2) the sorbent can be saturated with CO_2 within a reasonable time frame (no more than a few minutes) and (3) the sorbent is suitable for application in a gas-solid contactor which places restrictions on, for instance, the sorbent particles size.

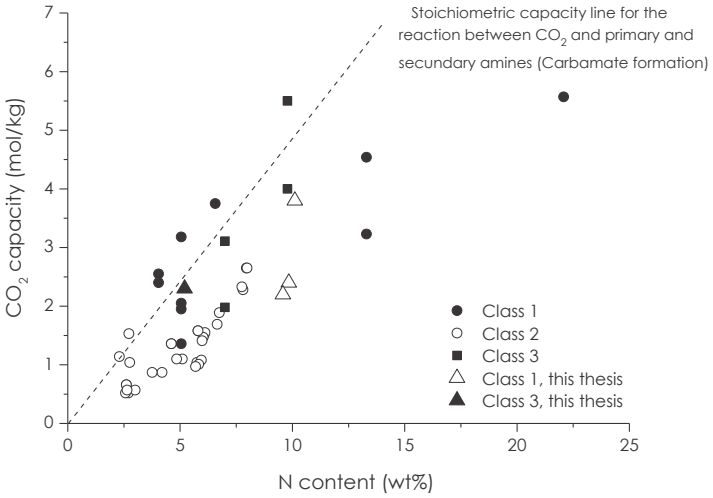

Figure 2: SAS adsorption capacities for grafted and impregnated sorbent materials as a function of the amine loading in moles N per kg sorbent for P_{CO2}<0.2 bar. The data depicted in this graph is summarized in Table 1 and 2 of Appendix A.

4.2 | Tolerance towards H_2O

Like CO_2, H_2O is a combustion product. Consequently, flue gas emitted by power plants also contains water. Water is also picked up by the flue gas in the flue gas clean up section. The conventional desulphurization system, which is deployed in most new coal-fired power plants to remove the SO_2 present in the gas, uses a wet scrubber usually with a slurry of lime or limestone. The amount of water present in flue gas depends on the configuration of the power plant but typically, the flue gas entering CO_2 capture facility will contain 7-10 vol% of H_2O.

Supported amine sorbents are tolerant towards the presence of water in the CO_2 containing gas i.e. the CO_2 capacity does not degrade in presence of H_2O (Figure 3). In many cases H_2O was even found to promote the CO_2 capacity [5, 18, 24, 42, 43]. This phenomenon is quite common for supported amine sorbents and is usually attributed to the interference of H_2O in the adsorption mechanism. Water vapor can act as a free-base, resulting in the formation of bicarbonate whereas carbamate is formed when water is not present. This changes the reaction stoichiometry; in the presence of water one amine group could theoretically react with one CO_2 molecule whereas two amine molecules are required to bind one molecule of CO_2 under dry conditions.

This is an important strength of this type of sorbents since flue gas contains as much if not more H_2O than CO_2. Still, these sorbent materials also capture significant amounts of H_2O under conditions relevant for post-combustion CO_2 capture. Franchi et al. [18] reported an adsorption capacities for DEA on pore expanded MCM-41 of 5.37 mol/kg at 28% relative humidity (Rh), and Xu et al. [24] measured the adsorption capacity for PEI on MCM-41 to be 2.63 mol/kg and 3.24 mol/kg at 26% Rh and 31% Rh respectively. Serna-Guerrero et al. reported capacities up to 7.5 mol/kg for aminopropyl-grafted pore-expanded MCM-41 silica at 74% Rh [44]. The sorption capacities reported for H_2O in these studies surpass the capacities measured for CO_2. Also other materials considered for applications in post-combustion capture as a sorbent or support material (13X, silica supported amines, carbons, etc..) are all known to capture large quantities of H_2O under flue gas conditions [45].

In terms of sorbent stability, the process may benefit from the co-adsorption of some of the water present in flue gas. The presence of water during sorbent regeneration suppresses the undesired formation of urea [42, 46-49]. Drage et al. [48] observed CO_2 induced deactivation of a PEI impregnated silica supported amine sorbents at temperatures above 135˚C. The loss of adsorption capacity was attributed to the bonding of CO_2 into

the PEI polymer through the formation of a urea type linkage. The reaction pathway for the formation of urea is given below.

$$2R_2NH+CO_2 \leftrightarrow R_2NCONR_2+H_2O \quad (3)$$

Sayari et al. [42] reported that water vapor greatly improved the stability of these type of sorbent material. It was observed that the formation of urea could be completely be reversed by adding steam via hydrolysis of such groups. Even at a low relative humidity (0.4%), urea formation was strongly inhibited. Desorption was performed here using a N_2 as a sweep gas. Therefore, higher partial pressures of water might be needed to prevent urea formation in case the sorbent material was to be regenerated in an atmosphere containing higher concentrations of CO_2. Another method to prevent the CO_2 induced degradation of supported amine sorbents was proposed by Sayari et al. [47]. Secondary and tertiary amine were found to be much more stable, even up to temperatures as high as 200°C, than primary amines with respect to undesired formation of urea. This difference was explained by Sayari et al. [47] in the following way: "The difference in the stability of primary vs secondary and tertiary amines was associated with the occurrence of isocyanate as intermediate species toward the formation of urea groups, since only primary amines can be precursors to isocyanate in the presence of CO_2."

Although the adsorption of small quantities of water might prevent CO_2 induced sorbent deactivation, the adsorption of large quantities of water could severely affect the energy demand of the process. In the desorber column temperatures are high and H_2O partial pressure are envisioned to be low [50]. Hence a large part of the co-adsorbed water will be released again in the desorber column. In addition to the heat required to desorb the captured CO_2, also energy is required to release the co-adsorbed water, resulting in an increase in the parasitic heat demand for capture.
In summary, the role of water in this process is complex as the H_2O present in flue gas (1) interferes with the CO_2 adsorption mechanism [18, 24] and affects (2) the sorbent stability [42, 46-49] as well as (3) the process energy demand. However, the studies on the H_2O adsorption by supported amine sorbents are limited. Moreover, there is not yet a clear strategy how to deal with the co-adsorption of water on a process scale.

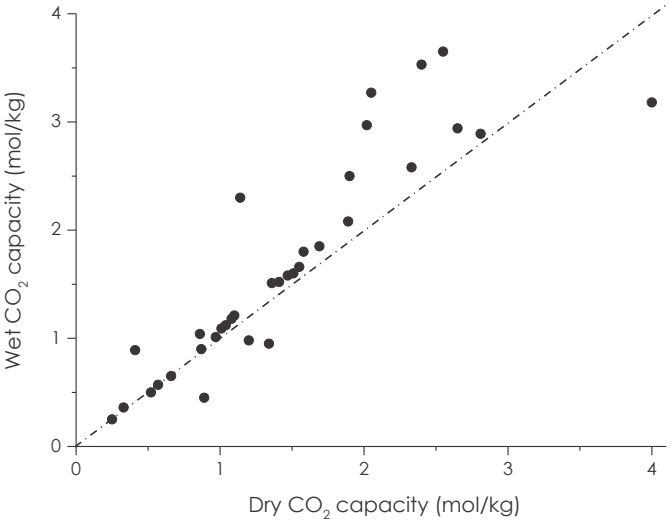

Figure 3: Parity plot of the CO_2 capacity of supported amine sorbents that were both tested under 'dry' conditions and under 'wet' conditions. The literature data depicted in this graph is summarized in Table 3 of Appendix A.

4.3 | Tolerance towards O_2, NO_2, SO_2, NO and $H2_S$

Next to N_2, CO_2 and H_2O flue gas contains other gases like O_2 and traces of NO_x and SO_2. Supported amine sorbents show high CO_2/N_2 and CO_2/O_2 selectivities and co-adsorption of these gasses is not expected [51]. However, the presence of O_2 does impact the stability of supported amine sorbents. Several researcher reported deactivation of both Class 1 and Class 2 supported amine sorbents in an oxidizing environment. Heydari-Gorji et al. [49] reported that the presence of O_2 induced degradation of PEI impregnated sorbent materials and they also observed amine-grafted pore expanded MCM-41 to suffer from degradation in presence of O_2 [52].
With respect to O_2 induced degradation, the amine type (i.e. primary, secondary or tertiary) [52], the temperature [49] and the CO_2 concentration [49] in the gas were found to greatly influence the degradation rate: (1) lower temperatures significantly lower the degradation rate, (2) primary amines were found to be more stable than secondary or mixed amines in presence of oxygen [52-54] and (3) higher CO_2 concentration in the O_2 containing gas resulted in less degradation.

After 30 h of exposure to carbon-free air at 120˚C, the PEI impregnated sorbent material lost its CO_2 capacity completely. However, at 75˚C only 6% of the capacity was lost after 30 h of exposure [49]. Moreover, the sorbent samples were found to be more stable if, next to O_2, also CO_2 was present in the gas mixture. Long-term exposure to wet CO_2- and O_2-containing gas mixtures did not result in sorbent degradation. This might indicate that carbamate and bicarbonate species formed in the reaction between amines and CO_2 are more resistant towards oxygen attacks.
With respect to the presence of SO_2, NO_2 and H_2S, amines sorbents show a different behavior. In contrast to O_2, all of these gasses adsorb onto the same active sites as CO_2.

SO_2 was found to adsorb as sulfates and sulfites on primary amine-grafted SBA-15 [55]. Although the adsorption rate of SO_2 was slower than that of CO_2, the adsorption of SO_2 is not reversible under CO_2 regeneration conditions and S surface species are capable of blocking the active amine sites resulting a significant loss in capacity. Other researchers confirmed these findings for PEI impregnated sorbent materials as well as three different grafted sorbent materials [56].
Also Hallenbeck et al. [57] reported irreversible adsorption of SO_2 on their primary amine based sorbent. However, treatment of the sorbent with a NaOH solution partially reversed the SO_2 poisoning.

The above mentioned PEI impregnated and grafted sorbent materials all showed very high nitrogen dioxide adsorption capacities upon exposure to NO_2. Moreover, all adsorbents treated with NO_2 exhibited a dramatic reduction in CO_2 capacity, which corresponds to the deactivation of amine groups due to the irreversible binding of NO_2 [56]. In another work, these amine-NOx complexes were identified as nitrite and nitrosamine derivatives, which cannot be thermally degraded to regenerate the amine [58]. Supported amine sorbents do seem to favor the adsorption of CO_2 over NOx [59]. This might limit the degradation rate but since the sorbent material need to be stable over many adsorption-regeneration cycles and considering the irreversible nature of the amine-NO_2 complex, even a small loss of activity per cycle might severely impact sorbent make-up cost.

In contrast to NO_2, H_2S adsorbs reversibly on supported amine sorbents. As H_2S binds to the amine active groups, H_2S capacities lie in the same range as the capacities measured for CO_2, and CO_2 and H_2S compete for the same active sites. The heat of adsorption was found to be slightly lower than that of CO_2, around 40 kJ/mol [60]. Supported amines show a low affinity for NO. Furthermore, exposing grafted and impregnated amine sorbents to NO did not result in a significant reduction in CO_2 capacity [56].

The main findings regarding the chemical stability of supported amines are summarized in Table 2. In most new power plants both NOx and SO_2 are removed upstream of the CO_2 capture facility in the selective catalytic reformer (SCR) and flue gas desulphurization (FGD) unit. Still even traces of these compounds cause deactivation of the sorbent material. Since the affinity of the supported amine sorbents towards these compounds is high and regeneration is difficult, the deactivation rate will be directly related to the concentration of these gasses in the flue gas entering the adsorber of the CO_2 capture process. Regarding the O_2 induced degradation, it seems that the oxidative degradation of these sorbent materials in the adsorption stage of the process could be managed by choosing low adsorption temperatures. This will also be beneficial to the CO_2 adsorption capacities. Moreover, since the sorbent materials show no significant uptake of O_2, the O_2 levels in the regenerator, where temperatures are envisioned to be higher, are expected to be very limited.

Table 2: Summary of main findings on chemical deactivation of amine sorbents.

Component	Deactivation	Source
CO_2	Yes: Formation of Urea. Deactivation is reversible by treatment with H_2O. Secondary and tertiary amine are more resistant.	[47]
SO_2	Yes: Poisoning of amine groups. Partially reversible in case of secondary amines. Poisoning can be reversed when sorbent is treated with a NaOH solution	[56, 57]
NO_2	Yes: Poisoning of amine groups. Irreversible binding	[56]
O_2	Yes: Oxidation of amine groups. Significant deactivation at temperatures above 100°C. Carbamate groups are more resistant. Primary amines are more resistant	[52]
NO	No deactivation	[56]
H_2S	No deactivation Competitive adsorption. Fully reversible adsorption.	[60, 61]

4.4 | Desorption

Supported amine sorbents can be regenerated by applying a thermal swing, a pressure swing or a combination of both. For applications in post-combustion CO_2 capture it is critical to regenerate the sorbent material in such a way that the CO_2 is released at a high purity (>95%). These high purities are essential for cost-effective transportation and storage of CO_2.
This high purity places restrictions on the sorbent regeneration method and three viable options are considered in literature: (1) the use of steam (or another easily condensable gas) as sweep gas to regenerate the sorbent material via a combined pressure/thermal swing, (2) a vacuum/thermal swing regeneration or (3) regeneration of the sorbent in pure CO_2 at atmospheric, or preferably higher than atmospheric pressures [9], using a temperature swing.

A temperature swing is the most applied method to regenerate supported amine sorbents. Regeneration in pure CO_2 by applying a thermal swing was demonstrated to combine good cyclic capacities with high product gas purities. Drage et al. measured an operating capacity of 2 mol/kg at a regeneration temperature of 140˚C [48]. Still, even at these relatively low temperatures, Class 1 sorbent materials suffer from amine losses due to evaporation and from CO_2 induced deactivation [48, 62]. Class 2 sorbent materials have been found to be more stable under these conditions. Alesi et al. [7] found that primary amine-functionalized ion-exchange resin shows excellent thermal stability and can be regenerated completely in pure CO_2 at 150˚C. A working capacity of around 1.5 mol/kg was achieved using this sorbent material.

Each of the above mentioned regeneration strategies have their own specific advantages. A combined thermal/pressure swing allows for lower desorption temperatures which is beneficial in view of the sorbent's thermal and chemical stability. In a pure thermal swing there is no need for a sweep gas or expensive vacuum equipment. The main challenge remains the selection of the best regeneration strategy and finding the most suitable regeneration conditions. Subsequently, this regeneration method should be evaluated under process conditions and over a large number of adsorption-desorption cycles.

5.0

Summary

Looking back on what has been discussed in this chapter we can conclude that supported amine sorbents are strong sorbent candidates especially for applications in post-combustion capture where the CO_2 partial pressure is low.

The capacities reported for supported amine sorbents rank among the highest reported for CO_2 sorbents under CO_2 partial pressures ranging from 0.04-0.15 bar. For both impregnated [17, 20, 24] amine sorbents as well as for grafted amine sorbents [15, 37, 63] adsorption capacities higher than 3 mol/kg have already been reported. Also, supported amine sorbents possess excellent CO_2/N_2 and CO_2/O_2 selectivity's [51] and are tolerant towards the presence of water in the CO_2 containing gas [64]. Moreover, supported amines can be regenerated at relatively low temperatures [48] and compared to other chemical sorbents like K_2CO_3, Na_2CO_3 and CaO, supported amine sorbents require a relatively small amount of heat to release the captured CO_2.

Although excellent work has already been published on the development and testing of SAS, still several critical issues remain which require additional attention. This is reflected in the outline of this thesis.

6.0

Scope & Outline

The work presented in this thesis focusses on the demonstration and evaluation of a new post-combustion CO_2 capture process based on SAS technology. The main objective is to advance the development of a CO_2 capture process with lower operational and capital costs than the conventional MEA based technology.

Chapter 2 focusses on sorbent preparation and improvement of the sorption characteristics of the prepared sorbent materials by changing the support type, amine type, amine loading and the pore size of the support material. The aim is to develop sorbent materials with a capacity of at least 1.5 mol/kg, which is the minimum capacity required to achieve the desired energy savings. In the second part of Chapter 2 thermal and chemical degradation of the sorbent material is investigated in more detail.

Chapter 3 focusses on the co-adsorption of H_2O on supported amine sorbents. As discussed in section 4.2, the role of water in this sorbent based process is complex as the H_2O present in flue gas (1) interferes with the CO_2 adsorption mechanism and affects (2) the sorbent stability as well as (3) the process energy demand. However, the studies on the H_2O adsorption by supported amine sorbents are limited. Moreover, there is not yet a clear strategy to deal with the co-adsorption of water on a process scale. The aim here is to analyze H_2O adsorption and to identify the best strategy to handle H_2O in this process i.e. to minimizes the impact of H_2O co-adsorption on capture costs.

Although both sorbent- and process development will have an essential role in realizing the envisioned cost savings, reports on process design remain rare. Several gas-solid reactor concepts exist but it is unclear which one is the most suitable. Also, testing of supported amine sorbents has mostly been limited to small-scale sorbent testing in a fixed- or fluid bed set-ups or by thermal gravimetric analysis. In Chapter 4 we present a systematic selection and design of the contactor required to facilitate sorbent based CO_2 capture. The most suitable adsorber and desorber reactor type were selected, designed and constructed for experimental validation of the reactor concept in Chapter 5. Focus here lies on analyzing the performance of the lab-scale capture facility in terms of capture efficiency, productivity

and energy demand.
Finally, Chapter 6 presents a preliminary process design for a sorbent based CO_2 capture facility at a 500 MWe coal-fired power plant and an extensive techno-economic comparison of the performance of the novel capture process with the state of the art technology.

Abbreviations

Amine types

MEA	Monoethanolamine
DEA	Diethanolamine
TEA	Triethanolamine
TEPA	Tetraethyleneamine
PEI	Polyethylenimine
APTES	3-aminopropyltriethoxysilane
APTS	3-aminopropyltrimethoxysilane
AEAPTS	aminoethyl-aminopropyl-trimethoxysilane
DAEAPTS	3-[2-(2-aminoethyl-amino)ethylamino]-propyltrimethoxysilane

Support materials

SBA-15	A silicon dioxide based support
PMMA	A poly(methyl acrylate) based support
MCM-41	Mobile composition of matter nr. 41: A silicon dioxide based support
MCM-48	Mobile composition of matter nr. 48: A silicon dioxide based support
PE-MCM-41	Pore expanded MCM-41
KIT-6	A silicon dioxide based support
HMS	Hexagonal mesoporous silicas
MC400/10	Type of mesoporous silica capsules

A.

Literature summary of capacities reported for CO_2 sorbents

Table A.1: Capacities for Class 1 amine sorbents for CO_2 pressures below or equal to 0.15 bar.

Support material	Amine type	Amine content (wt%)	CO_2 pressure (bar)	Temp. (°C)	N content (mol/kg)	Cap. (mol/kg)	Ref.
MCM-41	PEI	50	0.1	75	5.1	2.05	[16]
MCM-41	TEPA	50	0.05	75	13.3	4.54	[26]
SBA-15	TEPA	50	0.05	75	13.3	3.23	[17]
SBA-15	PEI	50	0.15	75	5.1	3.18	[65]
SBA-15	PEI	50	0.12	75	5.1	1.36	[66]
KIT-6	PEI	50	0.05	75	5.1	1.95	[67]
Monolith	PEI	65	0.05	75	6.6	3.75	[27]
MC400/10	TEPA	83	0.1	75	22.1	5.57	[68]
PMMA (diaion)	PEI	40	0.1	45	4.0	2.4	[22]
SiO_2 (CaRiaCT)	PEI	40	0.1	45	4.0	2.55	[22]
Diaion	TEPA	38	0.15	40	10.1	3.8	This thesis
Davisil grade 45	TEPA	37	0.15	40	9.8	2.4	This thesis
CaRiaCT Q-10	TEPA	36	0.15	40	9.6	2.2	This thesis

Table A.2: Capacities for Class 2 and 3 amine sorbents for CO_2 pressures below or equal to 0.15 bar.

Support material	Amine type	CO_2 press. (bar)	Temp. (°C)	N content (mol/kg)	Cap. (mol/kg)	Ref.

SBA-15	APTES	0.15	60	2.7	0.52	[69]
SBA-15	AEAPS	0.15	60	4.2	0.87	[69]
SBA-15	DAEAPTS	0.15	60	5.1	1.1	[69]
SBA-15	APTES	0.15	60	2.61	0.66	[70]
SBA-15	AEAPS	0.15	60	4.61	1.36	[70]
SBA-15	DAEAPTS	0.15	60	5.8	1.58	[70]
SBA-15	APTES	0.1	25	2.72	1.53	[71]
SBA-15	APTES	0.1	25	2.76	1.04	[71]
MCM-41	APTES	0.1	25	3	0.57	[71]
PE-MCM-41	DAEAPTS	0.05	25	7.95	2.65	[41]
PE-MCM-41	DAEAPTS	0.05	70	7.8	2.28	[72]
MCM-48	APTES	0.05	25	2.3	1.14	[73]
MCM-41	DAEAPTS	0.05	25	5.75	1.04	[41]
MCM-41	DAEAPTS	0.05	25	5.95	1.08	[41]
MCM-41	DAEAPTS	0.05	25	5.83	1.01	[41]
MCM-41	DAEAPTS	0.05	25	5.69	0.97	[63]
PE-MCM-41	DAEAPTS	0.05	25	6.07	1.51	[41]
PE-MCM-41	DAEAPTS	0.05	25	6.11	1.55	[41]
PE-MCM-41	DAEAPTS	0.05	25	6.03	1.47	[41]
PE-MCM-41	DAEAPTS	0.05	25	5.98	1.41	[63]
PE-MCM-41	DAEAPTS	0.05	25	7.75	2.33	[41]
PE-MCM-41	DAEAPTS	0.05	25	7.98	2.65	[41]
PE-MCM-41	DAEAPTS	0.05	25	6.75	1.89	[41]
PE-MCM-41	DAEAPTS	0.05	25	6.65	1.69	[41]
SBA-15 (wet)	aziridine polymer	0.1	25	9.78	5.5	[15]
SBA-15 (wet)	aziridine polymer	0.1	75	9.78	4	[15]
SBA-15 (wet)	aziridine polymer	0.1	75	7	1.98	[37]
SBA-15 (wet)	aziridine polymer	0.1	25	7	3.11	[37]
Lewatit VP OC 1065		0.15	40	5.2	2.3	This thesis

Table A.3: Literature data comparison of dry and wet capacities reported for SAS.

Support type	Amine type	Capacity (dry) (mol/kg)	Capacity (wet) (mol/kg)	CO_2 Pressure (atm)	Temp. (°C)	Ref.
PE- MCM-41	DEA	2.81	2.89	0.05	25	[18]
MC400/10	TEPA	5.57	7.93	0.1	75	[68]
PMMA (diaion)	PEI	2.4	3.53	0.1	45	[22]
SiO_2 (CaRiaCT)	PEI	2.55	3.65	0.1	45	[22]
MCM-41	PEI	2.02	2.97	0.15	75	[24]
SBA-15	TEPA/DEA	4	3.18	1	75	[74]
SBA-15	APTES	0.52	0.5	0.15	60	[69]
SBA-15	AEAPS	0.87	0.9	0.15	60	[69]
SBA-15	DAEAPTS	1.1	1.21	0.15	60	[69]
SBA-15	APTES	0.66	0.65	0.15	60	[70]
SBA-15	AEAPS	1.36	1.51	0.15	60	[70]
SBA-15	DAEAPTS	1.58	1.8	0.15	60	[70]
silica gel	APTES	0.41	0.89	1.01	22	[34]
HMS	APTES	0.86	1.04	0.91	20	[75]
MCM-48	APTES	1.14	2.3	0.05	25	[73]
HMS	AEAPS	0.89	0.45	0.91	20	[35]
HMS	DEA	1.2	0.98	0.91	20	[36]
MCM-41	DAEAPTS	1.04	1.12	0.05	25	[41]
MCM-42	DAEAPTS	1.08	1.18	0.05	25	[41]
MCM-43	DAEAPTS	1.01	1.09	0.05	25	[41]
MCM-44	DAEAPTS	0.97	1.01	0.05	25	[63]
PE-MCM-41	DAEAPTS	1.51	1.6	0.05	25	[41]
PE-MCM-41	DAEAPTS	1.55	1.66	0.05	25	[41]

PE-MCM-41	DAEAPTS	1.47	1.58	0.05	25	[41]
PE-MCM-41	DAEAPTS	1.41	1.52	0.05	25	[63]
SBA-15	AEAPS	0.57	0.57	0.15	25	[76]
PE-MCM-41	DAEAPTS	2.33	2.58	0.05	25	[41]
PE-MCM-41	DAEAPTS	2.65	2.94	0.05	25	[41]
PE-MCM-41	DAEAPTS	1.89	2.08	0.05	25	[41]
PE-MCM-41	DAEAPTS	1.69	1.85	0.05	25	[41]
PE-MCM-41	APTES	2.05	3.27	0.05	25	[44]
SBA-15	APTES	0.25	0.25	0.15	60	[70]
SBA-15	APTES	0.33	0.36	0.04	25	[77]
HMS	DAEAPTS	1.34	0.95	0.9	20	[36]
PE-MCM-41	DAEAPTS	1.9	2.5	0.1	50	[51]

References

1. Vos, R., Linking the chain: Integrated CATO$_2$ knowledge prepares for the next step in CO_2 capture and storage. 2014, Zutphen: CPI.
2. SASKPower. http://saskpowerccs.com/ccs-projects/boundary-dam-carbon-capture-project/. [cited 2015 11-06-2015].
3. Statoil. http://www.statoil.com/en/OurOperations/ExplorationProd/ncs/sleipner/Pages/default.aspx. [cited 2015 11-06-2015].
4. Fisher, K.S., et al., Integrating MEA regeneration with CO_2 compression and peaking to reduce CO_2 capture costs, 2005.
5. Ebner, A.D., et al., Suitability of a solid amine sorbent for CO_2 capture by pressure swing adsorption. Industrial and Engineering Chemistry Research, 2011. 50(9): p. 5634-5641.
6. Choi, S., J.H. Drese, and C.W. Jones, Adsorbent materials for carbon dioxide capture from large anthropogenic point sources. Chemsuschem, 2009. 2: p. 796-854.
7. Alesi, W.R. and J.R. Kitchin, Evaluation of a primary amine-functionalized ion-exchange resin for CO_2 capture. Industrial & Engineering Chemistry Research, 2012. 51(19): p. 6907-6915.
8. Filburn, T., J.J. Helble, and R.A. Weiss, Development of supported ethanolamines and modified ethanolamines for CO_2 capture. industrial & engineering chemistry research, 2005. 44: p. 1542-1546.
9. Veneman, R., H. Kamphuis, and D.W.F. Brilman, Post-Combustion CO_2 capture using supported amine sorbents: A process integration study. Energy procedia, 2013. 37: p. 2100-2108.
10. Rochelle, G., et al., Aqueous piperazine as the new standard for CO_2 capture technology. Chemical Engineering Journal, 2011. 171(3): p. 725-733.
11. Caplow, M., Kinetics of carbamate formation and breakdown. J. Am. Chem. Soc., 1968. 90: p. 6795–6803.
12. Danckwerts, P.V., The reaction of CO_2 with ethanolamines. Chem. Eng. Sci., 1976. 34: p. 443–446.
13. Samanta, A., A. Zhao, G.K.H. Shimizu, P. Sarkar, and R. Gupta, Post-combustion CO_2 capture using solid sorbents: A review. Industrial and Engineering Chemistry Research, 2012. 51(4): p. 1438-1463.
14. Kim, Y.E., et al., Comparison of carbon dioxide absorption in aqueous MEA, DEA, TEA, and AMP solutions. Bulletin of the Korean Chemical Society, 2013. 34(3): p. 783-787.
15. Drese, J.H., et al., Synthesis-structure-property relationships for hyper-

branched aminosilica CO_2 adsorbents. Advanced Functional Materials, 2009. 19(23): p. 3821-3832.
16. Xu, X., C. Song, J.M. Andresen, B.G. Miller, and A.W. Scaroni, Novel polyethylenimine-modified mesoporous molecular sieve of MCM-41 type as high-capacity adsorbent for CO_2 capture. Energy & Fuels, 2002. 16: p. 1463-1469.
17. Yue, M.B., Y. Chun, Y. Cao, X. Dong, and J.H. Zhu, CO_2 capture by as-prepared SBA-15 with an occluded organic template. Advanced Functional Materials, 2006. 16(13): p. 1717-1722.
18. Franchi, R.S., P.J.E. Harlick, and A. Sayari, Applications of pore-expanded mesoporous silica. 2. Development of a high-capacity, water-tolerant adsorbent for CO_2. Industrial & engineering chemistry research, 2005. 44: p. 8007–8013.
19. Houshmand, A., W.M.A.W. Daud, M.G. Lee, and M.S. Shafeeyan, Carbon dioxide capture with amine-grafted activated carbon. Water, Air and Soil Pollution, 2011: p. 1-9.
20. Su, F.S., C.Y. Lu, S.C. Kuo, and W.T. Zeng, Adsorption of CO_2 on amine-functionalized Y-Type zeolites. Energy & Fuels, 2010. 24: p. 1441-1448.
21. Lee, S., T.P. Filburn, M. Gray, J.W. Park, and H.J. Song, Screening test of solid amine sorbents for CO_2 capture. Industrial & engineering chemistry research, 2008. 47(19): p. 7419-7423.
22. Gray, M.L., et al., Parametric study of solid amine sorbents for the capture of carbon dioxide. Energy & Fuels, 2009. 23: p. 4840-4844.
23. Xu, X., J.M. Andresen, C. Song, B.G. Miller, and A.W. Scaroni. Preparation of novel CO_2 "molecular basket" of polymer modified MCM-41. 2002.
24. Xu, X., C. Song, B.G. Miller, and A.W. Scaroni, Influence of moisture on CO_2 separation from gas mixture by a nanoporous adsorbent based on polyethylenimine-modified molecular sieve MCM-41. Industrial and Engineering Chemistry Research, 2005. 44(21): p. 8113-8119.
25. Bhagiyalakshmi, M., L.J. Yun, R. Anuradha, and H.T. Jang, Synthesis of chloropropylamine grafted mesoporous MCM-41, MCM-48 and SBA-15 from rice husk ash: their application to CO_2 chemisorption. Journal of Porous Materials, 2010. 17(4): p. 475-484.
26. Yue, M.B., et al., Efficient CO_2 capturer derived from As-synthesized MCM-41 modified with amine. Chemistry - A European Journal, 2008. 14: p. 3442-3451.
27. Chen, C., S.T. Yang, W.S. Ahn, and R. Ryoo, Amine-impregnated silica monolith with a hierarchical pore structure: Enhancement of CO_2 capture capacity. Chemical Communications, 2009(24): p. 3627-3629.
28. Heydari-Gorji, A., Y. Yang, and A. Sayari, Effect of the pore length on

CO_2 adsorption over amine-modified mesoporous silicas. Energy and Fuels, 2011. 25(9): p. 4206-4210.
29. Kim, S., J. Ida, V.V. Guliants, and J.Y.S. Lin, Tailoring pore properties of MCM-48 silica for selective adsorption of CO_2. Journal of Physical Chemistry B, 2005. 109(13): p. 6287-6293.
30. Belmabkhout, Y. and A. Sayari, Effect of pore expansion and amine functionalization of mesoporous silica on CO_2 adsorption over a wide range of conditions. Adsorption, 2009. 15(3): p. 318-328.
31. Ko, Y.G., S.S. Shin, and U.S. Choi, Primary, secondary, and tertiary amines for CO_2 capture: Designing for mesoporous CO_2 adsorbents. Journal of Colloid and Interface Science, 2011. 361(2): p. 594-602.
32. S. Choi, J.H.D., C. W. Jones, Adsorbent Materials for Carbon Dioxide Capture from Large Anthropogenic Point Sources. ChemSusChem, 2009. 2(9): p. 796-854.
33. Zhao, W.Y., Z. Zhang, Z.S. Li, and N.S. Cai, Investigation of thermal stability and continuous CO_2 capture from flue gases with supported amine sorbent. Industrial & engineering chemistry research, 2013. 52(5): p. 2084-2093.
34. Leal, O., C. Bolívar, C. Ovalles, J.J. García, and Y. Espidel, Reversible adsorption of carbon dioxide on amine surface-bonded silica gel. Inorganica Chimica Acta, 1995. 240: p. 183-189.
35. Knowles, G.P., S.W. Delaney, and A.L. Chaffee, Amine-functionalised mesoporous silicas as CO_2 adsorbents. Studies in Surface Science and Catalysis, 2005. 156: p. 887-896.
36. Knowles, G.P., S.W. Delaney, and A.L. Chaffee, Diethylenetriamine[propyl(silyl)]-functionalized (DT) mesoporous silicas as CO_2 adsorbents. Industrial & engineering chemistry research, 2006. 45: p. 2626-2633.
37. Hicks, J.C., et al., Designing adsorbents for CO_2 capture from flue gas-hyperbranched aminosilicas capable of capturing CO_2 reversibly. Journal of the American Chemical Society, 2008. 130(10): p. 2902-2903.
38. Xu, X., C. Song, J.M. Andresen, B.G. Miller, and A.W. Scaroni, Adsorption separation of CO_2 from simulated flue gas mixtures by novel CO_2 'molecular basket' adsorbents. Int. J. Environ. Technol. Manage., 2004. 4: p. 32–52.
39. Veneman, R., Z.S. Li, J.A. Hogendoorn, S.R.A. Kersten, and D.W.F. Brilman, Continuous CO_2 capture in a circulating fluidized bed using supported amine sorbents. Chemical Engineering Journal, 2012. 207: p. 18-26.
40. Zhao, W., L. Wang, Z. Li, and N. Cai, Thermal stability of various amine CO_2 absorbents. Huagong Xuebao/CIESC Journal, 2012. 63(10): p.

3304-3309.
41. Harlick, P.J.E. and A. Sayari, Applications of pore-expanded mesoporous silica. 5. triamine grafted material with exceptional CO_2 dynamic and equilibrium adsorption performance. Industrial & engineering chemistry research, 2007. 46: p. 446–458.
42. Sayari, A. and Y. Belmabkhout, Stabilization of amine-containing CO_2 adsorbents: Dramatic effect of water vapor. Journal of the American Chemical Society, 2010. 132(18): p. 6312-6314.
43. Li, W., et al., Steam-stripping for regeneration of supported amine-based CO_2 adsorbents. Chemsuschem, 2010. 3(8): p. 899-903.
44. Serna-Guerrero, R., E. Da'na, and A. Sayari, New insights into the interactions of CO_2 with amine-functionalized silica. industrial & engineering chemistry research, 2008. 46: p. 446-458.
45. Wang, Y. and M.D. Levan, Adsorption equilibrium of carbon dioxide and water vapor on Zeolites 5A and 13X and Silica Gel: Pure components. Journal of Chemical and Engineering Data, 2009. 54(10): p. 2839-2844.
46. Sayari, A., A. Heydari-Gorji, and Y. Yang, CO_2-induced degradation of amine-containing adsorbents: Reaction products and pathways. Journal of the American Chemical Society, 2012. 134(33): p. 13834-13842.
47. Sayari, A., Y. Belmabkhout, and E. Da'na, CO_2 deactivation of supported amines: Does the nature of amine matter? Langmuir, 2012. 28(9): p. 4241-4247.
48. Drage, T.C., A. Arenillas, K.M. Smith, and C.E. Snape, Thermal stability of polyethylenimine based carbon dioxide adsorbents and its influence on selection of regeneration strategies. Microporous and mesoporous materials, 2008. 116(1-3): p. 504-512.
49. Heydari-Gorji, A. and A. Sayari, Thermal, oxidative, and CO_2-induced degradation of supported polyethylenimine adsorbents. Industrial & Engineering Chemistry Research, 2012. 51(19): p. 6887-6894.
50. Veneman, R., Z.S. Li, J.A. Hogendoorn, S.R.A. Kersten, and D.W.F. Brilman, Continuous CO 2 capture in a circulating fluidized bed using supported amine sorbents. Chemical Engineering Journal, 2012.
51. Serna-Guerrero, R., Y. Belmabkhout, and A. Sayari, Further investigations of CO_2 capture using triamine-grafted pore-expanded mesoporous silica. Chemical Engineering Journal, 2010. 158: p. 513–519.
52. Heydari-Gorji, A., Y. Belmabkhout, and A. Sayari, Degradation of amine-supported CO_2 adsorbents in the presence of oxygen-containing gases. Microporous and mesoporous materials, 2011. 145(1-3): p. 146-149.
53. Bollini, P., S. Choi, J.H. Drese, and C.W. Jones, Oxidative degradation of aminosilica adsorbents relevant to post-combustion CO_2 capture. En-

ergy & Fuels, 2011. 25(5): p. 2416-2425.
54. Bali, S., T.T. Chen, W. Chaikittisilp, and C.W. Jones, Oxidative stability of amino polymer-alumina hybrid adsorbents for carbon dioxide capture. Energy & Fuels, 2013. 27(3): p. 1547-1554.
55. Khatri, R.A., S.S.C. Chuang, Y. Soong, and M. Gray, Thermal and chemical stability of regenerable solid amine sorbent for CO_2 capture. Energy & Fuels, 2006. 20(4): p. 1514-1520.
56. Rezaei, F. and C.W. Jones, Stability of supported amine adsorbents to SO_2 and NOx in post-combustion CO_2 capture. 1. Single-component adsorption. Industrial & Engineering Chemistry Research, 2013. 52(34): p. 12192-12201.
57. Hallenbeck, A.P. and J.R. Kitchin, Effects of O_2 and SO_2 on the capture capacity of a primary-amine based polymeric CO_2 sorbent. Industrial and Engineering Chemistry Research, 2013. 52(31): p. 10788-10794.
58. Diaf, A. and E.J. Beckman, Thermally reversible polymeric sorbents for acid gases. 4. Affinity tuning for the selective dry sorption of NOx. Reactive Polymers, 1995. 25(1): p. 89-96.
59. Xu, X., C. Song, B.G. Miller, and A.W. Scaroni, Adsorption separation of carbon dioxide from flue gas of natural gas-fired boiler by a novel nanoporous "molecular basket" adsorbent. Int. J. Environ. Technol. Manage., 2004. 4: p. 32–52.
60. Belmabkhout, Y., N. Heymans, G. De Weireld, and A. Sayari, Simultaneous adsorption of H_2S and CO_2 on triamine-grafted pore-expanded mesoporous MCM-41 silica. Energy and Fuels, 2011. 25(3): p. 1310-1315.
61. Belmabkhout, Y., G. De Weireld, and A. Sayari, Amine-bearing mesoporous silica for CO_2 and H_2S removal from natural gas and biogas. Langmuir, 2009. 25(23): p. 13275-13278.
62. Xu, X.C., C.S. Song, J.M. Andresen, B.G. Miller, and A.W. Scaroni, Novel polyethylenimine-modified mesoporous molecular sieve of MCM-41 type as high-capacity adsorbent for CO_2 capture. Energy & Fuels, 2002. 16(6): p. 1463-1469.
63. Harlick, P.J.E. and A. Sayari, Applications of pore-expanded mesoporous silicas. 3. Triamine silane grafting for enhanced CO_2 adsorption. Industrial and Engineering Chemistry Research, 2006. 45(9): p. 3248-3255.
64. Veneman, R., W. Zhao, Z. Li, N. Cai, and D.W.F. Brilman, Adsorption of CO_2 and H_2O on supported amine sorbents. Energy Procedia, 2014. 63(0): p. 2336-2345.
65. Ma, X., X. Wang, and C. Song, "Molecular basket" sorbents for separation of CO_2 and H_2S from various gas streams. J. Am. Chem. Soc., 2009.

131: p. 5777-5783.
66. Dasgupta, S., et al., Carbon di-oxide removal with mesoporous adsorbents in a single column pressure swing adsorber.
67. Son, W.J., J.S. Choi, and W.S. Ahn, Adsorptive removal of carbon dioxide using polyethyleneimine-loaded mesoporous silica materials. Microporous Mesoporous Mater, 2008. 113: p. 31–40.
68. Qi, G., et al., High efficiency nanocomposite sorbents for CO_2 capture based on amine-functionalized mesoporous capsules. Energy Environ. Sci., 2011. 4: p. 444-452.
69. Hiyoshi, N., K. Yogo, and T. Yashima, Adsorption of carbon dioxide on amine modified SBA-15 in the presence of water vapor. Chemistry Letters, 2004. 33: p. 510.
70. Hiyoshi, N., K. Yogo, and T. Yashima, Adsorption characteristics of carbon dioxide on organically functionalized SBA-15. Microporous and mesoporous materials, 2005. 84: p. 357–365.
71. Zeleňák, V., et al., Amine-modified ordered mesoporous silica: Effect of pore size on carbon dioxide capture. Microporous and mesoporous materials, 2007. 99: p. 79–85.
72. Serna-Guerrero, R., Y. Belmabkhout, and A. Sayari, Influence of regeneration conditions on the cyclic performance of amine-grafted mesoporous silica for CO_2 capture: An experimental and statistical study. Chemical Engineering Science, 2010. 65: p. 4166-4172.
73. Huang, H.Y., R.T. Yang, D. Chinn, and C.L. Munson, Amine-grafted MCM-48 and silica xerogel as superior sorbents for acidic gas removal from natural gas.
74. Yue, M.B., et al., Promoting the CO_2 adsorption in the amine-containing SBA-15 by hydroxyl group.
75. Knowles, G.P., J.V. Graham, S.W. Delaney, and A.L. Chaffee, Aminopropyl-functionalized mesoporous silicas as CO_2 adsorbents. Fuel Processing Technology, 2005. 86: p. 1435-1448.
76. Zheng, F., et al., Ethylenediamine-modified SBA-15 as regenerable CO_2 sorbent. Div. Fuel Chem., Am. Chem. Soc.Prepr. Symp., 2004. 49: p. 261-262.
77. Chang, A.C.C., S.S.C. Chuang, M. Gray, and Y. Soong, In-situ infrared study of CO_2 adsorption on SBA-15 grafted with γ-(aminopropyl)triethoxysilane. Energy & Fuels, 2003. 17: p. 468-473.

Chapter 02

Evaluation of supported amine sorbents for CO_2 capture

This chapter is based on the following articles:

(1) Veneman, R., Li, Z.S., Hogendoorn, J.A., Kersten, S.R.A., Brilman, D.W.F., Continuous CO_2 capture in a circulating fluidized bed using supported amine sorbents, Chemical Engineering Journal, 2012. 207–208, p. 18–26.

(2) Veneman, R., Kamphuis, H., Brilman, D.W.F., Post-Combustion CO_2 capture using supported amine sorbents: A process integration study, Energy Procedia, 2013. 37, p. 2100-2108.

Abstract

This chapter focusses on evaluating the sorption performance of supported amine sorbents in view of their application in CO_2 capture. Sorbents were prepared by physical impregnation of silica and polymer based support materials with different types of amine molecules. The CO_2 capacity of the impregnated sorbents was significantly improved by tuning the amine loading and the pore volume of the support. However, exposing the impregnated sorbent materials to temperatures above 130˚C led to sorbent degradation as a result of (1) the loss of active amine material due to evaporation and (2) the undesired formation of urea. Although the impregnated sorbent material Diaion® HP-2MG (38wt%) showed the highest CO_2 capacity by far (3.8 mol/kg), the commercially grafted sorbent Lewatit® VP OC 1065 (3.2 mol/kg) showed excellent thermal stability. Using the developed sorbent(s) we can potentially reduce the thermal energy requirement for CO_2 capture from 3-4 GJ/t to around 2.2 GJ/t.

1.0

Introduction

Applying supported amine sorbents (SAS) in CO_2 capture may offer a low-cost alternative to the MEA based process. Switching to a sorbent based process could greatly reduce the energy required for CO_2 capture as; (1) the evaporation of water can be inhibited and (2) the energy required for heating the sorbent up to the desorption temperature is much lower due to the lower specific heat capacity of solid supports compared to water.
These supported amine sorbents consist of a high internal surface-area support with amine functional groups immobilized on their surface [1]. As discussed in Chapter 1, the key strengths of these type of sorbent materials include high CO_2 capacities, fast CO_2 uptake rates, low heats of adsorption and relatively mild regeneration conditions compared to other chemical sorbents [2]. In this chapter we focus on evaluating the sorption performance of the impregnated sorbent materials as well as that of a commercial grafted sorbent material. For impregnated sorbent materials, the effects of support pore size, amine loading and support type on capacity were investigated. All sorbents were tested under a wide range of temperatures and pressures to identify the operating window of the sorption process and to select the most suitable desorption strategy. Stability tests were performed and a preliminary energy analysis was conducted based on the experimental results obtained in an attempt to quantify the potential savings in energy discussed above.

2.0

Experimental section

2.1 | Sorbent development

Class 1 supported amine sorbents were prepared by physical impregnation of silica (CARiACT® and Davisil® grade 646, Aldrich), polymethylmethacrylate (Diaion® HP-2MG, Aldrich) and styrene divinylbenzene (Diaion® HP-20, Aldrich) with tetraethylenepentamine (TEPA, CAS: [112-57-2]Aldrich) and polyethylenimine (Mn = 600 g/mol, CAS: [25987-06-8] and Mn = 10000 g/mol, CAS: [9002-98-6] Aldrich). The sorbents were prepared by so-called 'wet impregnation' [3]. The amine compound was dissolved in methanol and physically mixed with the porous support particles. After impregnation, the solvent was evaporated leaving behind the amine, dispersed on the internal and external surface of the support particle. The amine loading was controlled by tuning the amine concentration in the amine/methanol solution. In addition, Lewatit® VP OC 1065 (Lanxess) was studied. Lewatit® VP OC 1065 is a polystyrene based ion exchange resin (IER) containing primary benzyl amine units [4]. The structural characteristics of the support materials and the IER are summarized in Table 1.

Table 1: Support structural characteristics.

Support	Pore size (nm)	Pore volume (ml/g)	Surface area (m^2/g)	Particle size (µm)
CARiACT Q-3	3	0.43	663	75-500
CARiACT Q-10	10	1.24	263	75-500
Davisil® grade 646	15	1.15	300	250-500
Diaion® HP-2MG	17	1.20	500	300-600
Diaion® HP-20	26	1.3	500	250-850
Lewatit® VP OC 1065	25	0.27	50	688*

*Mean particle size

2.2 | Thermal gravimetric analysis

A NETSZCH STA 449 F1 Jupiter thermal gravimetric analyzer (TGA) was used to assess the adsorption and desorption performance of the sorbent materials. In a typical adsorption experiment, around 15 mg of sorbent was placed inside the TGA furnace. The sample was heated up to 80˚C in N_2 to desorb any pre-adsorbed CO_2 and moisture. The temperature was kept constant until the sample mass stabilized. Then, the sample was cooled down to the desired adsorption temperature after which CO_2 was fed to the TGA. The uptake of CO_2 by the sorbent sample resulted in an increase in the sample mass. The sorbent CO_2 uptake, in mole per kilogram sorbent, was calculated from the weight change of the sample during adsorption. After adsorption, sorbent regeneration was achieved by increasing the temperature inside the TGA. Adsorption and regeneration experiments were performed at different temperatures and CO_2 partial pressures. Desired gas compositions were obtained by mixing high purity (grade 5.0) N_2 and high purity (grade 5.0) CO_2. The specific configuration of the TGA equipment limited the CO_2 concentration to a maximum of 80 vol% of CO_2 at 1 atm.

The amine loading of the sorbent was determined by heating the sorbent sample in N_2 up to 360˚C (TEPA bp.: 340˚C), after an initial desorption step at 80˚C. The sample mass decreased upon heating due to amine evaporation at temperatures above 130˚C. Again, the temperature was kept constant until the sample mass stabilized. The amine loading, defined as the mass percentage of amine of the total sorbent mass, was calculated from the sample weight loss during the evaporation experiment.

3.0

Results and discussion

3.1 | On the effect of pore size and amine loading

Figure 1 shows CO_2 uptake curves for TEPA, a viscous liquid at room conditions, and TEPA impregnated on the Diaion® HP-2MG particles. The capacity is expressed as the amount of moles CO_2 adsorbed per mole of N. Theoretically, under dry conditions, a maximum amount of 0.5 moles of CO_2 can be adsorbed per mole of N and considering that there is enough adsorption time, both TEPA and the supported TEPA should adsorb the same amount of CO_2 molecules per mole of N. The role of the support becomes clear when we compare the uptake rate of the amine liquid to that of the amine dispersed over the internal surface of the support material. The porous support provides an open, accessible backbone resulting in a large contact area for the reaction between the amine and CO_2. This results in a much faster CO_2 uptake. The uptake of CO_2 by the support material, HP-2MG, was also studied. The data is however not shown as there was no noticeable amount of CO_2 adsorbed by the support itself.

In the work described below, we have tried to improve the accessibility of the amine groups by tuning the support pore size, and increase the amount of active sites on the sorbent particles, by changing the amine loading, in order to improve the capacity of the sorbent material.
Four different types porous particles (Table 1) were impregnated with different amounts of TEPA, yielding a set of sorbents with different amine loadings (15-48 wt%) and support characteristics. For each prepared sorbent, CO_2 adsorption experiments were performed. CO_2 adsorption curves for the Diaion® HP-2MG based sorbents with various amine loadings are presented in Figure 2. An optimum was observed in sorbent CO_2 capacity as a function amine loading. This is due to a trade-off between the amount of active sites present in the pores of the support and the accessibility of these active sites. Below the optimal loading, a higher amine loading results in a higher capacity as there are more active sites available for reaction. However, due to pore blocking and filling effects at higher amine loadings, the accessibility of these active sites is reduced resulting in a lower effective CO_2 capacity, as evaluated after 50 min. of adsorption time at higher amine loadings [5, 6]. Analysis of the pore size distribution of the original support material and impregnated support material showed that the reduction in pore volume with increasing amine loading is larger than what was theo-

retically calculated based on the amine liquid density, especially at higher amine loadings, illustrating the blocking of pores at higher amine loadings. In the initial adsorption stage, uptake rates of around 2 mol/kg/min were measured for both the silica-based Davisil® grade 646 sorbents and the polymer-based Diaion® HP-2MG sorbents. Only sorbents with an amine loading higher than the optimal amine loading displayed significantly lower initial CO_2 uptake rates. The above mentioned uptake rates were estimated based on TGA-experiments. No dedicated tests were performed to measure intrinsic CO_2 reaction kinetics in this chapter and the observed uptake rates may very well be (partially) limited by mass/heat transfer limitations present inside the TGA furnace. In Chapter 5 the uptake rate of the sorbent particles is studied in detail by combining experimental work with mathematical modelling.

In Figure 3, the sorbent CO_2 capacity is plotted against the sorbent amine loading for all four types of impregnated sorbents. As a reference, the stoichiometric CO_2 capacity is also plotted, assuming 2 amine groups are needed to bind 1 CO_2 molecule. Diaion® HP-2MG impregnated with 20 wt% of TEPA adsorbed 2.39 mol of CO_2 per kilogram sorbent. This corresponds to an amine efficiency of 0.45 mol CO_2 per mole N_2 which is typical for these kind of sorbent materials. For all sorbent types, the CO_2 capacity was found to be a strong function of the sorbent amine loading. From Figure 3, it becomes clear that large pores are favorable for achieving high CO_2 capacities, most probably due to better accessibility of the active amine molecules. It is hard to conclude the effect of pore size and pore volume on the position of the optimum in amine loading based on the presented data.

However, the amine loading at which an optimum in sorbent capacity is observed seems to correlate with the support pore volume; the higher the pore volume of the support material, the higher the optimal amine loading. Impregnation of CARiACT Q-3 porous particles, with an average pore size of 3 nm, resulted in sorbents having almost no CO_2 capacity. On the other hand, both Davisil® grade 646 and CARiACT Q-10 sorbents, having larger pores, achieved CO_2 capacities up to 2.4 and 2.2 mol/kg respectively. In this study, Davisil® grade 646 (37 wt%) with an average pore size of 15 nm was identified as the best performing silica based sorbent. The polymer based Diaion® HP-2MG (17nm pores) sorbents clearly outperformed all silica based sorbents achieving CO_2 capacities up to 3.8 mol/kg. Although a few sorbents have been reported [7] that perform better in terms of capacity, the CO_2 capacities reported here suffice to reach the target set for

the operating capacity in the process analysis study presented in Chapter 1. Moreover, as mentioned in Chapter 1, increasing the sorbent operating capacity further, will not result in a large reduction in the thermal energy requirement of the capture process. Therefore, from an energy point of view, a further improvement of the CO_2 capacity was not our first priority.

Since, the nature of the support material of the Diaion® HP-2MG (PMMA) based sorbents compared to the Davisil® grade 646 (Silica) based sorbents is completely different, sorbent characteristics like fluidization behavior might also be different. Selecting sorbent material at this stage, based solely on capacity, seemed premature. Both Davisil® grade 646 (37 wt%) and Diaion® HP-2MG (38 wt%) possess reasonable CO_2 capacities compared to the calculated stoichiometric capacity and good uptake rates. Therefore, both sorbents were further tested over a wide range of conditions for their CO_2 capacity to identify the operating window of the adsorption process.

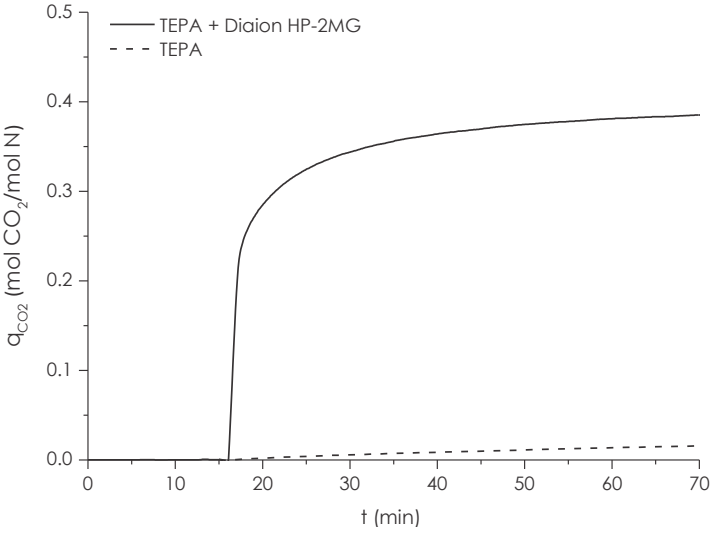

Figure 1: CO_2 uptake curves for TEPA, the support material Diaion® HP-2MG and the TEPA impregnated Diaion® HP-2MG (15 vol% CO_2, 85 vol% N_2, 40˚C, P_{total}=1 bar).

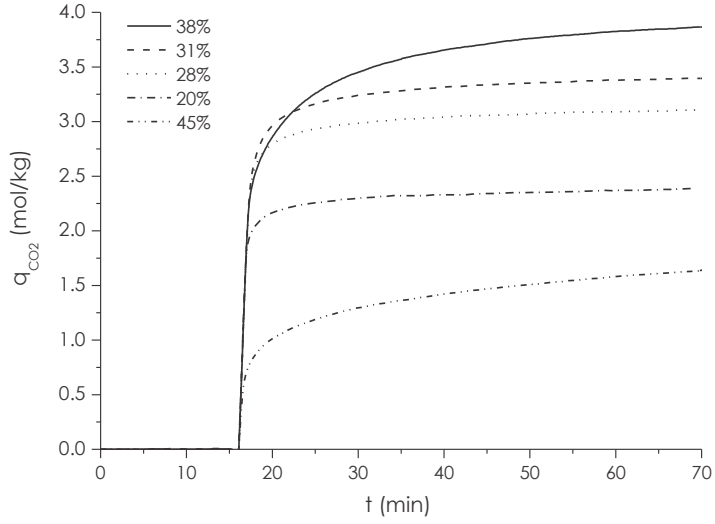

Figure 2: CO_2 uptake curves for Diaion® HP-2MG based sorbents for different wt% of amine loadings (CO_2 capacity tested using 15 vol% CO_2, 85 vol% N_2, 40˚C, P_{total}=1 bar).

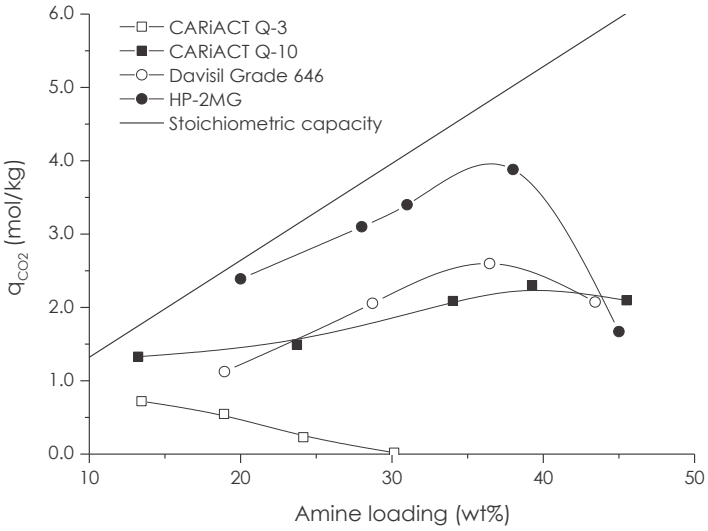

Figure 3: CO_2 adsorption capacity as a function of amine loading for CARiACT Q-3, Q-10, Davisil® grade 646 and Diaion® HP-2MG as support material (CO_2 capacities tested using 15 vol% CO_2, 85 vol% N_2, 50 min adsorption time, 40˚C, P_{total}=1 bar).

3.2 | On the effect of temperature and CO_2 pressure

The experiments performed in the TGA apparatus provide the CO_2 adsorption capacities at different adsorption temperatures and CO_2 partial pressures. This allows us to evaluate the cyclic capacity of the sorbent materials under different adsorption and regeneration conditions.
In Figures 4, 5 and 6, adsorption isobars are presented for Davisil® grade 646 (37 wt%), Diaion® HP-2MG (38wt%) and Lewatit® VP OC 1065. The sorbent sample was heated from 40˚C up to 140˚C at a heating rate of 0.1 ˚C/min in 1 vol%, 10 vol%, 14 vol% and 80 vol% CO_2 atmosphere (balance N_2) at a total flow rate of 100 ml/min. CO_2 adsorbed at 40˚C gradually desorbs with an increase in temperature due to a shift in chemical reaction equilibrium.

These slow heating rates provide sufficient time for the adsorption process to approach equilibrium. From Figure 2, 98% of the adsorption process is completed within the first 30 min of the adsorption time. In this time frame, with a heating rate of 0.1˚C/min, the temperature will increase by only 3˚C. Therefore, these measurements are expected to give a good indication of the equilibrium capacity although the effects of internal mass transfer limitations and reaction kinetics are still to some extent reflected in Figure 4 as a slight increase in CO_2 capacity with increasing temperature for the Davisil® grade 646 (37 wt%) sorbent. These effects seem less dominant in case of the Diaion® HP-2MG based sorbent (Figure 5). This could be associated with the larger pore size of the Diaion® HP-2MG based sorbent.

Two important observations can be made based on the isobars presented in Figures 4, 5 and Figure 6. Firstly, the tested sorbent materials possess high CO_2 capacities even at low CO_2 partial pressures. This makes them very suitable for CO_2 capture from gas fired power plants, where flue gas CO_2 concentrations are around 4 vol%, and are much lower than in flue gas from coal-fired power plants (~12 vol%). Moreover, CO_2 capture from gas streams with even lower CO_2 partial pressures, can also be considered. Although this is not the main focus of this thesis, the application of supported amine sorbents for air capture purposes was studied as well [8-10].
The second observation is related to the selection of the most suitable regeneration method for supported amine sorbents. For applications in post-combustion CO_2 capture, it is critical to regenerate the sorbent material in such a way that the CO_2 is released at a high purity (>95%). This high purity places restrictions on the sorbent regeneration method and three viable options are considered in literature: (1) the use of steam (or another easily condensable gas) as sweep gas to regenerate the sorbent material via

a combined pressure/thermal swing, (2) a vacuum/thermal swing regeneration or (3) regeneration of the sorbent in pure CO_2 at atmospheric, or preferably higher than atmospheric pressures [11], using a temperature swing. It should be noted that applying a vacuum swing [1] or steam regeneration [12] without a temperature swing will not result in a sufficiently high working capacity. Even at low CO_2 partial pressures as low as 1 kPa, the adsorption capacity of the sorbents is considerable due to the steep adsorption isotherms and this limits the working capacity in a pure pressure swing process.

The first option is very similar to the regeneration method used in the MEA based process. The use of steam as a sweep gas and the use of a vacuum swing both allow lower regeneration temperatures since the effective CO_2 partial pressure in the sorbent regeneration step is lowered. This is beneficial for the sorbent stability as well as the heat demand of the system. However, from Figures 5 and 6 we see that the temperature required for sorbent regeneration in 80 vol% CO_2, is ~135˚C, only ~20˚C higher than the temperature required for sorbent regeneration in 10 vol% CO_2, which is ~115˚C. This means that, on a process scale, lowering the CO_2 partial pressure during sorbent regeneration from 0.8 bar to 0.1 bar, by implementing vacuum regeneration or steam regeneration, would only result in minor savings (~20%) in thermal energy. Hence, there is not much benefit to be gained from combining a thermal swing with a pressure swing.
There are additional disadvantages of using a vacuum swing or steam regeneration. In a vacuum swing, process electricity is needed to run the vacuum equipment which is in general more expensive than (waste) heat. In a steam sweep, a considerable amount of steam is required to lower the CO_2 partial pressure to below 0.1 bar. This steam has to be generated and also condensed again to separate it from the capture CO_2 to produce a high purity CO_2 product stream. Consequently, thermal swing adsorption using CO_2 as regeneration gas in the desorber column seems to be the best option for regeneration of these type of sorbents, when compared to steam regeneration or vacuum swing adsorption.

In Figure 7, the working capacity is plotted as a function of the regeneration temperature for Davisil® grade 646 (37 wt%), Diaion® HP-2MG (38 wt%) and Lewatit® VP OC 1065. The sorbent working capacity was calculated from the sorbent CO_2 uptake from gas containing 10vol% of CO_2 at an adsorption temperature of 40˚C and regeneration of the sorbent in 80 vol% CO_2. At the selected adsorption conditions Davisil® grade 646 (37 wt%) and Diaion®

HP-2MG (38 wt%) adsorb 2.2 and 3.5 mol/kg sorbent respectively. Lewatit® VP OC 1065 adsorbs 2.2 mol/kg under these conditions. The sorbent working capacity is calculated as the difference between the CO_2 capacity at the adsorption conditions mentioned above and the CO_2 capacity at elevated temperatures in 80 vol% CO_2 given by the adsorption isobars presented in Figures 4, 5 and 6.

On a process scale, higher working capacities will translate to lower solid circulation rates, which in turn results in a lower energy requirement as less sorbent needs to be heated from the adsorption temperature up to the desorption temperature per ton of CO_2 captured. At a regeneration temperature of 130˚C, working capacities of around 1.3 mol/kg sorbent can be achieved when using Davisil® grade 646 (37 wt%). Diaion® HP-2MG (38 wt%) is able to achieve a working capacity of 3.2 mol/kg at 140˚C. Lewatit® VP OC 1065 cyclically adsorbs 1.4 mol/kg at 140˚C.

Exposing the impregnated sorbent materials to temperatures above 130˚C leads to sorbent degradation as a result of (1) the loss of active amine material due to evaporation and (2) the undesired formation of urea [13]. Urea is more stable than the carbamate species formed in the reaction between CO_2 and amines at lower temperatures and this side-reaction influences the CO_2 capacity at higher temperatures. The formation of urea seems to be mainly of concern for the silica based sorbent. Here, the formation of urea is reflected by an apparent increase in capacity for the SiO_2 based sorbent when exposing it to CO_2 at high temperatures (Figure 4). Both the degradation as a result of the loss of active amine material due to evaporation as well as the undesired formation of urea are studied in more detail in section 3.3 of this chapter.

In this chapter the aim was to prepare sorbent materials with a working capacity of at least 1.5 mol/kg which is the minimum capacity required to achieve the desired energy savings (Chapter 1,section 3). Both Diaion® HP-2MG (38 wt%) and Lewatit® VP OC 1065 have cyclic capacities higher than this minimum; 3.2 mol/kg and 1.8 mol/kg, respectively, both measured at a regeneration temperature of 140˚C. We can now make a more accurate estimation of the energy required to capture CO_2 using these sorbent materials than the estimate presented in Chapter 1 of this thesis.
To do so, we also need an estimate for the reaction heat of these sorbent materials. Based on the experimental data presented in Figure 5 and 6, the isosteric heat of adsorption was estimated using the Clausius–Clapeyron

equation. The formation of urea affects the adsorption capacity of the silica based sorbent. Part of the CO_2 adsorbed on the silica based sorbent at higher temperatures is not adsorbed reversibly. Consequently, we cannot get a reliable estimate of the adsorption heat based on the adsorption data presented in Figure 4. The adsorption heat for Diaion® HP-2MG (38wt%) and Lewatit® VP OC 1065 were estimated to be 85 kJ/mol at a CO_2 loading of 2.5 mol/kg and 75 kJ/mol at a CO_2 loading of 1.5 mol/kg, respectively. Both values lie in the range typical for CO_2 adsorption by amine molecules [3, 12]. As a reference, MEA has an absorption heat of 89 kJ/mol [14].

Both sorbents have an estimated energy requirement that is significantly lower than values reported for the MEA based reference process. Although the benchmark process requires 3.7 GJ/t [15], switching to a supported amine based process could reduce this energy demand to around 2.2 GJ/t of CO_2 mainly due to the reductions in the sensible heat energy penalty of the CO_2 capture process. This clearly shows that there is incentive to further develop this sorbent technology. In these calculations it was assumed that 75% of the sensible heat required for heating the sorbent material can be recovered indirectly or directly in a solid-solid heat exchanger.

It should be noted that this is still a preliminary energy estimate. Several issues should be investigated in more detail to increase its accuracy. One of the issues that deserves more attention is the possible co-adsorption of water in the adsorber column, which will be studied in the next chapter of this thesis. In addition, we should take into account that (1) the reaction heat is a function of the CO_2 loading [16] rather than a constant (2) a heat exchange efficiency of 75% might not be economically viable in a solid-solid heat exchanger and (3) other energy consumers in the capture process, like the flue gas blower, need to be taken into account when calculating the energy demand of the capture plant. A more complete evaluation will be presented in Chapter 6 of this thesis.

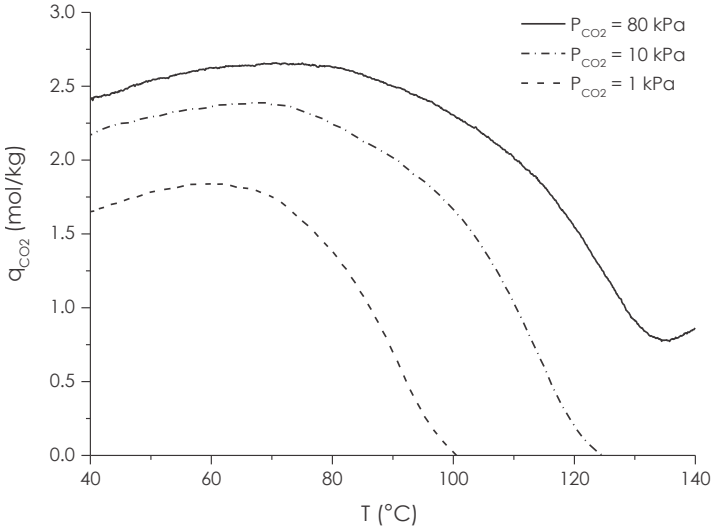

Figure 4: (Near-) Equilibrium CO_2 capacity as a function of temperature for Davisil® grade 646 (37 wt% of TEPA) (CO_2 capacities tested using 1 vol%, 10 vol%, 80 vol% CO_2, P_{total}=1bar)

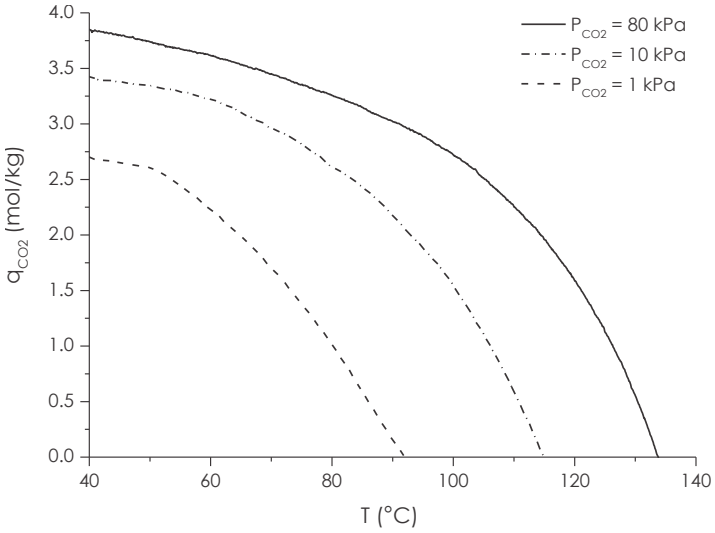

Figure 5: (Near-) Equilibrium CO_2 capacity as a function of temperature for Diaion® HP-2MG (38 wt% of TEPA) (CO_2 capacities tested using 1 vol%, 10 vol%, 80 vol% CO_2, P_{total}=1bar)

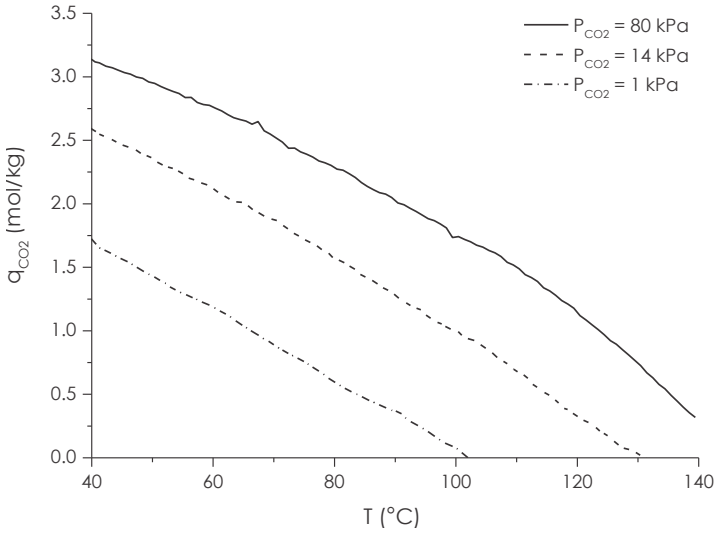

Figure 6: (Near-) Equilibrium CO_2 capacity as a function of temperature for Lewatit® VP OC 1065 (CO_2 capacities tested using 1 vol%, 14 vol%, 80 vol% CO_2, P_{total}=1bar)

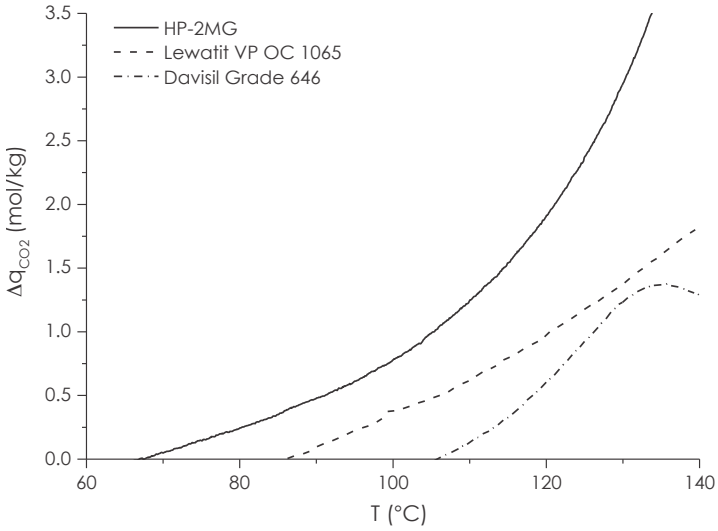

Figure 7: Sorbent working capacity as a function of temperature for adsorption at 40˚C, 0.1 bar P_{CO2} and regeneration in 0.8 bar P_{CO2}.

3.3 | On the thermal & chemical stability

Several sorbent materials were exposed to N_2, CO_2 and instrumental air in the TGA apparatus at different temperatures and for different time durations. The capacity of the sorbent material was measured at the start and at the end of the measurement in order to quantify the loss in activity.
Table 2 shows the sample weight loss and the capacity loss as a consequence of exposure to N_2 at 130˚C for 10 hours. The TEPA based sorbent material lost 58% of its initial capacity after 10 hours of exposure to the N_2. This deactivation is mainly associated with the evaporation of amine. During the measurement, the sorbent loses 22% of its initial weight. Since the amine loading of this sorbent material is approximately 49 wt%, a 22% loss in weight corresponds to a 45% loss in active material. One method to limit amine evaporation, investigated here, is to increase the boiling point of the amine impregnated into the support pore space. Amines with higher boiling points have a lower tendency to evaporate. Indeed, the TEPA impregnated sorbent materials lose much more mass during 10 hours at the same conditions when compared with that of the PEI 600 and PEI 10K based sorbent materials.

Exposing the TEPA based Diaion® HP-20 sorbent to CO_2 at high temperatures also resulted in a loss of capacity. The degree of deactivation was similar to the deactivation found when exposing the sorbent to N_2, but here the mass lost by the sample was much lower than in the experiment wherein the sorbent was exposed to N_2 only. Most probably part of the deactivation observed here is attributed to the undesired formation of urea. This CO_2-induced deactivation is especially severe for the TEPA impregnated SiO_2 based sorbent material. This sorbent practically loses all of its initial activity after treating it with CO_2 at high temperature. Still, there is almost no weight loss observed for this sorbent.

From Table 2 and Table 3, it can be concluded that Lewatit® VP OC 1065 is the most stable sorbent material tested here. The stability of Lewatit® VP OC 1065 was investigated under more severe conditions. The exposure time was increased to 50 hours and temperatures up to 200˚C were tested. No thermal deactivation was observed for temperatures lower than 150˚C, whereas the TEPA based sorbent materials showed significant deactivation beginning at 130˚C. As mentioned in the introduction of this chapter, for impregnated amine sorbents, the interaction between the support and the amine molecules is of a physical nature, whereas Lewatit® VP OC 1065 has an amine group chemically bonded to its internal surface and hence we

also expect Lewatit® VP OC 1065 to have better thermal stability due to the strong amine support interaction.
As shown, the evaporation rates of the PEI 600 and PEI 10K based sorbents are much lower than that of the TEPA impregnated materials. However, increasing the molar weight of the active amine compound can only help to lower the deactivation rate by evaporation but does not completely solve the issue because these PEI's also have a vapor pressure and deactivation due to evaporation of amine material will occur.

As in the case of the impregnated sorbent materials, Lewatit® VP OC 1065 also suffers from CO_2-induced deactivation starting at temperatures above 100˚C (Table 3). However, there are ways to prevent this CO_2 induced deactivation. In work by Sayari et. al. [17], it was reported for MCM-41 based supported amines that urea formation can be completely reversed via hydrolysis of such groups. Adding small amounts of steam to the CO_2 regeneration gas already inhibits the formation of urea, thereby allowing deeper regeneration of the sorbent. Another method to prevent the CO_2 induced degradation of supported amine sorbents was proposed by the same research group [18]. Secondary and tertiary amines were found to be much more stable than primary amines, even up to temperatures as high as 200˚C, with respect to the undesired formation of urea. Designing a sorbent with secondary amine groups attached to its surface might significantly reduce the CO_2 induced deactivation. Although the formation of urea might be counteracted by adding moisture to the gas phase [17], the loss of amine material is more difficult to prevent.

The specific combination of elevated temperatures and an oxidative environment result in the fast deactivation of the sorbent material (Table 3). Although the O_2 concentrations in flue gas are limited to values of around 5 vol%, this fast O_2-induced deactivation places restrictions on the adsorption temperature.

Table 2: The sample weight loss and the capacity loss as a consequence of exposure to N_2 and 80 vol% CO_2 at 130˚C for 10 hours for several impregnated sorbent materials and for Lewatit® VP OC 1065.

Sorbent	Exposed to:	Weight loss (%)	Capacity loss (%)
TEPA on HP-20	N_2	22%	58%
PEI 600 on HP-20	N_2	2%	0%
PEI 10K on HP-20	N_2	1%	0%
Lewatit® VP OC 1065	N_2	0%	0%
TEPA on Davisil grade 646	80% CO_2 in N_2	4%	90%
TEPA on HP-20	80% CO_2 in N_2	13%	63%
Lewatit® VP OC 1065	80% CO_2 in N_2	1%	0%

Table 3: The CO_2 capacity after exposure to N_2, 80 vol% CO_2, and Air at different temperatures for 50 hours for Lewatit® VP OC 1065. The initial capacity of Lewatit® VP OC 1065 at 15 vol% and 40˚C is 2.15 mol/kg.

Temperature (˚C)	N_2 (Thermal)	80% CO_2 in N_2 (Thermal + Urea)	Air (Thermal + Oxidative)
50	2.15	2.15	2.13
80	-	-	1.53
100	2.15	2.22	1.32
150	2.17	1.77	-
200	1.33	0.91	-

4.0

Conclusion

In the work presented in this chapter, we have focused on evaluating the sorption performance of impregnated and grafted sorbent materials. Impregnated amine sorbents were prepared by physical 'wet'-impregnation of silica, styrene-divinylbenzene and polymethylmethacrylate (PMMA) with tetraethylenepentamine (TEPA) and polyethylenimine (PEI) and were studied for application in post-combustion CO_2 capture.

For these sorbent materials we found that:

- The CO_2 capacity of the impregnated sorbent materials is a strong function of amine loading and pore volume. Significant improvement of the sorbent CO_2 adsorption capacity was achieved by tuning these variables.
- Exposing the TEPA impregnated sorbent materials to temperatures above 130˚C leads to sorbent degradation as a result of (1) the loss of active amine material due to evaporation and (2) the undesired formation of urea.
- Impregnating the support materials with amine molecules with a higher molecular weight resulted in a significant improvement of the thermal stability compared to the TEPA based sorbents.

Overall we conclude that:

- Thermal swing adsorption using CO_2 as regeneration gas in the desorber column seems to be the strongest regeneration option for these type of sorbents, compared to steam regeneration and to vacuum swing adsorption.
- Whereas TEPA impregnated Diaion® HP-2MG (38 wt%) showed by far the highest CO_2 capacity, Lewatit® VP OC 1065 (grafted) showed an excellent thermal stability. Further experimental work will focus on this commercial sorbent material.
- Using the developed sorbent(s) we can potentially reduce the thermal energy requirement for CO_2 capture from 3-4 GJ/t to around 2.2 GJ/t.

The potential of supported amine sorbents for post-combustion CO_2 capture by thermal swing adsorption was clearly demonstrated. Concluding from the presented experimental work, these sorbents have the potential to outperform aqueous amine solutions on working capacity and energy efficiency and can effectively be applied in a thermal-swing adsorption process for the production of high purity CO_2.

Acknowledgement

This research has been carried out in the context of the CATO-2-program. CATO-2 is the Dutch national research program on CO_2 Capture and Storage technology (CCS). The program is financially supported by the Dutch government (Ministry of Economic Affairs) and the CATO-2 consortium partners.

References

1. Ebner, A.D., et al., Suitability of a solid amine sorbent for CO_2 capture by pressure swing adsorption. Industrial and Engineering Chemistry Research, 2011. 50(9): p. 5634-5641.
2. Veneman, R., Z.S. Li, J.A. Hogendoorn, S.R.A. Kersten, and D.W.F. Brilman, Continuous CO_2 capture in a circulating fluidized bed using supported amine sorbents. Chemical Engineering Journal, 2012. 207: p. 18-26.
3. Gray, M.L., et al., Parametric study of solid amine sorbents for the capture of carbon dioxide. Energy & Fuels, 2009. 23: p. 4840-4844.
4. Alesi, W.R. and J.R. Kitchin, Evaluation of a primary amine-functionalized ion-exchange resin for CO_2 capture. Industrial & Engineering Chemistry Research, 2012. 51(19): p. 6907-6915.
5. Xu, X., C. Song, J.M. Andresen, B.G. Miller, and A.W. Scaroni, Novel polyethylenimine-modified mesoporous molecular sieve of MCM-41 type as high-capacity adsorbent for CO_2 capture. Energy & Fuels, 2002. 16: p. 1463-1469.
6. Yue, M.B., Y. Chun, Y. Cao, X. Dong, and J.H. Zhu, CO_2 capture by as-prepared SBA-15 with an occluded organic template. Advanced Functional Materials, 2006. 16(13): p. 1717-1722.
7. Samanta, A., A. Zhao, G.K.H. Shimizu, P. Sarkar, and R. Gupta, Post-combustion CO_2 capture using solid sorbents: A review. Industrial and Engineering Chemistry Research, 2012. 51(4): p. 1438-1463.
8. Brilman, W., L. Garcia Alba, and R. Veneman, Capturing atmospheric CO_2 using supported amine sorbents for microalgae cultivation. Biomass and Bioenergy, 2013. 53: p. 39-47.
9. Brilman, D.W.F. and R. Veneman, Capturing atmospheric CO_2 using supported amine sorbents. Energy Procedia, 2013. 37: p. 6070-6078.
10. Smal, I.M., Q. Yu, R. Veneman, B. Fränzel-Luiten, and D.W.F. Brilman, TG-

FTIR measurement of CO_2-H_2O co-adsorption for CO_2 air capture sorbent screening. Energy Procedia, 2014. 63(0): p. 6834-6841.
11. Veneman, R., H. Kamphuis, and D.W.F. Brilman, Post-Combustion CO_2 capture using supported amine sorbents: A process integration study. Energy procedia, 2013. 37: p. 2100-2108.
12. Li, W., et al., Steam-stripping for regeneration of supported amine-based CO_2 adsorbents. Chemsuschem, 2010. 3(8): p. 899-903.
13. Drage, T.C., A. Arenillas, K.M. Smith, and C.E. Snape, Thermal stability of polyethylenimine based carbon dioxide adsorbents and its influence on selection of regeneration strategies. Microporous and mesoporous materials, 2008. 116(1-3): p. 504-512.
14. Kim, Y.E., et al., Comparison of carbon dioxide absorption in aqueous MEA, DEA, TEA, and AMP solutions. Bulletin of the Korean Chemical Society, 2013. 34(3): p. 783-787.
15. Sanchez Fernandez, E., et al., Thermodynamic assessment of amine based CO_2 capture technologies in power plants based on European Benchmarking Task Force methodology. Fuel, 2014. 129: p. 318-329.
16. Serna-Guerrero, R., Y. Belmabkhout, and A. Sayari, Modeling CO_2 adsorption on amine-functionalized mesoporous silica: 1. A semi-empirical equilibrium model. Chemical Engineering Journal, 2010. 161(1-2): p. 173-181.
17. Sayari, A. and Y. Belmabkhout, Stabilization of amine-containing CO_2 adsorbents: Dramatic effect of water vapor. Journal of the American Chemical Society, 2010. 132(18): p. 6312-6314.
18. Sayari, A., Y. Belmabkhout, and E. Da'na, CO_2 deactivation of supported amines: Does the nature of amine matter? Langmuir, 2012. 28(9): p. 4241-4247.

Chapter 03

Adsorption of H_2O and CO_2 on supported amine sorbents

This chapter is based on the following article:

Veneman, R., Frigka, N., Zhao, W., Li, Z., Kersten, S.R.A., Brilman, D.W.F., Adsorption of H_2O and CO_2 on supported amine sorbents, International Journal of Greenhouse Gas Control, 2015, 41, 268-275.

Abstract

In this work the adsorption of H_2O and CO_2 on Lewatit® VP OC 1065 was studied in view of the potential application of this sorbent in post combustion CO_2 capture. Both CO_2 and H_2O were found to adsorb on the amine active sites present on the pore surface of the sorbent material. However, whereas the interaction between CO_2 and the amine groups is chemical, the adsorption behaviour of H_2O on Lewatit® VP OC 1065 shows the characteristics of physical multilayer adsorption. The difference in interaction is also clearly reflected in the differences in the adsorption heat (ΔH_{H2O} = 43 kJ/mol, ΔH_{CO2} = 70-80 kJ/mol) and differences in the final capacity. The highest capacity observed for H_2O was 12.5 mole/kg (at a relative humidity (RH) of 95%). The highest CO_2 capacity observed was 2.8 mol/kg (303K, PCO_2 = 81 kPa). Due to these high H_2O capacities the sorbent material can adsorb practically all water that enters the adsorber column. This increases the total energy demand of the sorbent based post-combustion capture process with 40%. To prevent the co-adsorption of large quantities of water several options were analyzed using the adsorption isotherms obtained for CO_2 and H_2O. Lowering the dew point of the flue gas upstream of the adsorber was identified as the most viable option.

1.0

Introduction

Application of carbon capture and storage (CCS) at fossil fuel burning plants is, among alternatives, a technically feasible method to significantly reduce the global anthropogenic emission of CO_2. Using current available technologies, this would result in an increase in the cost of electricity (COE) by 40% mainly due to high cost of carbon capture [1]. This increase in COE is a major hurdle in deployment and the development of a more cost effective capture technology is a main objective in CO_2 capture research.

The conventional capture process utilizes a mixture of amine molecules, typically MEA, and water to selectively absorb CO_2 from flue gases. Already at low temperatures, CO_2 dissolves in this absorption liquid (or solvent). By contacting the CO_2 containing gas with this solvent in an absorber column, the absorption liquid 'captures' the CO_2. Subsequently, the liquid with the dissolved CO_2 is transported to a second column, the desorber. Here, the liquid is heated, which causes the solvent to release the CO_2 again. This results in a stream of pure CO_2, which is compressed and stored, while the regenerated solvent is pumped back to the adsorber column to capture more CO_2. The main cost factor of the process is the high energy demand, for a large part associated with heating the aqueous amine solution from the absorption temperature to the desorption temperature.

Applying supported amine (solid) sorbents may offer a low-cost capture technology as alternative. The operational costs associated with the thermal energy input of the amine scrubbing process make up around 44% of the total CO_2 capture costs. A large part of this energy requirement is associated with heating of the aqueous amine solution from the absorption temperature to the desorption temperature and with the evaporation of solvent in the desorber column. Replacing H_2O as solvent by a solid support greatly reduces the energy required for CO_2 capture as; (1) the evaporation of water is inhibited and (2) the energy required for heating the sorbent up to the desorption temperature is much lower due to the lower specific heat capacity of solid supports (0.7 kJ/kg/K at 298 K) compared to water (4.2 kJ/kg/K at 298 K).

Supported amine sorbents (SAS) consist of a high internal surface-area support (e.g. silica's, polymers, zeolites) with amine functional groups immobilized on or grafted to its surface [2]. The key strengths of this type of sorbents material include high CO_2 capacities [3], fast CO_2 uptake rates, a low heat of adsorption (63.2 kJ/mol [4]) and relatively mild regeneration conditions (373-423 K) compared to other chemical sorbents [5].
Supported amine sorbents are tolerant towards the presence of water in the CO_2 containing gas i.e. the CO_2 capacity does not degrade in presence of H_2O. In many cases H_2O was even found to promote the CO_2 capacity [2, 6-9]. This is an important strength of these type of sorbents since flue gas contains as much, if not more H_2O, than CO_2. Still, these sorbent materials also capture significant amounts of H_2O under conditions relevant for post-combustion CO_2 capture. Franchi et al. [8] reported H_2O adsorption capacities for DEA on pore expanded MCM-41 siliceous molecular sieves of 5.37 mol/kg at 28%RH, and Xu et al. [9] measured the adsorption capacity for polyethyleneimine on MCM-41 to be 2.45 mol/kg and 3.01 mol/kg at 26% relative humidity (RH) and at 31%RH, respectively. The sorption capacities reported for H_2O in these studies surpass the capacities measured for CO_2. Also other materials considered for applications in post-combustion capture as a sorbent or as support material (13X, silica supported amines, carbons, etc..) are all known to capture large quantities of H_2O under flue gas conditions [10].

In terms of sorbent stability, the process may benefit from the co-adsorption of some of the water present in flue gas. The presence of water during sorbent regeneration suppresses the undesired formation of urea [6, 11-14]. Drage et al. [13] observed CO_2 induced deactivation of a PEI impregnated silica supported amine sorbents at temperatures above 135˚C. The loss of adsorption capacity was attributed to the bonding of CO_2 into the PEI polymer through the formation of a urea type linkage. Sayari and Belmabkhout [6] reported that water vapor greatly improved the stability of these type of sorbent material. It was observed that the formation of urea could be completely be reversed by adding steam via hydrolysis of such groups. Even at relative humidities as low as 0.4% urea formation was strongly inhibited. Desorption was performed here using a N_2 as a sweep gas. Therefore, higher partial pressures of water might be needed to prevent urea formation in case the sorbent material was to be regenerated in an atmosphere containing higher concentrations of CO_2.
Although the adsorption of small quantities of water might prevent CO_2-induced sorbent deactivation, the adsorption of large quantities of water

could severely increase the energy demand of the process. In the desorber column temperatures are high and H_2O partial pressure are envisioned to be low [3]. Hence a large part of the co-adsorbed water will be released again in the desorber column. In that case, and in addition to the heat required to desorb the captured CO_2, also energy is required to release the co-adsorbed water, resulting in an increase in the heat demand for capture. The role of water in this process is complex, as the H_2O present in flue gas (1) interferes with the CO_2 adsorption mechanism [9] and affects (2) the sorbent stability [6, 11-14] as well as (3) the process energy demand. However, the number of studies on the H_2O adsorption by supported amine sorbents is limited. Moreover, there is not yet a clear strategy how to deal with the co-adsorption of water on a process scale.

In this work, we aim to (1) better understand how water adsorbs on the sorbent material, (2) investigate how the presence of water affect the CO_2 adsorption process and (3) identify the best strategy to handle H_2O in this sorbent based process i.e. minimize the impact of H_2O co-adsorption on capture costs. CO_2 and H_2O adsorption measurements will be performed under a wide range of conditions relevant for post-combustion CO_2 capture. Based on the experimental work, adsorption isotherm equations for both H_2O and CO_2 will be fitted and used as input for process energy calculations.

2.0

Problem analysis

Flue gas emitted by a coal fired power plant typically contains around 12.3 vol% of CO_2 and around 9.4 vol% of H_2O. The water is picked up by the flue gas in the desulphurization unit which is deployed in most new coal-fired power plants to remove the SO_2 present in the gas. The conventional desulphurization system uses a wet scrubber usually using a slurry of lime or limestone. The dewpoint of the gas leaving the scrubber is 320 K corresponding to a saturation level of 67 %RH at the flue gas outlet temperature (328 K). The flue gas temperature, pressure and composition is summarized in Table 1.

Table 1: Flue gas conditions [1].

General plant data	
Net plant power (MWe)	500
Flue gas flow rate (Nm^3/s)	535
Capture efficiency (%)	90
Flue gas pressure (kPa)	111.2
Temperature (K)	328
Flue gas molar composition (vol%)	
N_2+Ar	73.5
CO_2	12.3
H_2O	9.4
O_2	4.8

Ideally, the adsorption of water should be prevented or at least kept to a minimum. In order to get a better understanding of the impact of water adsorption on the energy demand and to identify ways to circumvent the co-adsorption of water, we consider the overall mass balance over the adsorber.

From the ratio of the working capacity of H_2O (Δq_{H2O}) over that of CO_2 (Δq_{CO2}) we can deduce that:

$$\frac{\Delta q_{H_2O}}{\Delta q_{CO_2}} = \frac{X_{H_2O} E_{H_2O}}{X_{CO_2} E_{CO_2}} \qquad (1)$$

In this equation, X_{H2O} and X_{CO2} represent the molar fractions of H_2O and CO_2 in flue gas and are both given in Table 1. E_{H2O} and E_{CO2} represent the fraction of the incoming H_2O and CO_2 that is captured by the sorbent inside the adsorber column. Typically 90% of the incoming CO_2 is captured inside the adsorber column. The value capture efficiency for H_2O is dependent on the sorbents' uptake rate for H_2O. A slow H_2O uptake rate would limit the fraction of water captured by the sorbent.

Based on equation 1 we can calculate that for a coal fired power plant, in the worst case, i.e. in case all of the incoming H_2O is adsorbed (E_{H2O}=1, E_{CO2}=0.9), the sorbent particles leaving the adsorber contain 0.85 mol of H_2O per mol of CO_2. From this ratio we can directly calculate the energy penalty associated with the co-adsorption of water and it is therefore an important parameter in the adsorption process. Co-adsorption of H_2O would add 0.8 GJ/t CO_2 captured to the total heat demand of the process, estimated at 1.9 GJ/t CO_2 [5, 15] (not including H_2O co-adsorption). This corresponds to a 40% increase in the thermal energy penalty due to water co-adsorption which we deem unacceptable. In this calculation a H_2O desorption heat of 40.7 kJ/mol was assumed (equal to the evaporation heat at 373 K). It should be noted that for gas fired power plants the energy penalty will be even much higher since there is almost twice as much water in the flue gas as carbon dioxide.

We have identified several ways to prevent the co-adsorption of large quantities of H_2O:

- Increasing adsorber temperature: Higher adsorber temperatures will lower the equilibrium capacity of H_2O which will in turn limit the working capacity of water. Since there is a large amount of heat released during CO_2 adsorption this will not require additional energy. The decrease in water capacity must then outweigh the concurrent decrease in CO_2 capacity
- Kinetics: In case the uptake rate of H_2O is much slower than the uptake rate of CO_2, the capture efficiency of H_2O will be lower than the capture efficiency of CO_2 thereby limiting the H_2O working capacity.

- Preventing the desorption of water in the desorber: If water is added to the regeneration gas, like in steam generation, and ensure the H_2O partial pressure in the desorber is high enough, the desorption of water could be prevented.
- Pre-conditioning of the flue gas: By lowering the X_{H2O} in the flue gas upstream of the adsorber column the maximum working capacity of water is significantly lowered.

We would like to note here that the development of a sorbent that captures almost no H_2O under high saturation levels of H_2O would indeed solve the issue. However, most of the materials currently considered for post-combustion capture purposes (13X, silica supported amines, carbons, etc..) are all known to capture H_2O under flue gas conditions. Hence, for these materials, process based solutions, like the ones mentioned above, are necessary.

In the experimental section of this work we will focus on establishing H_2O and CO_2 adsorption isotherms and evaluating the uptake rate of H_2O and CO_2 on the sorbent Lewatit® VP OC 1065. The isotherm data will serve as a basis for calculation of the process energy demand. In this work we set the, somewhat arbitrary, goal of capturing no more than 0.25 mol of H_2O per mol of CO_2 captured i.e. the working capacity of CO_2 should be at least 4 times higher than the working capacity of H_2O. This would increase the energy demand of the process with no more than 0.25 GJ/t of CO_2 captured which we deem acceptable.

3.0

Experimental section

3.1 | Material

The sorbent materials used in this study are Lewatit® VP OC 1065 (obtained from Lanxess) and PEI impregnated Diaion® HP-20 (Aldrich). Lewatit® VP OC 1065 is a polystyrene based ion exchange resin (IER) containing primary benzyl amine units [16]. The resins are spherical shaped beads with a diameter of around 0.7 mm. The materials' pore volume, pore surface area and average pore size are 0.27 cm^3/g, 50 m^2/g and 25 nm, respectively. The Diaion® HP-20 based sorbent material was prepared by physical impregnation of Diaion® HP-20 with polyethyleneimine (PEI) with an average molecular weight of 10000 g/mol. This PEI-10K was dissolved in 10 ml of ethanol and physically mixed with the porous support particles. After impregnation, the ethanol was evaporated leaving PEI dispersed on the internal and external surface of the support particle. The amine loading was controlled by controlling the amine concentration in the PEI/ethanol solution. The amine loading we aimed for was 35wt% based on earlier optimization work [3]. The structural characteristics of the support material is summarized in Table 2.

Table 2: Sorbent properties.

Sorbent	N content (mole/kg)	Pore volume (cm^3/g)	Pore size (nm)	Pore area (m^2/g)
Lewatit® VP OC 1065	6.7 [16]	0.27	25	50
HP-20-PEI10K-35	8.4	1.3*	26*	500*

*Value reported for support before impregnation

3.2 | CO_2 and H_2O capacity measurements

The experimental work focusses on measuring adsorption capacities for CO_2 and H_2O at temperatures and partial pressure relevant for post combustion CO_2 capture.

A NETSZCH STA 449 F1 Jupiter thermal gravimetric analyzer (TGA) was used to assess the CO_2 adsorption capacity of the sorbent material. In a typical adsorption experiment around 15 mg of sorbent was placed inside the TGA furnace. The sample was heated up to 80˚C in N_2 to desorb any pre-adsorbed CO_2 and moisture. The temperature was kept constant until the sample mass stabilized. Then, the sample was cooled down to the desired adsorption temperature after which CO_2 was fed to the TGA furnace. The uptake of CO_2 by the sorbent sample results in an increase in the sample mass. The sorbent CO_2 uptake, in mole/kg sorbent, was calculated from the weight change of the sample during adsorption. Typically, after 4 hours of adsorption time the change in the sample mass was minimal (<0.01 mol/kg/hr) and the measurement was stopped. The adsorption experiments were performed at different temperatures and CO_2 partial pressures to obtain the data required to construct an adsorption isotherm. Desired gas compositions were obtained by mixing high purity (grade 5.0) N_2 and high purity (grade 5.0) CO_2. The specific configuration of the TGA equipment limited the CO_2 concentration to a maximum of 80 vol% of CO_2 at 1 atm.

The H_2O adsorption capacity of the sorbent material was measured in a custom built packed bed reactor equipped with a gas saturation bubble column, two humidity meters and an infrared CO_2 gas analyzer (Figure 1). The humidity meters (Hygrosens FF-20MA-INT-TE0) continuously measured the temperature and relative humidity of the gas entering and leaving the reactor (detection range: T=-30-70˚C, RH=0-100%). The CO_2 analyzer (SIDOR, SICK MAIHAK) was used to monitor the CO_2 concentration in the outlet gas of the packed bed column (detection range: 0-15 vol%). Two JULABO F32 water baths were used to control the temperature of the adsorber and the temperature of the H_2O saturation columns. The CO_2 and H_2O concentrations in the column inlet gas were controlled by mixing a flow of high purity (grade 5.0) N_2 and a high purity (grade 5.0) CO_2 flow with a third pre-saturated flow of N_2. The flow rates were controlled using three BROOKS mass flow controllers. After mixing of the three gas flows the humidity of the gas was measured. All of the gas lines were heated to temperatures just above the dew point of the gas mixture to prevent condensation of H_2O in the gas lines.

In a typical H_2O adsorption experiment around 10 g of dried sorbent material was loaded into the column. After closing the reactor, the reactor was heated up to 80˚C while flushing the column with N_2 (500 ml/min) to desorb any remaining CO_2 and H_2O. The reactor was subsequently cooled and when the desired adsorption temperature was reached, the N_2 flush was stopped and the H_2O containing gas (500-1000 ml/min) was fed to the column. The experiment was stopped when the inlet partial pressure of H_2O was equal to the outlet partial pressure of H_2O within the error margin of the humidity meters. CO_2/H_2O co-adsorption experiments were performed in a similar manner.

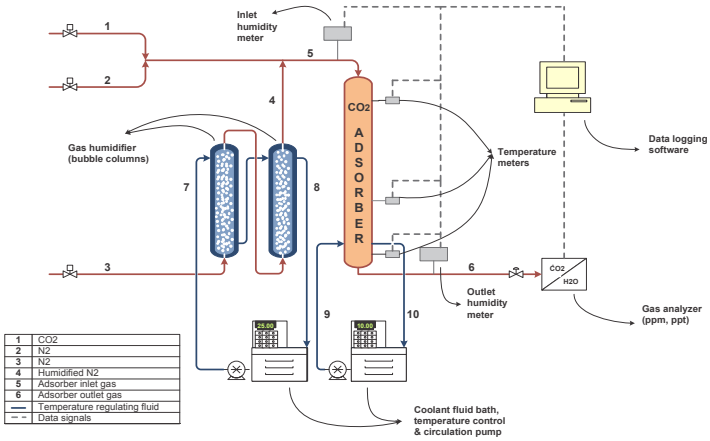

Figure 1: Schematic of the fixed bed set-up

4.0

Results

4.1 | Equilibrium adsorption capacities of CO_2

The experimental results obtained from the TGA apparatus provided CO_2 adsorption capacities at different adsorption temperatures and CO_2 partial pressures. Figure 2 shows the measured adsorption isotherms at 303 K, 313 K, 343 K, 353 K and 373 K for CO_2 on Lewatit® VP OC 1065. The CO_2 highest capacity observed in the measurements performed was 2.8 mol/kg resin measured at 303 K in 80 vol% of CO_2. Alesi and Kitchin [16] reported that the maximum theoretical amine loading is expected to be in the order of 6.7 mol N/kg resin for this type of IER. A CO_2 loading of 2.8 mol/kg then corresponds to an amine efficiency of 0.42 mol CO_2 per mol N, which is typical for these kind of sorbent materials since under dry conditions two amine groups are required to bind one molecule of CO_2.

One of the most important parameters in this capture process is the sorbent's cyclic operating capacity. This parameter will for a large part determine the heat demand of the process. Especially the partial pressure of CO_2 and the temperature during sorbent regeneration have a large impact on this cyclic adsorption capacity. Since we are aiming here to produce a high purity CO_2 product gas, the sorbent will be regenerated in an atmosphere with a high CO_2 content. This regeneration method has our preference over alternative regeneration methods like vacuum swing adsorption or steam regeneration [3]. Under the adsorption conditions summarized in section 1 and sorbent regeneration at 150°C at a CO_2 partial pressure of 100 kPa, the sorbent material can cyclically capture 1.4 mol/kg based on the isotherm calculations.

We have used the Toth isotherm model to describe the CO_2 adsorption behavior of the sorbent material [17]. In Figure 3 the calculated CO_2 capacities based on the isotherm fit are plotted against the experimental CO_2 capacity at the specific temperature and CO_2 partial pressure. The model accurately describes the experimental data. The CO_2 capacity can be calculated within an error margin of +/-0.08 mol/kg. The isotherm parameters are listed in Table 3. One of the parameters in the Toth isotherm model is the isosteric heat of adsorption at zero coverage (ΔH in Table 3) [17]. At an ΔH value of 87 kJ/mol the isotherm equation has the best fit to the experimental data plotted in Figure 2. Based on the isotherm equations we now

can calculate the isosteric heat of adsorption using the Clausius–Clapeyron equation. Also for Lewatit® VP OC 1065 the adsorption heat decreases with an increase in CO_2 loading [17]. At a CO_2 capacity of 1.5 mol/kg we find a heat of adsorption of 75 kJ/mol. This values lies in the range typical for CO_2 adsorption by amine molecules [4, 7].

Table 3: Toth isotherm parameters of the adsorption of CO_2 on Lewatit® VP OC 1065 using 353 K as reference temperature.

Parameter	Value
t_0	0.30
b_0 (1/bar)	408.84
ns_0 (mol/kg)	3.40
χ	0
α	0.14
ΔH (J/mol)	86.7×10^3

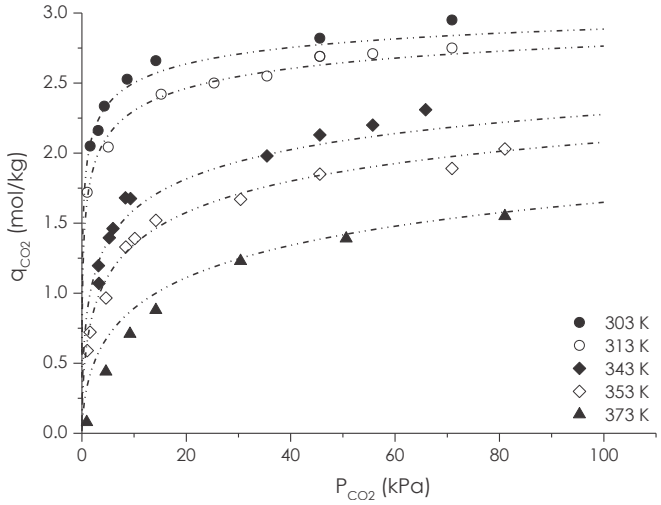

Figure 2: CO_2 adsorption isotherms for Lewatit® VP OC 1065 at 303 K, 313 K, 343 K, 353 K and 373 K. The lines represent capacities calculated using the equilibrium model.

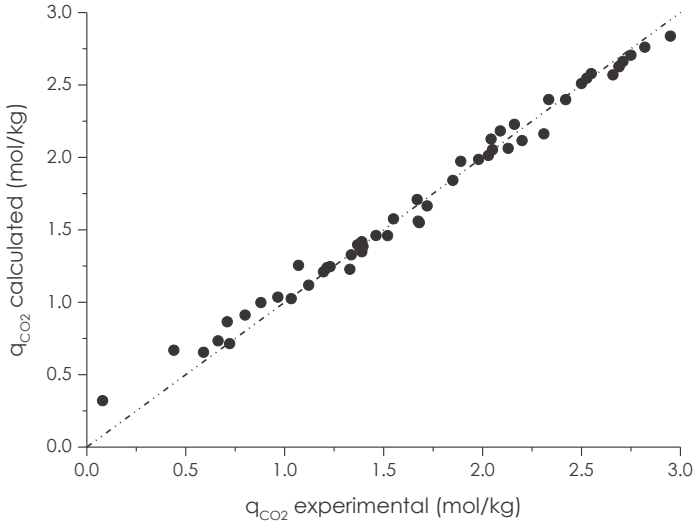

Figure 3: Parity plot in which the experimental CO_2 capacity of the sorbent is plotted against the capacity calculated using the equilibrium model at same partial pressure and temperature.

4.2 | Equilibrium adsorption capacities of H_2O

Figure 4 shows H_2O adsorption isobars for Lewatit® VP OC 1065. The highest observed H_2O sorption capacity for Lewatit® VP OC 1065 was 12.5 mol/kg at a P_{H2O}=2029 Pa and 291 K (RH=95%). At these high levels of saturation, water condenses inside the pores of the sorbent material and this high H_2O loading approaches the H_2O capacity for a completely filled pore space, being 14.4 mol/kg. However, analysis of the pore volume distribution showed that the sorbents' micropore volume was minimal (0.003272 cm^3/g) and more than 95% of the pore volume is attributed to pores larger than 10 nm. Hence, pore filling will most likely not be the main mechanism for H_2O uptake in the humidity range from 10%RH to 60%RH.

Based on the experimental data, the isosteric heat of adsorption was calculated using the Clausius–Clapeyron equation. The adsorption heat of 43 kJ/mol is close to the condensation heat of water. The enthalpy of vaporization of water ranges from 44.0 kJ/mol at 298 K to 40.7 kJ/mol at 373 K.
In Figure 5, the data points presented in Figure 4 are plotted as a function of the relative humidity in the adsorption gas. From Figure 5 we see that the H_2O adsorption capacity for Lewatit® VP OC 1065 is mainly a function of the relative humidity in the gas phase. This behavior was also observed for HP-20-PEI10K-35 (Figure 6). This points towards multilayer adsorption behavior of water on these sorbent materials. In the derivation of the BET multilayer adsorption isotherm one of the assumptions is that adsorbed molecules in the second and higher adsorption layers behave liquid like. Consequently, the heat of desorption for molecules in these layers is equal to the evaporation heat of the adsorbed molecule and the adsorbed amount is a function of the relative pressure of the adsorbate in the gas. The adsorption behavior of water on the tested sorbent materials is in line with what we would expect based on theory.

The adsorption behavior of H_2O on polymeric resins with a poly (styrene-divinylbenzene) matrix was investigated in literature. Lewatit® VP OC 1065 also has a styrene-divinylbenzene based backbone. These type of materials were found to have a very limited H_2O capacity (<1 mol/kg) at relative humidities lower than 60%RH [18, 19] due to the hydrophobic nature of the material. Also we have found that HP-20, a styrene-divinylbenzene based material, possesses a very limited H_2O capacity even at high relative humidities (Figure 6). However, after impregnation with PEI the H_2O adsorption capacity of the material increased dramatically. While before impregnation adsorption capacities were smaller than 1 mol/kg, after impregnation ca-

pacities up to 15 mol/kg were measured. Based on these experiments we conclude that the high H_2O capacities as observed for Lewatit® VP OC 1065 and HP-20-PEI10K-35 can be attributed to the presence of amine groups on the pore surface increasing the sorbent's affinity towards the adsorption of water.

Clearly, the interaction between the H_2O and the amine groups is different from the interaction between CO_2 and the amine groups. The first is more physical while the latter is chemical. This difference is also reflected in the differences in adsorption heat (ΔH_{H2O} = 43 kJ/mol, ΔH_{CO2} = 70-80 kJ/mol) and in capacity (CO_2/N=0.42, H_2O/N=2.5). However, since both molecules are attracted by the same sites, it is interesting to investigate how these molecules interfere with each other in the adsorbed phase. This will be discussed further in paragraph 4.3.

Figure 7 shows the H_2O adsorption capacity of Lewatit® VP OC 1065 compared to other sorbent materials studied for their application in post combustion CO_2 capture. The adsorption capacities of DEA on pore expanded MCM-41 [8] and PEI on MCM-41 [9] were plotted in the same graph as well as the H_2O sorption capacity of Zeolite 13X and SiO_2 gel.
The adsorption capacities of DEA on pore expanded MCM-41 (5.37 mol/kg at 28%RH, [8]) and PEI on MCM-41 (2.63 mol/kg and 3.24 mol/kg at 26%RH and 31%RH, respectively, [9]) are in the same order of magnitude as the capacities measured for the IER and also both well above the targeted working capacity, even at relatively low saturation levels of around 30%RH. The adsorption capacities observed for Zeolite 13X under the same conditions are even higher than that of Lewatit® VP OC 1065 and the MCM-41 based supported amine sorbents shown in the graph. Especially at relative humidities below 60%RH, Zeolite 13X shows much higher adsorption capacities for water than the sorbent studied here. This is most probably attributed to the smaller pore sizes of 13X, compared to the sorbent studied here, in which pore filling occurs at lower relative humidities.

The dewpoint of flue gas is around 47˚C before entering the adsorber column, which corresponds to a saturation level of 67%RH at the gas inlet temperature. Under these conditions this sorbent material is capable of adsorbing around 8 mol H_2O/kg. This means that Lewatit® VP OC 1065 can adsorb far more H_2O than CO_2 under conditions relevant for post-combustion CO_2 capture.

These high saturation capacities lead to the following important conclusion regarding the co-adsorption of water in the sorbent based process. The adsorption of H_2O in the adsorber column of the post combustion capture process is not limited by the equilibrium capacity of the sorbent material under adsorption conditions. Instead, the H_2O working capacity is supply limited, i.e. the sorbent will adsorb practically all H_2O entering the column, given there is enough contact time. This is not only true for this particular sorbent. Any sorbent with a H_2O capacity higher than its CO_2 capacity will adsorb practically all water entering the adsorber. This includes also Zeolite 13X.

Increasing the adsorber temperature was identified as one of the potential solutions in section 2 to lower the amount of water adsorbed. Concluding from Figure 2 and 5, a higher adsorption temperature significantly lowers the H_2O capacity and consequently the sorbent adsorbs much less water per mole of CO_2 adsorbed. The ratio of the equilibrium capacity of H_2O over that of CO_2 drops from 3.4 mol H_2O per mol of CO_2 at flue gas inlet conditions (P_{H2O}=10452 Pa, P_{CO2}=13677 Pa, T =328 K) to 1.6 at 373 K. But even at 373 K the sorbent adsorbs much more water than the targeted amount (0.25 mol of H_2O/mol of CO_2). Higher temperatures will not improve the selectivity of the sorbent further as at higher adsorption temperatures the CO_2 capacity is lower as well. Hence increasing the adsorption temperature does not seem like a viable option to prevent the co-adsorption of large amounts of water.

Adding water to the regeneration gas, like in steam regeneration, could prevent the desorption of the adsorbed water. If the relative humidity in the desorber is equal to the relative humidity in the adsorber the water will, in theory, not desorb. However, this would require a large amount of steam to be effective since achieving a relative humidity of 67%RH (i.e. the relative humidity of the incoming flue gas) under regeneration conditions requires a much higher partial pressure of H_2O than under adsorption conditions. Moreover, as can be seen from Figure 2, there is no large benefit from lowering the CO_2 partial pressure in the regenerator i.e. it will not yield a much higher sorbent working capacity as under regeneration conditions the CO_2 capacity is not a strong function of the CO_2 partial pressure.

As briefly discussed before, the development of a sorbent that does not bind water would solve the issue entirely. However, since we now know that the presence of amine groups causes the affinity of supported amine sor-

bents towards the adsorption of H_2O, it will not be easy to develop a supported amine sorbent with a H_2O capacity that is low enough to achieve the energy target set in the section 2.

In this work we set the goal of capturing no more than 0.25 mol of H_2O per mol of CO_2 captured. The working capacities for supported amine sorbents are typically in the order of 2 mol per kilogram sorbent. Now we can calculate that, according to equation 1, the equilibrium capacity of the sorbent material we are looking for should not be able adsorb more than 0.5 mol of water per kilogram sorbent in the relative humidity range of 60-90%. The sorbent material evaluated here can adsorb close to 4 times more H_2O than CO_2 under flue gas conditions (q_{H2O} at 67%RH=7.5 mol/kg, q_{CO2} at 12.3 vol% and 328 K is 2.0 mol/kg). This means that the water capacity of the sorbent material tested here has to be reduced with a factor 16 in order to achieve the target set in section 2.

Still there might be promising routes to reduce the affinity of supported amines towards the adsorption of H_2O. For instance, it might be interesting to bind a secondary amine to the internal surface of the support structure instead of the primary amine that is bonded to the internal surface of Lewatit® VP OC 1065. This secondary amine could have a hydrophobic group as a side chain to create a more hydrophobic surface. This is however outside of the scope of this paper.

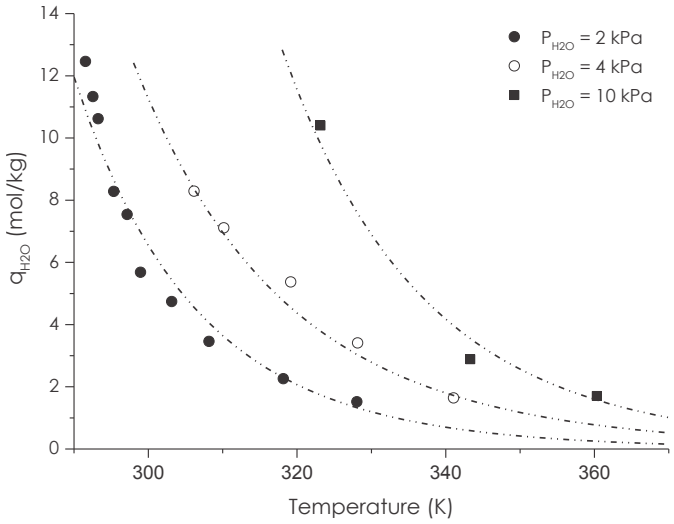

Figure 4: H_2O adsorption isobars for Lewatit® VP OC 1065 at H_2O partial pressures of 2 kPa, 4 kPa and 11 kPa, respectively.

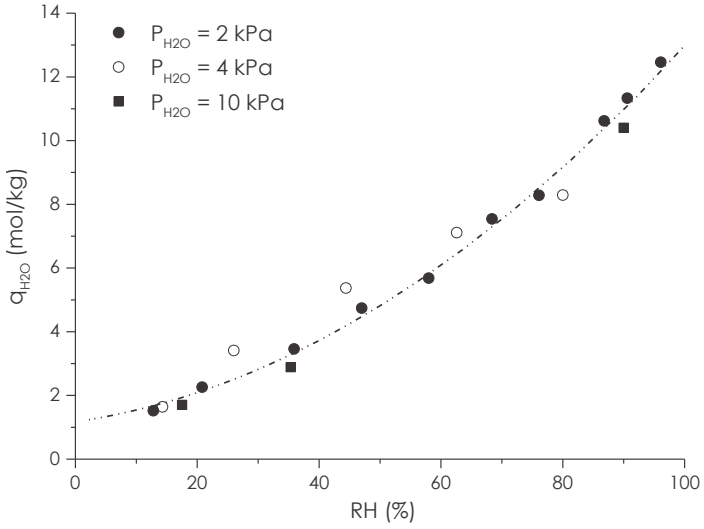

Figure 5: H_2O adsorption capacity of Lewatit® VP OC 1065 plotted against the relative humidity in the gas phase.

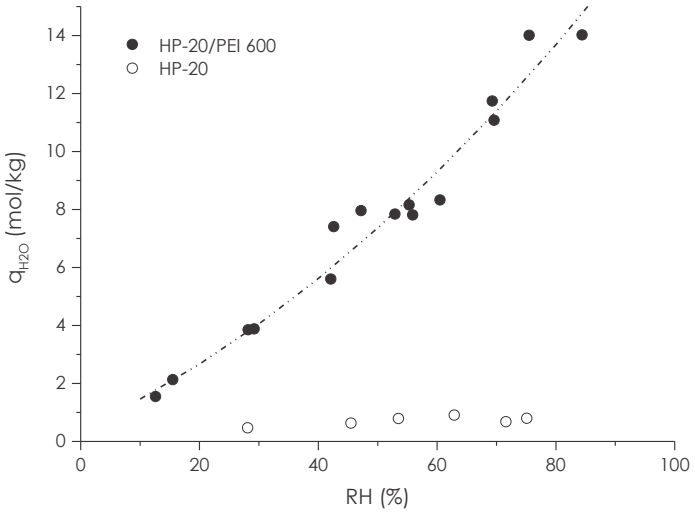

Figure 6: H_2O adsorption capacity of HP-20-PEI10K-35 and HP-20 plotted against the relative humidity in the gas phase.

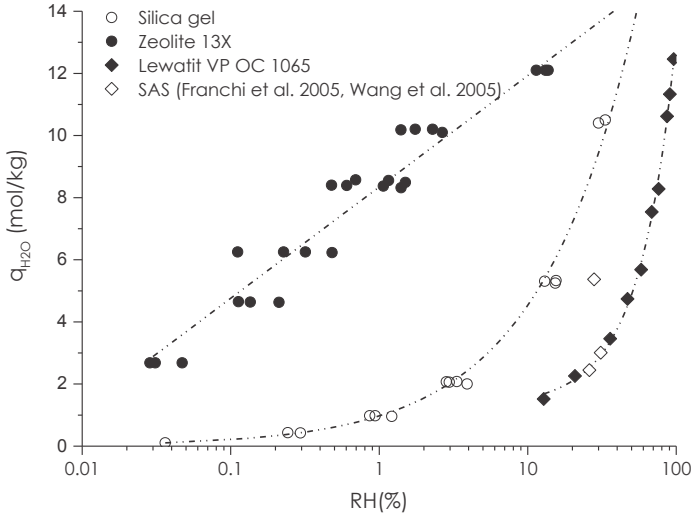

Figure 7: H_2O capacity as a function of the relative humidity for Zeolite 13X, silica gel, Lewatit® VP OC 1065 and sorbents prepared by Franchi et al. [8] and Xu et al. [9].

4.3 | Adsorption of CO_2 in presence of H_2O

Subsequently, the simultaneous adsorption of CO_2 and H_2O is studied. The sorbent was contacted with gas containing CO_2, H_2O and N_2 and fixed bed breakthrough curves were measured for both CO_2 and H_2O. Figure 8 shows the CO_2 adsorption capacity of Lewatit® VP OC 1065 measured in these experiments as a function of the relative humidity in the gas phase. Figure 9 shows the H_2O capacities measured in these experiments.

In Figure 9 we see that the H_2O capacity seems largely unaffected by the co-adsorption of CO_2. Still, the adsorbed H_2O could influence the sorption of CO_2 through for example physical interaction between CO_2 and H_2O or shielding of amine active sites by H_2O. Figure 8 shows the CO_2 adsorption capacities for Lewatit® VP OC 1065 under dry and humid conditions. The presence of water does not seem to have a detrimental effect on the CO_2 capacity; the measured CO_2 capacities are even significantly higher in the experiments with water present. This phenomenon has been noticed before for supported amine sorbents [8, 20-22] and is usually attributed to the interference of H_2O in the adsorption mechanism. Water can act as a free-base, resulting in the formation of bicarbonate ions in the presence of water, whereas carbamate is formed when water is not present. This changes the reaction stoichiometry; in the presence of water one amine group could theoretically react with one CO_2 molecule, whereas two amine molecules are required to bind one molecule of CO_2 under dry conditions. Alesi and Kitchin [16] applied in-situ DRIFTS IR to study the nature of the groups formed during the adsorption of CO_2 by Lewatit® VP OC 1065. They confirmed the formation of both carbamate- and bicarbonate groups during the adsorption process. At higher relative humidities it seems that more carbamate groups are converted to bicarbonate groups and the effect of H_2O on the CO_2 capacity becomes more apparent.

Concluding from the co-adsorption experiments performed we found that the adsorption of H_2O is not significantly slower that the adsorption of CO_2. This does not come as a surprise. Mass transfer rates to and in the sorbent particle are comparable for both adsorbates and physical adsorption processes are in general fast compared to chemical adsorption processes. Consequently, the process does not benefit from a kinetic selectivity of CO_2 over H_2O.

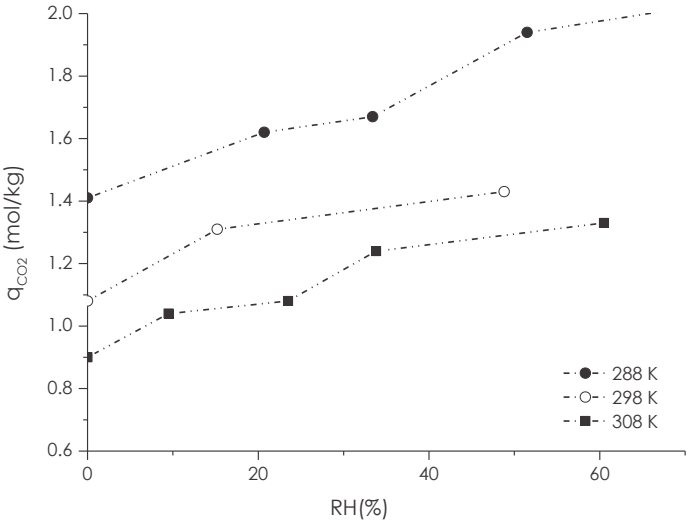

Figure 8: CO_2 adsorption capacity of Lewatit® VP OC 1065 as a function of the relative humidity in the feed gas at three different temperatures (P_{CO2} = 40 Pa).

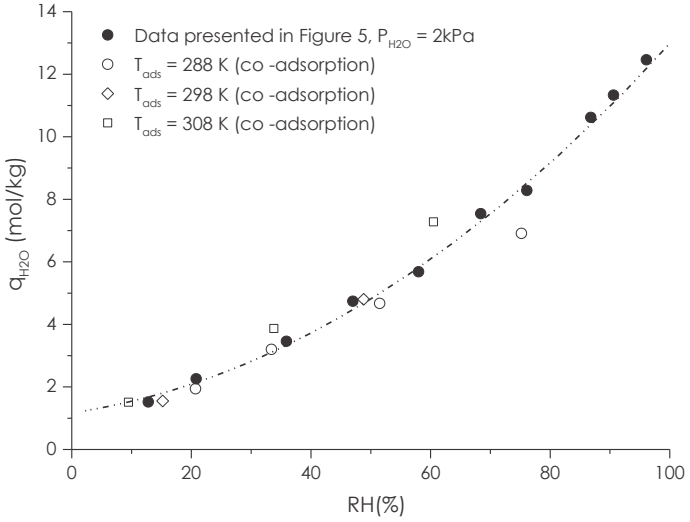

Figure 9: H_2O equilibrium capacities for Lewatit® VP OC 1065, with and without CO_2 present, at varying relative humidity (RH%).

4.4 | Energy penalty

Concluding from the experimental results presented here, the sorbent particles have a high affinity towards the adsorption of water. Consequently the sorbent material will capture significant amounts of H_2O in the adsorber when applied in post-combustion CO_2 capture. This could lead to an increased energy demand of the process. Conditioning of the flue gas upstream of the adsorber will prevent this co-adsorption of large amounts of water. Effectively the dewpoint of the incoming flue gas should be lowered (e.g. by condensation), to remove the major part of the water present in the flue gas.

By lowering the dew point of the incoming gas from 47˚C to 30˚C, the amount of water adsorbed can be lowered from 0.85 to 0.25 mol of H_2O per mol of CO_2. For Lewatit® VP OC 1065, the desorber energy demand is then lowered from 3 GJ to 2.6 GJ per ton of CO_2 captured. The 2.6 GJ per ton heat demand includes 0.25 GJ for desorption of co-adsorbed H_2O, 1.8 GJ for the desorption of CO_2 and 0.5 GJ for the heating of the sorbent material from the adsorption temperature (328 K) to the desorption temperature (423 K). In the calculations we have assumed that 75% for the sensible heat can be exchanged between the hot and the cold solid particles. In these calculations we have also assumed a solid heat capacity of 1.5 kJ/kg/K. The H_2O desorption heat of 43 kJ/mol and a CO_2 desorption heat of 78 kJ/mol (at q_{CO2}=0.5 mol/kg) were calculated based on the adsorption data as mentioned earlier. The sorbent working capacity was calculated based on the presented data as well.

The cooling duty required to lower the temperature of the flue gas and to condense the water is 0.74 GJ per ton of CO_2 captured, in addition to the 2.6 GJ of heat required to desorb the captured CO_2. This cooling duty can be supplied by relatively cheap cooling water, whereas co-adsorbed water is desorbed in the desorber column using steam extracted from the power plants steam cycles. At a cooling water price of $0.8 per GJ cooling duty and a low pressure steam price of $ 6.6 per GJ heat duty, handling water in the process would add $2.3 per ton of CO_2 to the total capture costs [23]. These calculations do not include costs associated with the capital investment for the cooler/condenser.

5.0

Conclusions

In this work we have evaluated the H_2O and CO_2 adsorption characteristics of Lewatit® VP OC 1065 in view of the potential application of solid sorbents in post combustion CO_2 capture at a coal-fired power plant. It was found that:

- Under flue gas conditions this sorbent material adsorbs much more H_2O than CO_2. Consequently, this sorbent material will adsorb all water present in the flue gas.
- H_2O does not seem to compete with CO_2 for active sites but does interfere in the adsorption process of CO_2. The presence of H_2O enhances the CO_2 capacity.
- The presence of amine groups causes the high affinity of the sorbent towards the adsorption of H_2O. The development of an hydrophobic amine based sorbent material is therefore challenging.

A viable strategy to prevent the co-adsorption of large quantities of water is to lower the dewpoint of the incoming flue gas. This way the impact of water adsorption on cost can be effectively lowered. The co-adsorption of water is estimated to add $2-3 to the total costs for capturing one ton of CO_2.

Acknowledgement

This research has been carried out in the context of the CATO-2-program. CATO-2 is the Dutch national research program on CO_2 Capture and Storage technology (CCS). The program is financially supported by the Dutch government (Ministry of Economic Affairs) and the CATO-2 consortium partners.

References

1. Fisher, K.S., et al., Integrating MEA regeneration with CO_2 compression and peaking to reduce CO_2 capture costs, 2005.
2. Ebner, A.D., et al., Suitability of a solid amine sorbent for CO_2 capture by pressure swing adsorption. Industrial and Engineering Chemistry Research, 2011. 50(9): p. 5634-5641.
3. Veneman, R., Z.S. Li, J.A. Hogendoorn, S.R.A. Kersten, and D.W.F. Brilman, Continuous CO_2 capture in a circulating fluidized bed using supported amine sorbents. Chemical Engineering Journal, 2012. 207-208: p. 18-26.
4. Gray, M.L., et al., Parametric study of solid amine sorbents for the capture of carbon dioxide. Energy & Fuels, 2009. 23: p. 4840-4844.
5. Sjostrom, S. and H. Krutka, Evaluation of solid sorbents as a retrofit technology for CO_2 capture. Fuel, 2010. 89(6): p. 1298-1306.
6. Sayari, A. and Y. Belmabkhout, Stabilization of amine-containing CO_2 adsorbents: Dramatic effect of water vapor. Journal of the American Chemical Society, 2010. 132(18): p. 6312-6314.
7. Li, W., et al., Steam-stripping for regeneration of supported amine-based CO_2 adsorbents. Chemsuschem, 2010. 3(8): p. 899-903.
8. Franchi, R.S., P.J.E. Harlick, and A. Sayari, Applications of pore-expanded mesoporous silica. 2. Development of a high-capacity, water-tolerant adsorbent for CO_2. Industrial & engineering chemistry research, 2005. 44: p. 8007–8013.
9. Xu, X., C. Song, B.G. Miller, and A.W. Scaroni, Influence of moisture on CO_2 separation from gas mixture by a nanoporous adsorbent based on polyethylenimine-modified molecular sieve MCM-41. Industrial and Engineering Chemistry Research, 2005. 44(21): p. 8113-8119.
10. Wang, Y. and M.D. Levan, Adsorption equilibrium of carbon dioxide and water vapor on Zeolites 5A and 13X and Silica Gel: Pure components.

Journal of Chemical and Engineering Data, 2009. 54(10): p. 2839-2844.
11. Sayari, A., A. Heydari-Gorji, and Y. Yang, CO_2-induced degradation of amine-containing adsorbents: Reaction products and pathways. Journal of the American Chemical Society, 2012. 134(33): p. 13834-13842.
12. Sayari, A., Y. Belmabkhout, and E. Da'na, CO_2 deactivation of supported amines: Does the nature of amine matter? Langmuir, 2012. 28(9): p. 4241-4247.
13. Drage, T.C., A. Arenillas, K.M. Smith, and C.E. Snape, Thermal stability of polyethylenimine based carbon dioxide adsorbents and its influence on selection of regeneration strategies. Microporous and mesoporous materials, 2008. 116(1-3): p. 504-512.
14. Heydari-Gorji, A. and A. Sayari, Thermal, oxidative, and CO_2-induced degradation of supported polyethylenimine adsorbents. Industrial & Engineering Chemistry Research, 2012. 51(19): p. 6887-6894.
15. Veneman, R., H. Kamphuis, and D.W.F. Brilman, Post-Combustion CO_2 capture using supported amine sorbents: A process integration study. Energy procedia, 2013. 37: p. 2100-2108.
16. Alesi, W.R. and J.R. Kitchin, Evaluation of a primary amine-functionalized ion-exchange resin for CO_2 capture. Industrial & Engineering Chemistry Research, 2012. 51(19): p. 6907-6915.
17. Serna-Guerrero, R., Y. Belmabkhout, and A. Sayari, Modeling CO_2 adsorption on amine-functionalized mesoporous silica: 1. A semi-empirical equilibrium model. Chemical Engineering Journal, 2010. 161(1-2): p. 173-181.
18. Long, C., Y. Li, W.H. Yu, and A.M. Li, Adsorption characteristics of water vapor on the hypercrosslinked polymeric adsorbent. Chemical Engineering Journal, 2012. 180: p. 106-112.
19. Bardina, I.A., O.S. Zhukova, N.V. Kovaleva, and S.N. Lanin, The adsorption of H_2O and D_2O on porous polystyrene adsorbents. Russian Journal of Physical Chemistry A, 2007. 81(9): p. 1525-1531.
20. Su, F.S., C.Y. Lu, S.C. Kuo, and W.T. Zeng, Adsorption of CO_2 on amine-functionalized Y-Type zeolites. Energy & Fuels, 2010. 24: p. 1441-1448.
21. Hicks, J.C., et al., Designing adsorbents for CO_2 capture from flue gas-hyperbranched aminosilicas capable of capturing CO_2 reversibly. Journal of the American Chemical Society, 2008. 130(10): p. 2902-2903.
22. Hiyoshi, N., K. Yogo, and T. Yashima, Adsorption of carbon dioxide on amine modified SBA-15 in the presence of water vapor. Chemistry Letters, 2004. 33: p. 510.
23. Peters, M.S., K.D. Timmerhaus, and R.E. West, Plant design and economics for chemical engineers. 5th ed. McGraw-Hill chemical engineering

series. 2003, New York: McGraw-Hill. xvii, 988 p.

Chapter 04

Selection, modelling and design of a supported amine based CO_2 capture process

This chapter is based on the following article:
Veneman, R., Hilbers, T., Brilman, D.W.F., Kersten, S.R.A., CO_2 capture in a continuous gas-solid trickle flow reactor, submitted to Chemical Engineering Journal.

Abstract

This chapter focusses on the selection and design of an adsorber and desorber for adsorption-based post-combustion CO_2 capture using supported amine sorbents. This process selection and design study involves detailed modelling of the sorbent particle and the adsorber reactor.

Based on the particle model developed we can conclude heat transfer rates are not limiting the overall CO_2 uptake rate of the sorbent particles. Under typical flue gas conditions (T= 328 K, P_{CO2} = 0.137 bar), Lewatit® VP OC 1065 can be saturated with CO_2 in around 80 seconds.

With respect to the process configuration, we believe that solid circulation is essential. This will reduce the adsorption-desorption cycle time and in this way improve the volumetric productivity of the process. We selected a gas solid trickle flow reactor as the most suitable adsorber type as it provides counter current gas-solid contacting, and allows for high operating gas velocities, while the adsorber pressure drop is relatively low. A multistage fluid bed was selected as desorber. A staged fluid bed desorber combines good heat exchange characteristics with solid phase staging, which is essential to keep the required solids inventory in the desorber column to a minimum.

A full scale design of a gas solid trickle flow column for a CO_2 capture facility at a 500 MWe coal-fired power plant was presented as well. Capture efficiencies up to 90% can be achieved in a column of 13 meters high. The sorbent particles can attain 90% of their equilibrium capacity in this column. At these working capacities we expect a significantly lower process heat demand than in the conventional process; 2.3 GJ/t compared to 4 GJ/t for the conventional MEA based process. Moreover, it was found that the higher mass transfer rates in the adsorption column when compared to the mass transfer rates typical for MEA scrubbers allow for a more compact adsorber design. In comparison with the conventional technology, next to the energy savings, also the column size of the scrubber can significantly be reduced by 50-70%, when switching to a adsorption based process.

1.0

Introduction

The overall aim of this research is to reduce CO_2 capture costs by applying supported amine sorbents in a new post-combustion CO_2 capture process. This process is anticipated to have lower operational costs than the conventional amine scrubbing technology.

The operational costs associated with the thermal energy input of the amine scrubbing process make up around 44% of the total CO_2 capture costs. A large part of this energy is associated with heating of the aqueous amine solution from the absorption temperature to the desorption temperature and with the evaporation of solvent in the desorber column. Replacing H_2O as solvent by a solid support greatly reduces the energy required for CO_2 capture as; (1) the evaporation of water is inhibited and (2) the energy required for heating the sorbent up to the desorption temperature is much lower due to the lower heat capacity of solid supports compared to water. In addition to these savings on operational costs, we expect to save on capital costs as well. The cost of the absorber accounts for 40% of the total purchased equipment cost of the capture process. Application of supported amine sorbents could potentially reduce the size of the absorber column due to higher overall conversion rates expected in gas-solid systems. For conventional MEA scrubbers, overall mass transfer rates depend on the type of packing and are reported to be in the order of 10^{-2} to 10^{-1} (k_La, 1/s) [1] compared to gas-solid systems for which typical values are in the order of 10^{-1}-10^{0} (k_Ga, 1/s) [2]. Volumetric CO_2 uptake rates are thus expected to be higher in the sorbent based process which would reduce equipment size and hence capital cost.

The selection of a suitable contactor and process configuration will have an essential role in realizing the envisioned cost savings. However, reports on process design remain rare [3] and the impact of process design on the economic performance of the capture system is not yet clear. In this chapter we focus on the selection and design of the process technology required to facilitate adsorption-based CO_2, based on detailed particle and reactor modelling. In Chapter 5 the selected reactor will be tested at lab-scale and model predictions will be compared with experimental results. In Chapter 6, the economic performance of the process will be evaluated.

2.0

Design basis

The process design will be based on the use of Lewatit® VP OC 1065 sorbent particles, studied in Chapter 2 and 3. The performance of the adsorber will be compared with the performance of a typical MEA scrubber. The reactor performance comparison is based on a process evaluation study performed by Fisher et al. [4] for a MEA-based capture facility at a 500 MWe pulverized coal plant. The CO_2 capture system is designed to capture at least 90% of the CO_2 emitted by the coal-fired power plant. The power plant general data used in this study is presented in Table 1. The flue gas composition given in Table 1 represents the molar composition of the gas downstream of the wet flue gas desulphurization scrubber.

Table 1: Base case definition [4].

Net plant power (MWe)	500
Flue gas flow rate (m^3/s)	576
Capture efficiency (%)	90
Flue gas pressure (kPa)	111.2
Temperature (K)	328
Flue gas molar composition (vol%)	
N_2+Ar	73.5
CO_2	12.3
H_2O	9.4
O_2	4.8

Thermal swing desorption using CO_2 as the regeneration gas in the desorber was identified in Chapter 2 as a strong option for regeneration of these type of sorbents when compared to steam regeneration or vacuum swing adsorption. This thermal swing adsorption process consist of at least four basic steps; (1) selective adsorption of CO_2, (2) heating of the sorbent material, (3) desorption of CO_2 at elevated temperatures and (4) cooling of the sorbent material before starting a new sorption cycle. Depending on the process configuration, transportation of the solid material is required from the adsorption vessel to the desorption vessel and back. In the follow-

ing sections we will decide on the mode of operation and on what type of gas-solid contactor would be most suitable for the capture and subsequent release of CO_2.

3.0

Process selection procedure

The goal here is to identify a process with a low capital investment and a low energy demand, as these cost elements have a large contribution to the overall cost of the process as mentioned in the introduction. To guide the process selection procedure in a systematic way we have adopted the selection strategy proposed by Krishna and Sie [5]. The problem of reactor selection is analysed on two levels of detail; the particle level and the reactor level. Decisions are made based on a list of desired process characteristics; a reactor 'wish' list. We have defined process 'wants' that have a large impact on the capital investment and/or on the energy demand of the process. A process that meets these criteria is likely to require less capital and a smaller amount of energy than a process that does not meet these criteria. These 'wants' are here defined as quantifiable indicators, given below.

(i) | High system productivity

The productivity of the capture system is here defined as the amount of CO_2 captured per second per cubic meter of installed reactor volume. This productivity is a measure for the 'compactness' of the process and relates to the investment cost for the process equipment. An adsorber column with a high productivity is expected to have lower investment cost than one with a low productivity.

This productivity is mainly a function of the (1) particle hold-up, (2) the sorbent residence time i.e. depending on adsorption and desorption kinetics and (3) the bed effectiveness. The latter is a measure for how effective the solids participate in the sorption process. At a 100% bed effectiveness all sorbent particles leaving the adsorber or desorber column have attained a CO_2 loading equal to the equilibrium CO_2 capacity at the columns inlet conditions, hence at maximum CO_2 partial pressure. The bed effectiveness is highly dependent on the mode of operation and the state of solid phase mixing in the adsorber and desorber column. For MEA, a productivity of 0.6 mol/m^3/s has been reported for the scrubber and a productivity of 2.1 mol/m^3/s for the stripper [4].

(ii) | High solids conversion

The process design should facilitate G-S contacting in such a way that the capacity of the sorbent particles is used optimally. This will minimize the

sorbent circulation rate and maximize the sorbent working capacity resulting in lower sensible heat energy penalties. To ensure that the sorbent particles are used efficiently: (1) sufficient G-S contact area and gas residence time should be provided in both the adsorber and the desorber column and (2) a suitable G-S flow contact pattern should be selected in the adsorber column. This will guarantee all sorbent particles have attained their equilibrium CO_2 capacity at the given inlet CO_2 concentration at the end of the adsorption step.

(iii) | Low adsorber pressure drop

The selection of a low pressure drop adsorber design is essential considering the high gas flows involved in post-combustion CO_2 capture. The cost associated with the adsorber pressure drop is directly related to the electrical compression energy required to overcome the adsorber pressure drop. Here, it should be mentioned that the selection of a low pressure drop adsorber is even more important when CO_2 is captured from a gas fired power plant. Flue gas from a NGCC plant contains around three times less CO_2 per unit volume of flue gas compared to flue gas at a PC plant and the pressure drop will therefore have a much larger impact on the energy required per unit of CO_2 captured. For post-combustion CO_2 capture, a system pressure drop higher larger than 210 mbar is considered unacceptable [3]. In the amine scrubbing process around 7% of the total energy is used to overcome the system pressure drop (100-170 mbar) [4, 6]. Since gas flow rates will be much smaller in the desorption step, the energy penalty related to desorber pressure drop is expected to be smaller and therefore of less importance.

(iv) | High operating gas velocities in the adsorber

As the volumetric gas flow rates in the adsorber column are extremely high, gas velocities should preferably be in the same range as or higher than the gas velocities applied in a MEA scrubber. This will reduce the footprint of the process and will result in a more viable aspect ratio. In the amine scrubbing process gas velocities in the range of 1-3 m/s are applied.

Typical values for the productivity, the pressure drop, the working capacity, the gas velocity and the process heat demand for the MEA benchmark process are given in Table 2.

Table 2: Typical values for the selected performance indicators in the MEA benchmark process.

Parameter	MEA [4]
Capture efficiency (%)	90
Adsorber productivity (mol/m^3/s)	0.6
Adsorber pressure drop (mbar)	103
Working capacity (mol/kg)	0.94
Adsorber gas velocities (m/s)	1.8
Heat demand (GJ/tCO_2)	4.2

4.0

Adsorption on a particle level

4.1 | Model description

In this section we first take a closer look at CO_2 adsorption on a particle level to identify the key mass and heat transfer resistances in the uptake of CO_2 by the solids particles. A detailed particle model was developed describing (1) external mass transfer, (2) external heat transfer, (3) internal mass transfer, (4) internal heat transfer and (5) reaction kinetics. In Chapter 3 an adsorption isotherm was developed for Lewatit® VP OC 1065. This isotherm was incorporated in the kinetic rate expression given by equation 8 in Table 5. The isotherm equations and the isotherm parameters are given in Table 3 and Table 4.

The mass and energy balance equations are given in Table 5 [7]. Equation 5 represents the mass balance for CO_2 inside the pore space. CO_2 diffuses through the sorbent's pores with a diffusivity Dp and reacts with the amine groups attached to the surface of the support with a rate, R_A, given by Equation 8. The adsorption reaction rate is assumed to be first order in the gas-phase CO_2 concentration and first order in the amount of free adsorption sites, q_e-q. Experimental data supporting the form for the kinetic rate expression can be found in Appendix C of Chapter 5. The energy balance is described by equation 7. We assume that there is no temperature difference between the gas inside the particle and the particles themselves. The mass balance for the solid phase is given by Equation 6. As mentioned, the Toth isotherm model presented in Chapter 3 is used to describe the equilibrium capacity, q_e, as a function of the local CO_2 concentration in the pore space and the local temperature.

For particles with pore diameters in the order of 25 nm (250 Å), like the pores of Lewatit® VP OC 1065, the diffusion can be described as a combination of Knudsen and molecular diffusion. The mean free path for CO_2 is 39 nm at 273 K and atmospheric pressure and larger than the pore diameter. External heat and mass transfer coefficients were calculated from suitable Nusselt and Sherwood correlations [8].
The partial differential equations listed in Table 5 are solved simultaneously using Matlab's PDEPE solver. This solver can handle initial-boundary value problems for parabolic-elliptic (PE) partial differential equations (PDE).

Table 3: Toth isotherm equations.

$$q_e = \frac{n_S b P_{CO2}}{(1+(bP_{CO2})^t)^{\frac{1}{t}}} \quad (1)$$

$$b = b_0 \exp\left(\frac{\Delta H}{RT_0}\left(\frac{T_0}{T}-1\right)\right) \quad (2)$$

$$t = t_0 + \alpha\left(1-\frac{T_0}{T}\right) \quad (3)$$

$$n_s = n_{s0} \exp\left(\chi\left(1-\frac{T}{T_0}\right)\right) \quad (4)$$

Table 4: Toth isotherm parameters of the adsorption of CO_2 on Lewatit® VP OC 1065 using 353 K as reference temperature.

Parameter	Value	Unit	Description
t_0	0.30	-	-
b_0	408.84	l/bar	-
ns_0	3.40	mol/kg	Maximum CO_2 capacity
χ	0	-	-
α	0.14	-	-
ΔH	$86.7x10^3$	J/mol	Reaction heat
T_0	353	K	Reference temperature

Table 5: Mass balance equations describing the uptake of CO_2 on a particle level.

Equation describing the pore concentration of CO_2

$$\varepsilon \frac{\partial C_P}{\partial t} = \frac{1}{r^2}\frac{\partial}{\partial r}\left[r^2 D_P \frac{\partial C_P}{\partial r}\right] - \rho_s R_A \quad (5)$$

Equation describing the adsorbed phase CO_2 concentration

$$\frac{\partial q}{\partial t} = R_A \quad (6)$$

Equation describing the temParameter

$$\rho_s Cp_s \frac{\partial T}{\partial t} = \frac{1}{r^2}\frac{\partial}{\partial r}\left[r^2 \lambda_s \frac{\partial T}{\partial r}\right] + \Delta H \rho_s R_A \quad (7)$$

Equation describing the chemical reaction rate

$$R_A = k_1 C_P (q_e - q) \quad (8)$$

Boundary conditions for the particle model

$$\left.\frac{\partial C_P}{\partial r}\right|_{r=0} = \left.\frac{\partial T}{\partial r}\right|_{r=0} = 0 \quad (9)$$

$$D_P \left.\frac{\partial C_P}{\partial r}\right|_{r=r_S} = k_G (C_G - C_P) \quad (10)$$

$$\lambda_s \left.\frac{\partial T}{\partial r}\right|_{r=r_S} = h_G (T_G - T) \quad (11)$$

Initial conditions for the particle model

$$q\,(r,t0) = 0 \quad (12)$$

$$C_p(r,t0) = 0 \quad (13)$$

$$T(r,t0) = T_G \quad (14)$$

Table 6: Equations describing the mass and heat transfer rates.

Equations used to calculated the external mass transfer rate

$$Sh_G = 2 + 0.6\, Sc_G^{\frac{1}{3}} Re_G^{\frac{1}{2}} = \frac{k_G d_S}{D_{AB}} \tag{15}$$

$$Re_G = \frac{\rho_G d_S |u_S - u_G|}{\mu_G} \tag{16}$$

Equation used to calculated the external heat transfer rate

$$Nu_G = 2 + 0.6\, Pr_G^{\frac{1}{3}} Re_G^{\frac{1}{2}} = \frac{h_G d_S}{\lambda_G} \tag{17}$$

Equation used to calculate the Knudsen diffusion coefficient

$$D_{Kn} = \frac{d_p}{3} \sqrt{\frac{8RT}{\pi M}} \tag{18}$$

Equation used to calculate the pore diffusion coefficient

$$D = \left(\frac{1}{D_{AB}} + \frac{1}{D_{Kn}} \right)^{-1} \tag{19}$$

Equation describing the effective pore diffusivity

$$D_P = \frac{\varepsilon}{\tau} D \tag{20}$$

Table 7: Particle model input.

Parameter	Value	Unit	Description
C_P	-	mol_{CO2}/m_G^3	Pore concentration of CO_2
t	-	s	Time
r	-	m	Particle radius
D_p	$3.8\ 10^{-7}$	$m_G^3/m_s/s$	Effective pore diffusion coefficient calculated for pores of 25 nm
ρ_s	880	kg_s/m_s^3	Particle density
R_A	-	$mol_{CO2}/kg_s/s$	Intrinsic reaction rate

q	-	mol_{CO2}/kg_s	Particle CO_2 capacity
Cp_s	1500	$J/kg_s/K$	Particle heat capacity
λ_s	0.027	$W/m_s/K$	Effective particle conductivity
T	-	K	Temperature
k_1	0.014	$m_G^3/mol_{CO2}/s$	Intrinsic reaction rate
q_e	-	mol_{CO2}/kg_s	Particle equilibrium CO_2 capacity
k_G	-	$m_G^3/m_s^2/s$	External mass transfer coefficient
h_G	-	$W/m_s^2/s$	External heat transfer coefficient
C_G	-	mol_{CO2}/m_G^3	Bulk CO_2 concentration
T_G	-	K	Bulk gas temperature
Sh_G	-	-	Particle Sherwood number
Sc_G	0.83	-	Schmidt number
Re_G	-	-	Particle Reynolds number
D_{AB}	$1.65\ 10^{-5}$	m_G^2/s	Molecular diffusion coefficient of CO_2 in air at 313 K. [9]
ρ_G	1.1	kg/m^3	Gas density
d_s	$7\ 10^{-4}$	m_s	Particle size
u_s	0.10	m/s	Particle downward velocity
u_G	1.8	m/s	Superficial gas velocity
μ_G	$1.8\ 10^{-5}$	Pa s	Gas viscosity
Nu_G	-	-	Particle Nusselt number
Pr_G	0.71	-	Prandtl number
λ_G	0.027	$W/m_G/K$	Gas conductivity
d_p	$2.5\ 10^{-8}$	m	Averaged pore diameter
R	8.314	J/mol/K	Gas constant
M	44	g/mol	Molecular weight of CO_2
D_{Kn}	$3.2\ 10^{-6}$	m_G^2/s	Knudsen diffusion coefficient (at a pore diameter of 25 nm and 313 K)
τ	2.3	m_G/m_s	Pore tortuosity
ε	0.23	m_G^2/m_s^2	Particle voidage

4.2 | Model results

The particle effectiveness compares overall uptake rate with the intrinsic reaction rate between CO_2 and the amine groups on the support pore space. For slow reaction rates the particle effectiveness, η, is close to 1, indicating that the reaction rate limits the sorbent's overall CO_2 uptake rate. For fast reaction rates $\eta<<1$, indicating that the uptake of CO_2 is no longer only a reaction rate limited process but pore diffusion is playing a role as well.
To validate the particle model, the particle effectiveness, as calculated numerically by the particle model for unloaded particles (i.e. q=0), was compared to the theoretical particle effectiveness for a first order reaction with a first order reaction rate constant equal to the product of k_1 and q_e. The modelled effectiveness compared well with the theoretical value indicating that there are no errors in the mass and energy balance equations and that they are solved correctly.

For the sorbent particles considered here we calculate particle effectiveness factors in the range of 60-80%. This points towards a mostly reaction rate limited uptake of CO_2 by the sorbent particles. A value for the intrinsic reaction rate constant, k_1, was obtained by fitting k_1 to experimental data. A value of 1.4 10^{-2} $m_G^3/mol_{CO2}/s$ gave the best fit to the experimental data. Details regarding the experimental work and the fitting procedure can be found in Chapter 5.

Using the particle model, the influence of other mass and heat transport resistances on the overall particle uptake rate was investigated. In Figure 1, the particle effectiveness is plotted as a function of the particle's CO_2 loading for two different gas velocities. In addition, the particle effectiveness is plotted for the case that there are no external mass or heat transfer limitations. Based on this graph we can conclude that external mass and heat transfer do not significantly limit the uptake of CO_2 for gas velocities around the particle in the range 0-2 m/s. This is a typical velocity range for gas-solid reactors.

As in the MEA scrubbing process, heat management is an important aspect of the process design since the adsorption reaction is highly exothermic in both cases. The heat released during adsorption causes a rise in temperature inside the adsorber column and inside the sorbent particles. High temperatures limit the CO_2 capacity of the sorbent particles and so heat removal could limit the time required to saturate the particles.

In Figure 2, the particle effectiveness, as calculated by the particle model, is plotted as a function of the particle's CO_2 capacity for two different effective particle thermal conductivities, λs. Porous polystyrene typically has a thermal conductivity of around 0.027 W/m/K. The adsorption rate is clearly not affected by internal heat transfer limitations and we can conclude that the internal transfer of heat is fast enough to dissipate the heat produced in the adsorption reaction. This is also clearly reflected in Figure 3. Here, the temperature inside the sorbent particles is plotted as a function of the adsorption time. The two lines represent the temperature change over time at the particle's outer surface and at the centre of the particle. The peak temperature inside the particles is only ~5-7 K higher than the bulk gas temperature which was 328 K in this case. This small temperature increase will not significantly influence the adsorption process on a particle level.

However, this does not mean we can neglect temperature effects on a reactor level. The amount of heat released in the adsorption of 2 mol of CO_2 per kilogram of sorbent is enough to heat up the particles and the gas with around 90 K (the adiabatic temperature rise). As high temperatures will limit the uptake of CO_2, heat effects will severely influence the length of the mass transfer zone if the heat removal rate in the adsorber column is not fast enough. These heat effects will become increasingly dominant in the adsorption step at higher uptake rates. Installing heat exchange area in the adsorber column and desorber column is the most feasible way to extract adsorption heat in the adsorber and to supply desorption heat in the desorber column. Heat transfer to internals will be included in the energy balance of the reactor model that will be presented at the end of this chapter.

From the particle model we have learned that internal and external heat transfer resistances do not limit the overall uptake rate of the sorbent materials (See Figure 1 and 2). The external mass transfer resistances are also not expected to limit the adsorption process on a process scale (See Figure 1). In the following section, the aim is to select the most suitable reactor for the sorbent particles under consideration.

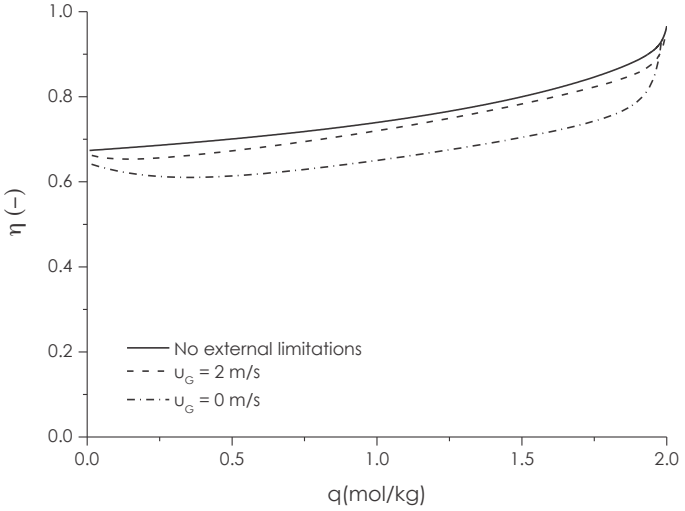

Figure 1: The particle effectiveness factor calculated by the particle model as a function of the capacity of the sorbent material. The gas velocity around the particle was changed to check for external heat or mass transfer limitations. The bulk gas CO_2 fraction was 12.3 vol% and the bulk gas temperature was 328 K.

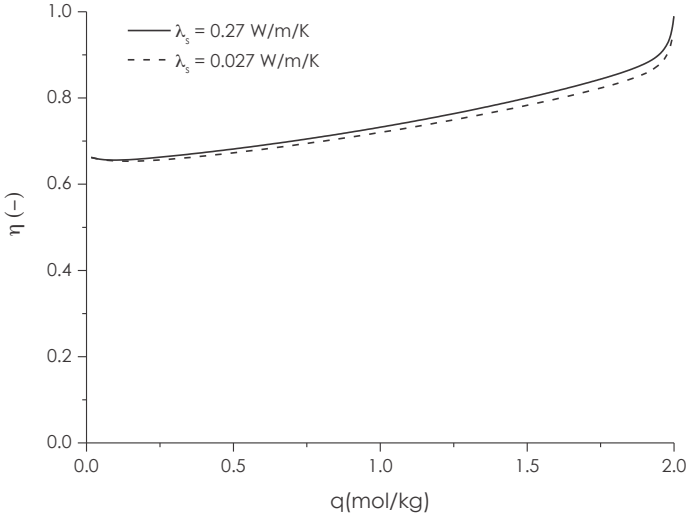

Figure 2: The particle effectiveness factor calculated by the particle model as a function of the capacity of the sorbent material. The conductivity of the sorbent material (λs) was changed to check for internal heat transfer limitations. The bulk gas CO_2 fraction was 12.3 vol% and the bulk gas temperature was 328 K.

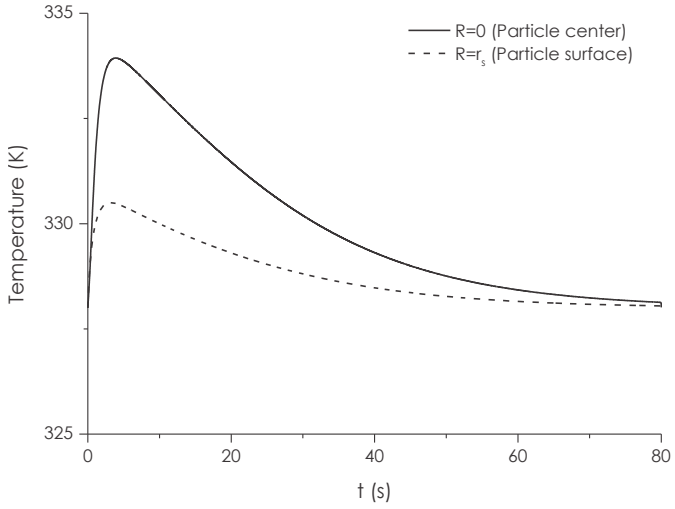

Figure 3: Temperature inside the sorbent particles as a function of the adsorption time. The bulk gas CO_2 fraction was 12.3 vol% and the bulk gas temperature was 328 K. The two lines represent the temperature change over time at different places in the sorbent particles for a λ_s of 0.027 W/m/K. (At the particle's outer surface and at the centre of the particle). The particle Reynolds number was 100.

5.0

Adsorption on a reactor level

5.1 | Mode of operation

Thermal swing adsorption (TSA) processes can have two modes of operation. Either (i) the sorption and regeneration are achieved by cyclic changes in temperature inside the vessel where the sorbent is contained or (ii) the process consists of a low-temperature adsorber and a high-temperature regenerator with the sorbent circulating between the adsorber and the desorber. If the sorbent is contained in one vessel during both sorption and regeneration, a minimum of two sorption vessels is required two allow for continuous process operation. One vessel would be in adsorption mode, while the other vessel is being regenerated. When sorbent regeneration takes longer than adsorption or the uptake of CO_2 by the sorbent particles is slow, a three-bed (or multi-bed) thermal swing adsorption process is often applied. CO_2 is allowed to break through the leading adsorber bed into a second adsorber bed, termed the trim bed, allowing full utilization of the leading adsorber bed. In the second step, the trim bed will become the lead bed and the third bed, meanwhile regenerated, will become the trim bed. The classical advantages of fixed beds are their easy operation and the simple design. Also, solid phase mixing is prevented and attrition of the sorbent is minimal. If the solids are circulated between the adsorption and desorption vessels, a transportation system should be fitted to transport the sorbent particles from the adsorber vessel to the desorber vessel. Therefore, the solid particles should be mechanically stable to avoid attrition.

For post-combustion CO_2 capture using solid sorbents in a TSA process, solid circulation between the adsorber and desorber column seems the most efficient process configuration for the reasons described below. Firstly, in a continuous mode of operation, the bed length can be kept to a minimum, namely equal to the length of the mass transfer zone, while the particles can be completely converted and capture efficiencies close to 100% can be achieved. In a fixed bed TSA process, in order to achieve a bed effectiveness of 80-90%, the adsorber bed should be at least 2.5-5 times as long as a continuously operated adsorber column (estimated based on Collins' length of unused bed method [7]). This implies a larger bed pressure drop and lower bed productivities compared to the continuous system.

A high bed effectiveness can also be achieved when solids are not circulating between the adsorption and desorption vessel by (1) allowing breakthrough of CO_2 i.e. settling for a lower capture efficiency, (2) using the three-bed (or multi-bed) TSA described earlier. However, the productivity of these systems is much lower than in a continuous operation mode, since a large part of the sorbent material in the column is inactive during operation. In a fixed bed adsorption process for example, the only solids that effectively participate in the sorption process are those located in the mass transfer zone. The other solids in the column are either saturated with CO_2 or not yet in contacted with CO_2 and are therefore only adding inactive volume to the reactor.
Secondly, sorbent heating times are expected to be much shorter when the solids are circulated. Total cycle times for thermal swing adsorption processes operated in batch mode are of the order of hours because of the thermal inertia of the packed bed [10]. As long cycle times would severely limit the productivity of the process, heating times should be kept as short as possible.
In summary, a process with sorbent circulation and the continuous injection of both sorbent material and flue gas to the adsorber and the desorber, we believe, is essential for achieving high bed efficiencies and productivities.

5.2 | Mixing and contacting pattern

To achieve high productivities and high sorbent conversions in the adsorber column, choosing an appropriate contact flow pattern and an appropriate state of mixing for both phases is essential. To do so, we have calculated the required sorbent inventory for five adsorber reactor concepts, each with a different state of mixing and/or a contacting pattern but all operated with the same sorbent particles and all capturing the same amount of CO_2. We have considered (1) an adsorber in which both the gas phase and the solid phase are well mixed, (2) one in which the solid phase is well mixed but the gas phase moves in plug flow, (3) one in which the gas phase is well mixed but the solid phase moves in plug flow and two plug flow reactors, (4) one in which the gas and the solids are contacted in co-current fashion and (5) one in which they are contacted in counter-current mode. The flue gas flow rate, composition, pressure and temperature used as input for these calculations are given in Table 1.

In Figure 4, the sorbent conversion is plotted on the x-axis. The sorbent conversion is defined here as the amount of CO_2 adsorbed by the sorbent particles leaving the reactor (q) divided by the equilibrium CO_2 capacity of the sorbent corresponding to flue gas inlet conditions (q_{max} = 2.0 mol/kg). The y-axis in Figure 4 represent the solid inventory in each reactor concept required to capture 90% of the incoming CO_2. Details about the calculation method can be found in Appendix B. We can draw several important conclusions from Figure 4 that will help us select the most suitable adsorber type:

- For all cases except for the counter-current plug flow reactor, the sorbent conversion is limited to values lower than ~60% (the asymptote in Figure 4). Since the sorbent particles leaving the reactor are contacted with flue gas also leaving the reactor, the sorbent capacity is limited to the equilibrium sorbent capacity at gas phase outlet conditions. This implies that only in a counter-current plug flow reactor we can make effective use of the CO_2 capacity of the sorbent material. A low sorbent conversion will limit the working capacity and this could translate into a high process heat demand.
- Especially the state of mixing of the gas phase has a large effect on the adsorber size. A gas phase in plug flow results in significantly higher driving forces for CO_2 uptake and hence in a more compact adsorber design.
- Due to the large spread in the residence time distribution of the sorbent particles in a well-mixed system, a large fraction of the particles will spend more time in the adsorber bed than required for full saturation by adsorption, resulting in an oversized adsorber column. This conclusion also holds for the design of the desorber column.

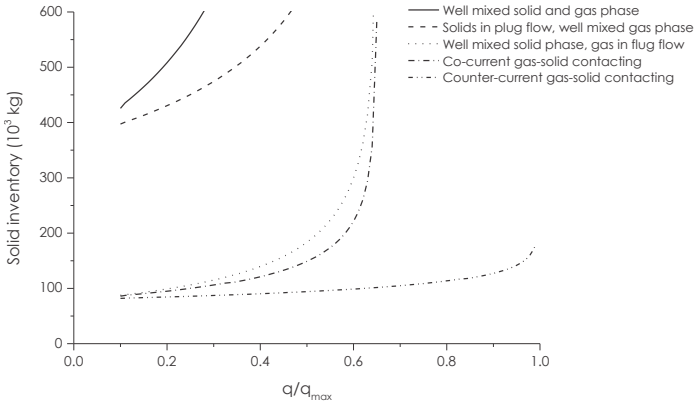

Figure 4: The adsorber solid inventory for the five specified cases as a function of the conversion of the sorbent particles leaving the reactor. Full sorbent conversion ($q/q_{max}=1$) is attained when the adsorption capacity is equal to the equilibrium capacity at the inlet CO_2 concentration (12.3 vol %).

5.3 | On the selection of a reactor type

So far we have concluded that the adsorber design should (1) allow for solid circulation, (2) prevent mixing of the gas and solid phase, (3) provide counter current G-S contacting, (4) allow high operating gas velocities and (5) have a low pressure drop, preferable lower than 100 mbar. In the desorber column, we would like (1) to prevent solid mixing in order to minimize the sorbent hold-up and (2) the reactor should possess excellent heat transfer properties to keep sorbent heating times as short as possible and prevent large temperature gradients in the desorber column. Since the sorbent material will be regenerated in a (almost) pure CO_2 atmosphere neither the desorber mass transfer characteristics nor the choice of G-S contacting flow pattern will significantly influence the performance of the desorber column. Since gas flows are much lower in the desorber column than in the adsorber column, the pressure drop energy penalty over the desorber is much less of an issue as well.

In our opinion there are two reactor types that best fit the above defined adsorber reactor profile, namely a staged fluid bed adsorber and a gas-solid trickle flow reactor (GSTF). A staged-fluid bed combines the excellent heat and mass transfer properties of a fluid bed reactor with a counter-current gas-solid contacting flow pattern. In a typical fluid bed the sorbent is moving freely inside one compartment, resulting in mixing of the solids phase. In a staged fluid bed adsorber, counter current G-S contacting is realised by dividing the fluid bed in several stages so preventing the undesired back mixing of solids. This will reduce the required solid inventory and reactor size. The pressure drop inside a staged fluid bed adsorber is however expected to be considerable [3] and operating gas velocities are limited.
In a gas-solid trickle flow adsorber the gas and the solid phase can be operated in plug-flow creating a counter current G-S contacting flow pattern, ideal for CO_2 adsorption. Expected gas velocities are well in the desired range; operating velocities up to 70% or 80% of the terminal velocity of the sorbent particles are permitted. Due to the high void fraction (>90%), the pressure drop is expected to be low at the cost of a somewhat lower productivity.

For the desorber, we believe that both a staged fluid bed and a cross flow fluid bed would perform well. Both reactors combine solids segregation with excellent heat transfer properties. With respect to solids staging, only a few stages (four or more) would be enough to prevent extensive mixing of

solids in the desorber column. The advantage of the staged fluid bed over the cross fluid bed is that the footprint of the staged fluid bed is smaller, albeit at the cost of a higher pressure drop. The CO_2 released by the sorbent material could be used to fluidize the fluid bed desorber column [3]. This would reduce the energy required to operate the fluidization gas blower as a lower inlet flow is required.

In Chapter 5 of this thesis, the performance of a lab-scale capture set-up, consisting of a gas-solid trickle flow adsorber and a staged-fluid bed desorber, will be studied experimentally. In the following section, the main focus is on the performance of the adsorber column, as this is the most expensive piece of equipment in the conventional process.

6.0

Reactor model

6.1 | Model description

In a trickle flow reactor, gas and solids are contacted in a counter-current manner over a packed column under dilute phase or trickle flow conditions [2]. The solids are introduced at the top of the adsorber column and move through the reactor under the influence of gravity. The gas is introduced at the bottom of the adsorber column. The purpose of the packing is to slow down the sorbent particles on their way down. This results in increased residence times and consequently higher solid holdups (β). Also the gas, flowing in counter current, slows down the solids. The sorbent holdup will be highest for densely packed columns operated at gas velocities close to the terminal velocity of the sorbent particles. The terminal velocity determines the upper limit for the operating gas velocity. At gas velocities close to the particle's terminal velocity flooding will occur. The heat exchange area required to remove the adsorption heat can be included in the structured 'packing'.

Since the solid hold-up directly relates to the specific interfacial surface area available for mass exchange between the solid particles and the gas it will, to a large extent, determine the productivity and efficiency of the column. The solid holdup is calculated using equation 21 [11]. In this equation the solid flux, S, is equal to the amount of solids circulated per second per square meter of cross-sectional area of the reactor and us represents the effective downward velocity of the sorbent particles.
In the trickle flow reactor, CO_2 is being selectively adsorbed by the sorbent particles causing a change in (1) the gas phase CO_2 concentration, (2) the CO_2 loading of the sorbent particles, (3) the temperature of the gas and (4) the temperature of the solids over the length of the reactor. The changes in concentration, loading and temperature are described by equation 22, 23 and 24. The variables C* and T* represent the gas phase CO_2 concentration and the gas phase temperature at the particle surface respectively. Their values are extracted from the particle model that is coupled to the reactor model. A more detailed description of the reactor model and the assumptions made is given in Appendix B at the end of this chapter. The main adsorber performance indicators, the capture efficiency E, the productivity P and the working capacity Δq, are defined by equations 30, 31 and 32 in Table 8.

Table 8: Mass and heat balance equations describing the reactor.

Equation describing the solid hold-up [11]

$$\beta = \frac{S}{\rho_s u_s} \tag{21}$$

Equation describing the CO_2 concentration profile

$$\frac{\partial(u_G C_G)}{\partial z} = -\frac{6 k_G \beta}{d_s} (C_G - C^*) \tag{22}$$

Equation describing the capacity profile

$$S\frac{\partial q}{\partial z} = -\frac{6 k_G \beta}{d_s} (C_G - C^*) \tag{23}$$

Equation describing the temperature profile inside the reactor column

$$\rho_G Cp_G \frac{\partial(u_G T_G)}{\partial z} = -\frac{6 h_G \beta}{d_s} (T_G - T^*) - h_w a (T_G - T_c) \tag{24}$$

The boundary conditions for the differential equation given above

$$C_G|_{L=0} = C_{G,in} \tag{25}$$

$$T_G|_{L=0} = T_{G,in} \tag{26}$$

Boundary conditions for the particle model

$$C(r)|_{L=L} = 0 \tag{27}$$

$$q(r)|_{L=L} = 0 \tag{28}$$

$$T_S(r)|_{L=L} = T_{S,in} \tag{29}$$

Equation used to calculate the capture efficiency

$$E = 1 - \frac{u_{G,out} C_{G,out}}{u_{G,in} C_{G,in}} \tag{30}$$

Equation used to calculate the column productivity

$$P = \frac{u_G C_{G,in} E}{L} \tag{31}$$

Equation used to calculate the working capacity

$$\Delta q = \frac{P L}{S} \tag{32}$$

Table 9: Reactor model input.

Parameter	Value	Unit	Description
C_P	-	mol_{CO2}/m_G^3	Pore concentration of CO_2
t	-	s	Time
r	-	m	Particle radius
D_p	$3.8\ 10^{-7}$	$m_G^3/m_s/s$	Effective pore diffusion coefficient calculated for pores of 25 nm
ρ_s	880	kg_s/m_s^3	Particle density
R_A	-	$mol_{CO2}/kg_s/s$	Intrinsic reaction rate
q	-	mol_{CO2}/kg_s	Particle CO_2 capacity
Cp_s	1500	$J/kg_s/K$	Particle heat capacity
λ_s	0.027	$W/m_s/K$	Effective particle conductivity
T	-	K	Temperature
k_1	0.014	$m_G^3/mol_{CO2}/s$	Intrinsic reaction rate
q_e	-	mol_{CO2}/kg_s	Particle equilibrium CO_2 capacity
k_G	-	$m_G^3/m_s^2/s$	External mass transfer coefficient
h_G	-	$W/m_s^2/s$	External heat transfer coefficient
C_G	-	mol_{CO2}/m_G^3	Bulk CO_2 concentration
T_G	-	K	Bulk gas temperature
Sh_G	-	-	Particle Sherwood number
Sc_G	0.83	-	Schmidt number
Re_G	-	-	Particle Reynolds number

6.2 | Model results

Figure 5 and Figure 6 show the gas phase CO_2 concentration profile and gas temperature profile over the length of the adsorber reactor. The amount of installed heat exchange area was varied to quantify the effect of cooling on the adsorber performance. The heat exchange coefficient between the gas and the heat exchange area inside the trickle flow adsorber was assumed to be 150 W/m^2/K [12]. Also in the reactor modelling we found that the temperature difference between the solids and the gas is small (<5K) throughout the adsorber column. Only near the gas inlet (L<0.2 m), the solid temperature is higher than the gas temperature.

In an adsorber without cooling, the gas reaches temperatures as high as 388 K. The increase in temperature limits the CO_2 capacity of the sorbent particles. At these increased temperatures the solids have an equilibrium CO_2 capacity of 0.72 mol/kg instead of 2 mol/kg which is the equilibrium capacity of the sorbent at the inlet conditions (12.3 vol% CO_2 and 328 K). As a result a large part of the adsorber column is inactive resulting in a low column productivity and a low capture efficiency. The adsorber reactor captures only 36% of the incoming CO_2.

The adsorber performance clearly improves with the installation of heat exchange area. For a column with 15 m^2/m^3 of heat exchange area the gas still reaches temperatures of around 360 K near the top of the reactor which is ~30 K higher than the inlet temperature of the gas. This rise in temperature still limits the uptake of CO_2, but the capture efficiency of the column is already much higher than that of the adiabatic column; 74%. The installation of more heat exchange area prevents high temperatures in the top of the reactor and further improves the capture efficiency to even 90% at 100 m^2/m^3.

Here, the cost of the heat exchange area should also be taken into account; the best performing reactor in terms of capture efficiency is not necessarily the most cost effective reactor design. We should consider the practical limitations to the amount of heat exchange area we can add to the reactor as well. Most probably it is more cost effective and more practical to accept a small rise in temperature (smaller than 20 K) and add around 30 m^2/m^3 of heat exchange area to the column instead.

In Table 10 we present a preliminary design of an adsorber column for a CO_2 capture facility at a 500 MWe coal-fired power plant. The flue gas flow

rate, composition, pressure and temperature used as input for these calculations are given in Table 1. The adsorber column was designed in such a way that 90% of the CO_2 introduced to the column is captured by the sorbent particles. We have selected a gas velocity of 1.8 m/s, which is similar to the gas velocity in the MEA benchmark process (Table 2). Although the upper limit for the gas velocity is set by the terminal velocity of the particles (2.6 m/s), practically, we cannot allow for gas velocities higher than 70% of this terminal velocity.

Table 10 shows the dimension and the performance of a gas solid trickle flow reactor adsorber column calculated based on the reactor model presented in this section. It should be noted that we did not report a column diameter here. Like in the MEA based process, rather than treating all flue gas in one adsorber column, there may be several adsorber columns operating in parallel each treating a fraction of the flue gas.

The installation of heat exchange area will add to the purchased equipment cost of the adsorber and hence we would like to minimize the installed amount. However, we would like to guarantee a good column performance as well. In the column design study we have added just enough heat exchange area to keep the maximum gas temperature below 340 K. In all cases shown in Table 10, the cooling water temperature was assumed to be 303 K except for the case shown in column one of Table 10. Here, the cooling water temperature was assumed to be 328 K. In all cases the inlet solid temperature was assumed to be equal to the inlet gas temperature.

We have considered several cases in Table 10. Firstly, a full scale design is presented for a gas solid trickle flow reactor operated with the Lewatit® VP OC 1065 sorbent particles. This sorbent is already commercially available and serves as a benchmark here. Secondly, we have presented a column design for a 'second generation sorbent'. This sorbent material has a higher CO_2 capacity than the benchmark sorbent. Instead of adsorbing 2.5 mol/kg, this improved sorbent material adsorbs 5.1 mol/kg at 303 K and at a gas phase CO_2 concentration of 12.3 vol%. In the model this is mimicked by doubling the value for ns0 in equation 4. Currently, sorbents with capacities above 5.1 mol/kg under flue gas conditions already exist. They are however not yet commercially available. For more information on sorbent capacities, the reader is referred to Chapter 1 of this thesis in which a detailed literature overview is given. Lastly, a 'third generation' sorbent is considered. This sorbent does not only adsorb more CO_2 than the benchmark sorbent

material, but also has a higher reactivity. In the model this is mimicked by doubling the value of k_1 in equation 8. The intrinsic reaction rate might be improved by tuning the amine type for instance.

Although there are sorbent materials that perform better than Lewatit® VP OC 1065, also this sorbent performs well in a post combustion capture process. The productivities of the adsorber operated with the benchmark sorbent are similar to the productivities reported for the scrubber in the MEA reference study [4]. However, the Lewatit® VP OC 1065 based process could significantly reduce the energy demand of the capture process from around 4 GJ/t to 2.4 GJ/t. The second column of Table 10 shows the performance of an adsorber column operated with Lewatit® VP OC 1065 but at a lower adsorption temperature; 303 K compared to 328 K. Clearly, a lower adsorption temperature improves the productivity as the sorbent shows a higher equilibrium capacity at these lower temperatures. However, 303 K is below the dew point of the flue gas. It is only possible to operate the column at these temperatures if water is removed upstream of the adsorber column. This was discussed in more detail in Chapter 3 of this thesis.

Applying the 'second generation' sorbent material would improve the productivity of the adsorber column from 1.1 to 1.3 mol/m^3/s and the working capacity from 1.8 mol/kg to 3.1 mol/kg. Sorbent materials with higher CO_2 capacities do not have to be saturated fully with CO_2 to achieve high working capacities. Since the rate of adsorption is higher at low particle saturation levels we expect slightly higher productivities as well. We see however that the higher working capacity (3.1 compared to 1.8 mol/kg) does not result in a much lower process heat demand (2.3 compared to 2.5 GJ/t). The process heat demand was calculated assuming a sorbent heat capacity of 1500 J/kg/K and a desorption temperature of 423 K. The reaction heat was assumed to be 87 kJ/mol. Applying the third generation sorbent material, with a higher reactivity, further improves the productivity of the adsorption process.

In short, we can conclude that switching to an adsorption based process could reduce the energy penalty of the conventional process from around 4 GJ/t to 2.3 GJ/t but also increase the productivity of the process to from 0.6 to 1.8 mol/m^3/s resulting in lower operating cost as well as lower capital cost.

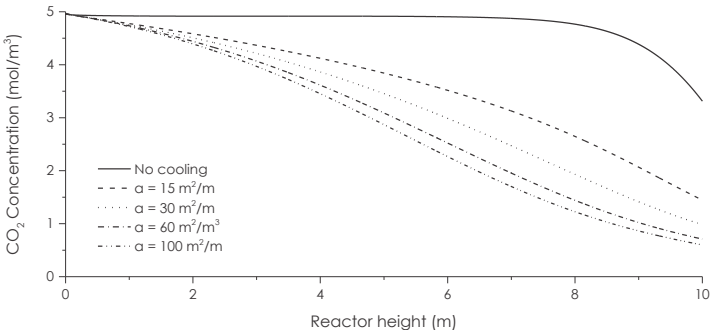

Figure 5: Gas phase CO_2 concentration profiles for different column cooling capacities. The gas velocity at the inlet was 1.8 m/s. The inlet CO_2 fraction was 12.3 vol%. The inlet gas and inlet solid temperature was 328 K. The solid flux was equal to 4.5 kg/m^2/s.

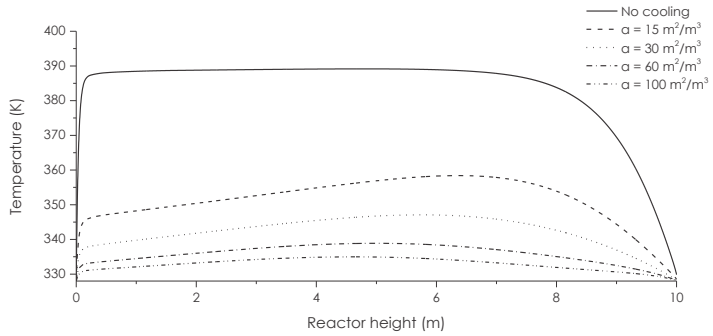

Figure 6: Gas Temperature profiles for different column cooling capacities. The temperature profiles correspond to the concentration profiles shown in Figure 5. The gas velocity at the inlet was 1.8 m/s. The inlet CO_2 fraction was 12.3 vol%. The inlet gas and inlet solid temperature was 328 K. The solid flux was equal to 4.5 kg/m^2/s.

Table 10: Design study preformed based on the reactor model presented in this chapter.

Sorbent	Lewatit® VP OC 1065		Second generation sorbent	Third generation
	Base case (2.0 mol/kg)	Base case (2.5 mol/kg) Low temperature	High capacity (5.1 mol/kg)	High capacity (5.1 mol/kg) Higher reactivity
Flue gas				
Flue gas flow (m^3/s)	576	532	532	532
Pressure (kPa)	111.2	111.2	111.2	111.2
Temperature (K)	328	303	303	303
Inlet CO_2 concentration (vol%)	12.3	12.3	12.3	12.3
Adsorber				
Gas velocity (m/s)	1.8	1.8	1.8	1.8
Cross sectional area total (m^2)	317	293	293	293
Total volume (m^3)	4126	2345	2052	1466
Height (m)	13	8	7	5

Max. Gas temperature (K)	340	334	330	337
Solid inventory (kg)	185759	114313	60014	42867
Solid holdup (%)	5.1%	5.5%	3.3%	3.3%
Amount of heat exchange area (m^2)	185671	58639	82095	58639
Moles CO_2 captured (t/s)	0.114	0.113	0.116	0.115
Sorbent flux ($kg/m^2/s$)	4.5	4.9	2.9	2.9
Capture efficiency (-)	0.91	0.90	0.92	0.92
Working capacity (mol/kg)	1.8	1.8	3.1	3.1
Heat removed from adsorber (GJ/t)	2.1	1.8	1.9	1.9
Productivity ($mol/m^3/s$)	0.6	1.1	1.3	1.8
Solid conversion (q/qmax)	0.9	0.71	0.61	0.60
Heat demand Estimated process heat demand (GJ/t)	3.7	4.2	3.3	3.3
Estimated process heat demand with heat exchange (@75%) (GJ/t)	2.4	2.5	2.3	2.3

7.0

Simplification of the model equations

A detailed particle model was presented for the adsorption of CO_2 on Lewatit VP OC 1065. This particle model was later coupled to a reactor model describing the performance of these sorbent materials in a gas-solid trickle flow reactor. Based on the simulation results presented here we can safely assume:

- That the external transport of heat and mass does not significantly influence the performance of the reactor.
- That the internal transport of heat is fast enough to dissipate the heat produced in the adsorption reaction and prevent large temperature gradients inside the sorbent particle.
- That the effectiveness of the sorbent particles is not a strong function of the CO_2 concentration nor the CO_2 loading of the sorbent particle. Under adsorption conditions, the effectiveness is approximately constant over the length of the reactor.
- Because the isotherm is nearly flat in the concentration range of 1 vol% to 15 vol%, the equilibrium sorbent capacity is not a strong function of the length of the reactor especially for lower capture efficiencies. Assuming the equilibrium capacity of the sorbent constant over the length of the reactor gives a good approximation of the actual uptake rate in the reactor.

These assumptions can greatly simplify the reactor model. A simplified reactor model is discussed in more detail in Chapter 5 where it is used to describe the experimental results obtained in a lab-scale capture facility.

8.0

Conclusion

This chapter focusses on the selection and design of an adsorber and desorber for adsorption-based post-combustion CO_2 capture using supported amine sorbents. This process selection and design study involves detailed modelling at the particle level and the adsorber reactor level. We concluded that:

- The adsorption rate of CO_2 by the sorbent particles studied here, is limited by a combination of external mass transfer, internal diffusion and reaction kinetics. Moreover, heat transfer, internal or external, will not have a significant effect on the performance of the sorbent particles. Under flue gas conditions (T= 328 K, P_{CO2} = 0.137 bar), the Lewatit® VP OC 1065 sorbent can be saturated with CO_2 in around 80 seconds.
- Since the rate of adsorption is a strong function of the gas phase CO_2 concentration, the performance of the adsorber column would greatly benefit from a counter-current contacting flow pattern.
- Especially a gas-solid trickle flow reactor would perform well as a CO_2 adsorber column. It provides counter current G-S contacting and can be operated at gas velocities equal or higher than the gas velocities applied in a MEA scrubber without resulting in unacceptable pressure drops.
- For desorption in (almost) pure CO_2 atmosphere neither the desorber mass transfer characteristics nor the choice of G-S contacting flow pattern will significantly influence the performance of the column. Here, good heat exchange characteristics and solid phase segregation is key and either a staged fluid bed or a cross-flow fluid bed are suitable reactor types.

A full scale design of a gas solid trickle flow column for a CO_2 capture facility at a 500 MWe coal-fired power plant was presented as well. Capture efficiencies up to 90% can be achieved in a column of 13 meters high. The sorbent particles can attain 90% of their equilibrium capacity in this column. At these working capacities we expect a significantly lower process heat demand than in the conventional process; 2.3 GJ/t compared to 4 GJ/t for the conventional MEA based process. Moreover, it was found that the higher mass transfer rates in the adsorption column allow for a more compact adsorber design. In comparison with the conventional technology, the column size of the scrubber can significantly be reduced when switching to an adsorption based process.

References

1. Jassim, M.S., G. Rochelle, D. Eimer, and C. Ramshaw, Carbon dioxide absorption and desorption in aqueous monoethanolamine solutions in a rotating packed bed. Industrial & engineering chemistry research, 2007. 46(9): p. 2823-2833.
2. Kiel, J.H.A., W. Prins, and W.P.M. Van Swaaij, Mass-Transfer between Gas and Particles in a Gas Solid Trickle Flow Reactor. Chemical Engineering Science, 1993. 48(1): p. 117-125.
3. Yang, W.C. and J. Hoffman, Exploratory design study on reactor configurations for carbon dioxide capture from conventional power plants employing regenerable solid sorbents. Industrial and Engineering Chemistry Research, 2009. 48(1): p. 341-351.
4. Fisher, K.S., et al., Integrating MEA Regeneration with CO_2 Compression and Peaking to Reduce CO_2 Capture Costs, 2005.
5. Krishna, R. and S.T. Sie, Strategies for Multiphase Reactor Selection. Chemical Engineering Science, 1994. 49(24A): p. 4029-4065.
6. Kothandaraman, A., L. Nord, O. Bolland, H.J. Herzog, and G.J. McRae, Comparison of solvents for post-combustion capture of CO_2 by chemical absorption. Greenhouse Gas Control Technologies 9, 2009. 1(1): p. 1373-1380.
7. Tien, C., 6 - Macroscopic description of adsorption processes, in Adsorption Calculations and Modelling. 1994, Butterworth-Heinemann: Boston. p. 87-98.
8. Bird, R.B., W.E. Stewart, and E.N. Lightfoot, Transport Phenomena 2nd ed. 2007, New York: John Wiley & Sons, Inc.
9. Massman, W.J., A review of the molecular diffusivities of H_2O, CO_2, CH_4, CO, O_3, SO_2, NH_3, N_2O, NO, and NO_2 in air, O_2 and N_2 near STP. Atmospheric Environment, 1998. 32(6): p. 1111-1127.
10. Thomas, W.J. and B.D. Crittenden, Adsorption technology and design. 1998, Boston.
11. Dudukovic, A.P., N.M. Nikacevic, D.L. Petrovic, and Z.J. Predojevic, Solids holdup and pressure drop in gas-flowing solids-fixed bed contactors. Industrial & engineering chemistry research, 2003. 42(12): p. 2530-2535.
12. Cheng, Y., C.N. Wu, J.X. Zhu, F. Wei, and Y. Jin, Downer reactor: From fundamental study to industrial application. Powder Technology, 2008. 183(3): p. 364-384.

B.

Detailed information about the simulation work

B.1 | Supplementary information to section 5.2

The following equations were solved to plot Figure 4. The equation were solved using Matlab's BVP4c solver. The values for the dispersion coefficients D1 and D2 were changed to mimic either a well-mixed phase or a plug flow. The input for the calculations is summarized in Table 7 of this chapter. The calculation procedure was as follows. For each value of q/qmax the reactor length was varied. The length was increased until the capture efficiency was 90%. Then the volume of the reactor was calculated and subsequently the weight of the solids inside this reactor assuming a gas velocity of 2 m/s and a reactor voidage of 0.6. For the counter current reactor the solid flux in equation B.2 has a negative value and boundary conditions B.8 are valid at L=L whereas B.9 is valid at L=0. In equation B.3, the value of q_e is evaluated at bulk gas conditions.

B.2 | Reactor model assumptions:

The assumptions made in the reactor model are listed below:

- The adsorption reaction rate is assumed to be first order in the gas-phase CO_2 concentration and first order in the amount of free adsorption sites.
- There is no temperature difference between the gas inside the particles and the particles themselves.
- Both the solid phase and the gas phase move in plug flow through the trickle flow column.
- There are no radial temperature and concentration profiles inside the trickle flow reactor.
- Pressure is constant over the length of the reactors.
- The effect of temperature on the mass transfer and kinetic rate is not taken into account.
- The effect of the local velocity on the overall solids holdup is not taken into account.
- Gas velocity, density and molar volume are not corrected for temperature changes

B.3 | Reactor model description

We have solved the gas-phase concentration profile and the gas-phase temperature profile in an iterative process. As an initial guess, both the CO_2 concentration and gas temperature were assumed constant over the length of the reactor and equal to the CO_2 inlet concentration and inlet gas temperature respectively. The particle model was solved for τ_s seconds i.e. the solid residence time in the reactor. This yields the sorbent capacity

profile of particles falling through the trickle flow column, in case the concentration of CO_2 and gas temperature are constant over the length of the reactor. In practice the CO_2 concentration inside the reactor will be lower that the CO_2 inlet concentration for L>0. Also the gas temperature will not be equal to the inlet gas temperature for L>0. As we have overestimated the CO_2 concentration, we have also overestimated the uptake of CO_2. Now a new better guess for the gas concentration profile can be calculated based on the sorbent capacity profile obtained from the particle model.
The reactor length is discretized and for each differential reactor volume the amount of CO_2 adsorbed by the solid particle during its stay in that particular control volume was calculated based on the sorbent capacity profile as calculated by the particle model. In a similar way a new better guess for the temperature profile can be calculated. The volume flow of the gas is corrected for the decrease in concentration. Now the particle model is solved again but with the new CO_2 concentration profile and temperature profile as boundary conditions. The model keeps iterating until the error in the mass and energy balance is smaller than 0.01%.

Table 9: Reactor model input.

Equation describing the CO_2 concentration profile for reactor

$$D_1 \frac{\partial^2 C}{\partial z^2} - u_G \frac{\partial C}{\partial z} + R_A \varrho_s \beta = 0 \quad \text{B.1}$$

Equation describing the capacity profile

$$D_2 \frac{\partial^2 q}{\partial z^2} - S \frac{\partial q}{\partial z} - R_A \varrho_s \beta = 0 \quad \text{B.2}$$

Equation describing the overall reaction rate

$$R_A = k_1 C_P (q_e - q) \eta \quad \text{B.3}$$

Thiele modulus and effectiveness for the sorbent particle

$$\eta = \frac{3}{\phi^2} (\phi \coth(\phi) - 1) \quad \text{B.4}$$

$$\phi = \frac{d_s}{2} \sqrt{\frac{k_1 (q_e - q) \rho_s}{D_p}} \quad \text{B.5}$$

Equation describing the CO_2 concentration profile for reactor concept 1-4

$$D_1 \left. \frac{\partial C}{\partial z} \right|_{L=0} = u_G C - u_G C_{G,in} \quad \text{B.6}$$

$$D_1 \left. \frac{\partial C}{\partial z} \right|_{L=L} = 0 \quad \text{B.7}$$

$$D_2 \left. \frac{\partial q}{\partial z} \right|_{L=0} = S\, q \quad \text{B.8}$$

$$D_2 \left. \frac{\partial q}{\partial z} \right|_{L=L} = 0 \quad \text{B.9}$$

Chapter 05

CO_2 capture in a continuous gas-solid trickle flow reactor

This chapter is based on the following article:
Veneman, R., Hilbers, T., Brilman, D.W.F., Kersten, S.R.A., CO_2 capture in a continuous gas-solid trickle flow reactor, submitted to Chemical Engineering Journal.

Abstract

A commercial supported amine sorbent, Lewatit® VP OC 1065, was applied in a continuous lab-scale CO_2 capture facility consisting of a trickle flow adsorber and a multi-stage fluid bed desorber.

The experimental work presented here summarizes over 300 hours of operating experience which is equivalent to approximately 350 adsorption/desorption cycles. The main focus here was on the performance of the adsorber column. We have measured the effect of process parameters like gas velocity, solid flux and CO_2 inlet concentration on adsorber performance in terms of the capture efficiency, productivity and working capacity. Typically around 5 kg of sorbent was circulated per hour. Capture efficiencies up to 81%, productivities up to 3.95 mol/m^3/s and working capacities up to 2.7 mol/kg were achieved.

The performance of the trickle flow adsorber was adequately described by a 1-D plug-flow model. The experimental results combined with the modeling work showed that a gas-solid trickle flow reactor is a suitable adsorber for the post-combustion capture of CO_2. The model was used to design an adsorber to capture 90% of the CO_2 emitted by a 500 MWe coal fired power plant. The trickle flow adsorber is expected to outperform the scrubber in the conventional MEA based process in terms of productivity; 1.1 compared to 0.6 mol/m^3/s in the MEA based process.

Finally, the energy demand of the lab scale capture facility was measured. Based on the measured desorber energy demand, the reaction heat of the sorbent material was estimated to be 62 kJ/mol. In total the energy associated with heating of the sorbent particles and desorption was 141 kJ/mol or 3.2 GJ/t at a working capacity of 1.2 mol/kg. At working capacities of 2.7 mol/kg the heat demand was reduced to values below 2 GJ/t. The experimental results obtained in the lab-scale CO_2 capture facility clearly show that these sorbents have the potential to outperform aqueous amine solutions on working capacity, column productivity and energy efficiency and hence there is a clear scope to develop this technology further.

1.0

Introduction

Application of carbon capture and storage (CCS) at fossil fuel burning plants is, among other alternatives, a technically feasible method to significantly reduce the global anthropogenic emission of CO_2. However, using the current state-of-art technology, this would result in an increase in the cost of electricity (COE) by 30-40% mainly due to the high cost of carbon capture. This increase in COE is a major hurdle in deployment and, hence, the development of a more cost effective capture technology is a main objective in CO_2 capture research.

Applying supported amine sorbents (SAS) may offer a low-cost alternative to the amine scrubbing process. The main cost driver in this conventional process is the heat demand of the process. A large part of this energy requirement is associated with heating of the aqueous amine solution from the absorption temperature to the desorption temperature and with the evaporation of solvent in the desorber column. Replacing H_2O as solvent by a solid support greatly reduces the energy required for CO_2 capture as the evaporation of water is inhibited and the energy required for heating the sorbent up to the desorption temperature is much lower due to the lower heat capacity of solid supports compared to water.
The design of an efficient adsorber column is critical to the performance of the novel CO_2 capture process. An efficient adsorber column would guarantee high solid conversions, assures high column productivities and capture efficiencies and has a low pressure drop. Especially the productivity deserves special attention as it is a measure for the systems' compactness. The productivity is defined as the amount of moles of CO_2 captured per unit of volume and time. Increasing this productivity reduces the size of the column and hence most probably also the cost of column. Since the absorber column in the MEA based benchmark process accounts for 40% of the total equipment cost we believe that the development of an adsorber with a higher productivity than the absorber in the benchmark process will help to further reduce the cost of CO_2 capture.
In addition to a high column productivity, the desorber should guarantee that the capacity of the sorbent particles is used optimally. This will minimize the sorbent circulation rate and maximize the sorbent working capacity resulting in lower sensible heat energy requirements. Also, the adsorber column should have a low pressure drop. The selection of a low pressure

drop adsorber design is essential considering the high gas flows involved in post-combustion CO_2 capture. The cost associated with the adsorber pressure drop is directly related to the compression energy required to overcome the adsorber pressure drop. Moreover, as the volumetric gas flow rates in the adsorber column are extremely high, gas velocities should preferably be high as well. This will reduce the footprint of the process and will result in a more viable aspect ratio.
The gas solids trickle flow reactor is expected to be perform well with respect to the above mentioned parameters as it provides counter-current gas solid contacting, high gas solid heat and mass transfer rates and allows for high gas velocities in the adsorption column. The counter-current gas solid contacting maximizes the driving force for mass transfer and allows high sorbent working capacities as the sorbents leaving the column will be nearly saturated with CO_2 at the inlet gas phase CO_2 concentration rather than at the outlet CO_2 concentration.
At the moment of writing, only a few articles have been published on application of supported amine sorbents in a continuous process [1-4]. In these studies the focus was mainly on testing the sorbent performance rather than on the performance of the system as a whole.

The aim of the experimental work presented here is twofold; (1) identify the effect process parameters on the performance of a lab-scale trickle flow adsorber and (2) verify the accuracy of a trickle flow reactor model developed here. The mathematical reactor model is developed to describe and interpret the experimental results and to be used in sizing studies. Finally, the performance of a typical MEA scrubber is compared to the performance of a full scale trickle flow adsorber in terms of efficiency and productivity. In addition we have measured the energy demand of the process under continuous operation.

2.0

Experimental

2.1 | Materials

The sorbent material used in this study is Lewatit® VP OC 1065 (obtained from Lanxess). It is a polystyrene based ion exchange resin (IER) containing primary benzyl amine units [5]. The resins are spherical shaped beads with an average diameter of 688 µm. The materials' pore volume, pore surface area and average pore size are 0.27 cm^3/g, 50 m^2/g and 25 nm respectively. The CO_2 adsorption isotherms for this sorbent material were presented in Chapter 3.

Table 1: Properties of Lewatit® VP OC 1065.

N content (mol/kg)	6.7 [5]
Pore volume (cm^3/g)	0.27
Pore size (nm)	25
Pore area (m^2/g)	50
Particle density (kg/m^3)	880
Average particle size (µm)	688
Terminal velocity (m/s) (in N_2 at 298 K)	2.5

2.2 | TGA testing

To better understand the adsorber's performance, sorbent uptake rates measured on small scale are compared to measurements done in the continuous setup. A NETSZCH STA 449 F1 Jupiter thermal gravimetric analyzer (TGA) was used to assess the CO_2 adsorption capacity of the sorbent material. In a typical adsorption experiment around 15 mg of sorbent was placed inside the TGA furnace. The sample was heated up to 80°C in N_2 to desorb any pre-adsorbed CO_2 and moisture. The temperature was kept constant until the sample mass stabilized. Then, the sample was cooled down to the desired adsorption temperature after which CO_2 was fed to the TGA furnace. The uptake of CO_2 by the sorbent sample results in an increase in the sample mass. The sorbent CO_2 uptake, in mol/kg sorbent, was calculated from the weight change of the sample during adsorption. Typically, after 4 hours of adsorption time the change in the sample mass was minimal (<0.01 mol/kg/hr) and the measurement was stopped. The adsorption experiments were performed at different temperatures and CO_2 partial pressures to ob-

tain the data required to construct an adsorption isotherm. Desired gas compositions were obtained by mixing high purity (grade 5.0) N_2 and high purity (grade 5.0) CO_2. The specific configuration of the TGA equipment limited the CO_2 concentration to a maximum of 80 vol% of CO_2 at 1 atm.

2.3 | Lab-scale continuous testing

Figure 1 shows a scheme of the set-up used in this study. The set-up consists of an adsorber column, a desorption column and solids transportation section. The adsorber, desorber and the riser are all interconnected by rotary valves to control the solid circulation rate and avoid back mixing of gas streams. These solid valves allow for solid circulation rates up to 12.5 kg/hr. Inside the adsorber, the gas and the solids are contacted in a countercurrent manner over a packed column under dilute phase or trickle flow conditions [7]. The solids are introduced at the top of the adsorber column and move through the reactor under the influence of gravity. The gas is introduced at the bottom of the adsorber column. The adsorber's internal diameter and height are 21 mm and 1300 mm respectively. The column is packed with sieve plates at every 30 mm. The sieve plates slow down the particles on their way down, increasing the sorbent residence time.

The desorber is a carbon steel fluidized bed of five stages (110 mm ID) interconnected via downcomers (30 mm ID, 270 mm H). The bottom stage is connected to a rotary valve which feeds the solids to the riser. The desorber can be fluidized with either N_2 of CO_2. The staged fluid bed contains 3-4 kg of particles and is electrically heated. The design of the multi-stage fluid bed prevents back mixing of the solids, providing a reasonable degree of plug flow of the solids phase. The average residence time of the solids inside the desorber ranges from 45 – 90 minutes depending on the solid circulation rate. Each tray of the desorber column was heated by a separate trace heater (5 x 220 W) and the duty of the each electrical heater was monitored continuously.
Generally, in a small lab scale set-up, a large amount of heat is lost to the environment and this has to be corrected for in order to get a reliable estimate of the heat demand of the system. To do so, the desorber was fluidized and heated to 100°C. The temperature was then kept constant and the duty of the desorber was monitored over a long period of time. During this time no solids were circulated and hence no CO_2 was captured. The measured desorber duty gives an estimate for the amount of heat lost to the environment. Subsequently, the heat demand of the desorber was measured for different solid circulation rates. In these experiments the adsorber

column was operated with CO_2-free gas. This gives an estimate of the heat required to heat up the solid material from the adsorber to the desorber temperature.

The solids transportation section consists of a rotary valve controlling the solids circulation rate, a riser column to transport the regenerated particles back to the adsorber column and a cyclone to separate riser gas from the solids. The riser is a metal pipe (ID 8.5 mm, 2900 mm) through which the solids are pneumatically transported from the desorber to the adsorber. The top end of the riser is connected to a cyclone that separates the solids from the transport gas, in this case N_2. Two infrared gas analyzers (SICK MAIHAK, SIDOR Extractive Multi-component Gas Analyser) were used to monitor the CO_2 concentration in the adsorber outlet gas (detection range: 0-15 vol%) and the desorber gas (detection range: 0-50 vol%). Due to the specific configuration of the CO_2 analyzers used in this study it was not possible to detect CO_2 concentrations higher than 50 vol%. Hence, no measurements were conducted with gas containing more than 50 vol% of CO_2. Table 2 shows a summary of the setup's characteristics.

Table 2: Set-up characteristics.

Adsorber properties	
Type	Gas Solid Trickle flow reactor
Packing	Perforated trays
Internal diameter (cm)	2.1
Reactor length (cm)	180
Reactor volume (cm^3)	442
Internals volume fraction (%)	2.5
Solid flux range ($kg/m^2/s$)	1-5
Gas velocity range (m/s)	0-1
Capture efficiency (-)	<90%
Productivity ($mol/m^3/s$)	<6
Maximum capacity of the sorbent (mol/kg)	2.8
Solid holdup (m_S^3/m_R^3)	<3%
Desorber properties	
Type	Multistage fluid bed
Number of stages (-)	5
Solid hold-up (kg)	3-4
Heating capacity (W)	5 x 220
Temperature (°C)	90-120

As mentioned in the introduction, the sorbent working capacity, the column productivity, CO_2 capture efficiency and the energy demand of the system are used in this study to assess the performance of the adsorber column. These performance parameters will be measured and compared to typical values reported for the amine scrubber in the MEA based process, summarized in the Table 4.

Table 3: Definition of performance parameters studied here.

Equation used to calculate the capture efficency

$$E=1-\frac{u_{G,out}C_{G,out}}{u_{G,in}C_{G,in}} \quad (1)$$

Equation used to calculate the column productivity

$$P=\frac{u_G C_{G,in} E}{L} \quad (2)$$

Equation used to calculate the working capacity

$$\Delta q=\frac{P L}{S} \quad (3)$$

Table 4: Typical values for the selected performance indicators in the MEA benchmark process.

Parameter	MEA [6]
Capture efficiency (%)	90
Productivity (mol/m^3/s)	0.6
Pressure drop (mbar)	103
Working capacity (mol/kg)	0.94
Gas velocities (m/s)	1.8
Heat demand (GJ/tCO_2)	4.2

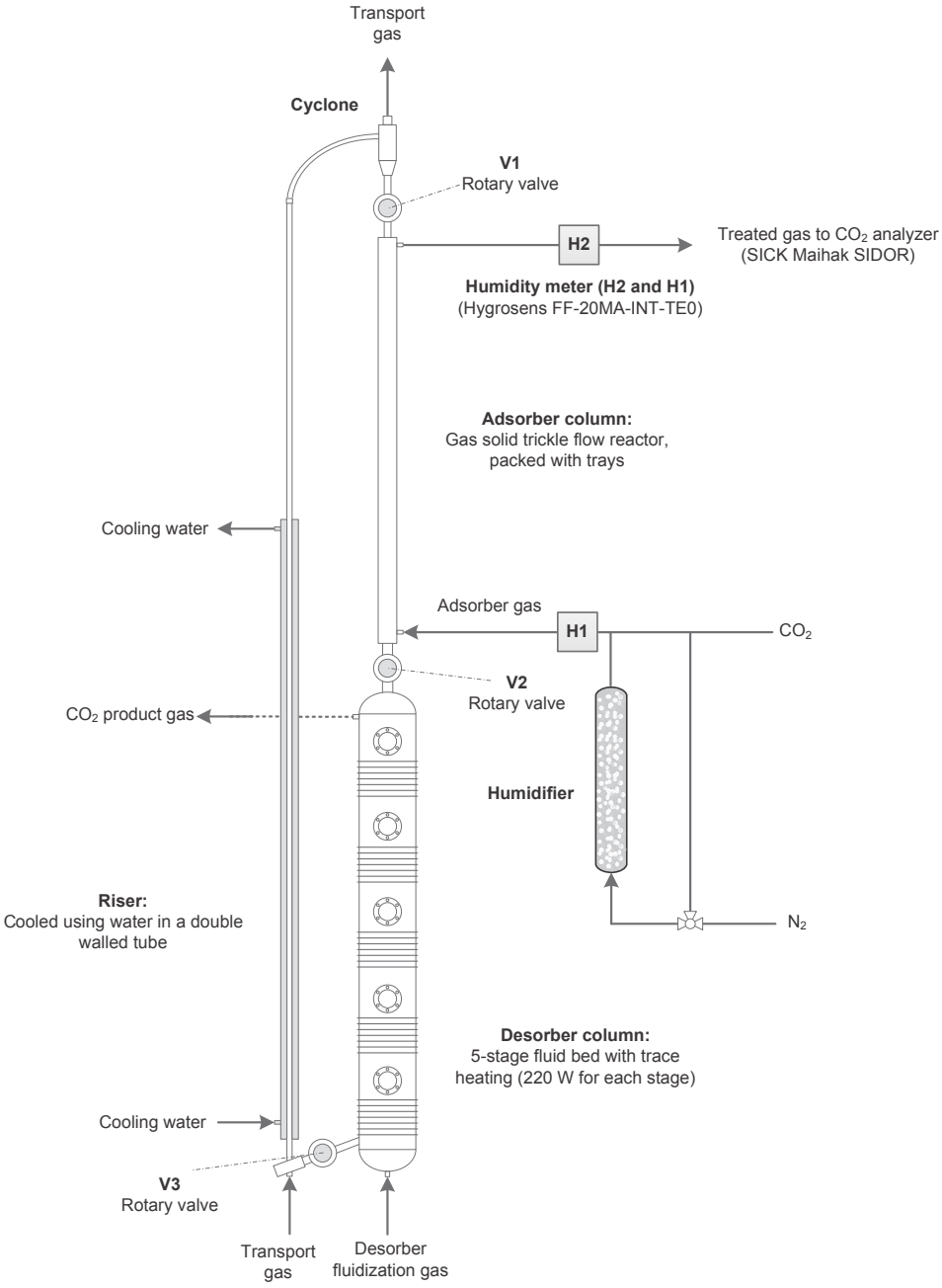

Figure 1: Schematic of the experimental set-up

3.0

Column hydrodynamics & Reactor modelling

3.1 | Column hydrodynamics

In a trickle flow reactor, gas and solids are contacted in a counter-current manner over a packed column under dilute phase or trickle flow conditions [7]. The purpose of the packing is to slow down the sorbent particles on their way down. This results in increased residence times and consequently in a higher solid holdup. Also the gas, flowing in counter current direction, slows down the solids. The sorbent holdup will be highest for densely packed columns operated at gas velocities close to the terminal velocity of the sorbent particles. The terminal velocity determines the upper limit for the operating gas velocity. At gas velocities very close to the particle's terminal velocity flooding will occur.

Since the solid hold-up, β, directly relates to the specific interfacial surface area available for mass exchange between the solid particles and the gas, it will, to a large extent, determine the productivity and efficiency of the column. The solid holdup is calculated using equation 4 in Table 5 [8]. In this equation the solid flux, S, is equal to the amount of solids circulated per second per square meter of cross-sectional area of the reactor and us represents the effective downward velocity of the sorbent particles. This trickle velocity is mainly a packing characteristic. Below the so-called loading point of the column, the solid hold-up linearly increases with an increase in the solid flux and the trickle velocity is constant [9].

Here, this trickle velocity of the solids (u_s in equation 4) was calculated based on dedicated solid holdup measurements presented in Appendix C. The solid hold-up was determined for different solid fluxes and gas velocities by simultaneously closing Valve 1 and Valve 2 and measuring the volume of the solids trapped in the adsorber section. Figure 2 shows a plot of the trickle velocity as a function of the relative velocity. The relative velocity was defined here as the ratio of the linear gas velocity in the column, u_G/ε, and the particle's terminal velocity, u_t. For this packing, the trickle velocity was found to be 0.24 m/s. In literature, values for the trickle velocity range from 0.2-0.05 m/s (See Figure 2).

In general both the dynamic holdup of solids and the static holdup of solids are considered in trickle flow columns. The dynamic holdup refers to the solids that flow through the column with a velocity equal to us. The static solid holdup refers to the solids that remain in the column. The static solid-holdup is however a strong function of the configuration of the packing in the column [9] and in the column considered here the contribution of the static solid hold-up was negligible (<0.1vol%).

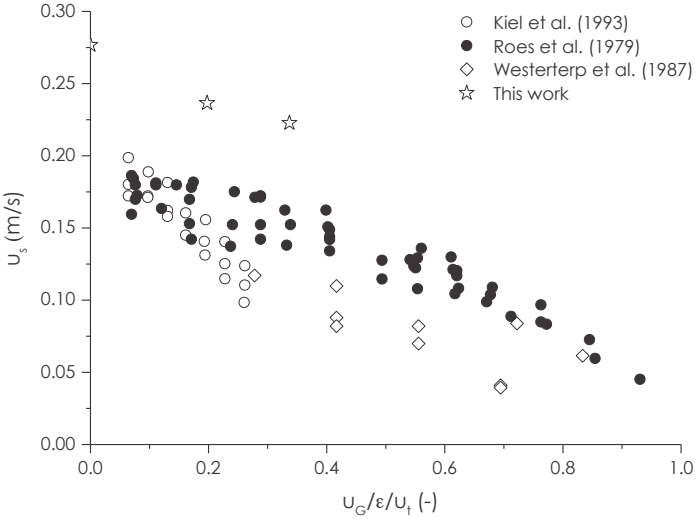

Figure 2: A plot of the trickle velocity as a function of the relative gas velocity in the column. Comparison of the experimental downward solid velocity to values presented by Roes et al. [9], Kiel et al. [7] and Westerterp et al. [10] for solid fluxes between 0.1 and 6 kg/m^2/s. The solid flux used in the base case was 4.1 kg/m^2/s.

3.2 | Reactor modelling

A mathematical, Matlab® based, model of the adsorber was developed and the modelling results are compared with data obtained from the continuous gas-solid trickle flow column. The model includes external mass transfer limitations, inter-particle mass transfer limitations and reaction kinetics as well as the effect of temperature and pressure on the equilibrium CO_2 adsorption capacity of the sorbent particles. The adsorption isotherm equation was presented in Chapter 3. In the description of the trickle flow adsorber and the sorbent particles it was assumed that:

- The adsorption reaction rate is first order in the gas-phase CO_2 concentration and first order in the amount of free adsorption sites. More information on the form of the rate equation can be found in Appendix C.
- Both the solid phase and the gas phase move in plug flow through the trickle flow column.
- The solids velocity is constant over the length of the reactor and the gas velocity does not influence the solid holdup.
- Heat effects can be neglected.

The governing equations describing the mass transfer of CO_2 are summarized in Table 5. The equations were solved using the BVP4c solver in Matlab®. The only unknown parameter in the model equations presented in Table 5 is the kinetic rate constant k. The effective diffusion coefficient, D_p, was calculated based on correlations for the pore diffusion coefficient. The value for the intrinsic reaction rate constant was obtained by fitting k to experimental data. The value for k that gave the best fit to the experimental data was 0.014 m_G^3/mol/s.

Based on this fitted kinetic rate constant, we calculate particle effectiveness factors in the range of 60-70%. The particle effectiveness compares the rate of pore diffusion with the intrinsic reaction rate between CO_2 and the amine groups on the support pore space. For slow reaction rates the particle effectiveness, η, is close to 1, indicating that the reaction rate limits the sorbent's overall CO_2 uptake rate. For fast reaction rates, $\eta << 1$, indicating that the uptake of CO_2 is no longer only a reaction rate limited process but diffusion limitations are playing a role as well. A particle effectiveness of 60-70% points towards an uptake rate of CO_2 determined by a combination of pore diffusion and reaction kinetics.

Figure 3 shows a parity plot of the fraction of CO_2 in the outlet gas, as measured in experiments performed in the lab-scale capture set-up and the outlet fraction as calculated by the developed model. The experimental work includes measurements done at a range of different gas velocities, a

range of different solid flows and a range of different inlet CO_2 concentrations. Figure 3 shows that the model is capable of predicting the measured outlet fraction adequately. The calculated outlet concentrations are within 15% of the measured value. The deviation between the model and the experimental results was found to be largest for measurements done at high gas velocities and then especially in combination with high solid fluxes. This and other results, will be discussed in more detail below.

Table 5: Model equations.

Solid holdup

$$\beta = \frac{S}{\rho_s u_s} \tag{4}$$

Gas phase mass balance

$$\frac{du_G C_G}{dz} = -\frac{6\, k_G \beta}{d_s} (C_G - C^*) \tag{5}$$

Solid phase mass balance

$$S\frac{dq}{dz} = -\frac{6\, k_G \beta}{d_s} (C_G - C^*) \tag{6}$$

Uptake rate equation

$$\frac{6\, k_G \beta}{d_s} (C_G - C^*) = k\, C^* (q_e - q) \beta \rho_s \eta \tag{7}$$

Boundary conditions

$$q\,(L) = 0 \tag{8}$$

$$C_p(0) = Cin \tag{9}$$

Thiele modulus and effectiveness for the sorbent particle

$$\eta = \frac{3}{\phi^2} (\phi \coth(\phi) - 1) \tag{10}$$

$$\phi = \frac{d_s}{2} \sqrt{\frac{k(q_e - q)\rho_s}{D_p}} \tag{11}$$

Equations used to calculated the external mass transfer rate

$$Sh_G = 2 + 0.6 \cdot Sc_G^{\frac{1}{3}} Re_G^{\frac{1}{2}} = \frac{k_G d_S}{D_{AB}} \tag{12}$$

$$Re_G = \frac{\rho_G \cdot d_S |U_S - U_G|}{\mu_G} \tag{13}$$

Equation used to calculate the Knudsen diffusion coefficient

$$D_{Kn} = \frac{d_p}{3} \sqrt{\frac{8RT}{\pi M_i}} \tag{14}$$

Equation used to calculate the pore diffusion coefficient

$$D = \left(\frac{1}{D_{AB}} + \frac{1}{D_{Kn}} \right)^{-1} \tag{15}$$

Equation describing the effective pore diffusivity

$$D_P = \frac{\varepsilon}{\tau} D \tag{16}$$

Table 6: Model input.

Parameter	Symbol	Value	Unit
Particle diameter	d_p	$7.0\ 10^{-4}$	m_p
Particle density	ρ	880	kg_p/m_p^3
Ratio of particle voidage and pore tortuosity	$\frac{\varepsilon}{\tau}$	0.10	m_G^2/mp
Particle voidage	ε	0.23	m_G^3/m_p^3
Prandtl number (For air at 313 K)	Pr	0.71	-
Schmidt number	Sc	0.83	-
Pore diameter	d_{pore}	$2.5\ 10^{-8}$	m
Molecular diffusion coefficient (For CO_2 in air at 313 K)	D_{AB}	$1.65\ 10^{-5}$ [11]	m_G^2/s
Knudsen diffusion coefficient (at a pore diameter of 25 nm and 313 K)	D_{Kn}	$3.2\ 10^{-6}$	m_G^2/s
Effective pore diffusion coefficient	D_p	$3.8\ 10^{-7}$	$m_G^3/m_p/s$
Intrinsic reaction rate	k	0.014	$m_G^3/mol_{CO2}/s$
Adsorber temperature	T_{ads}	313	K
Adsorber pressure	P_{ads}	1.1	bar

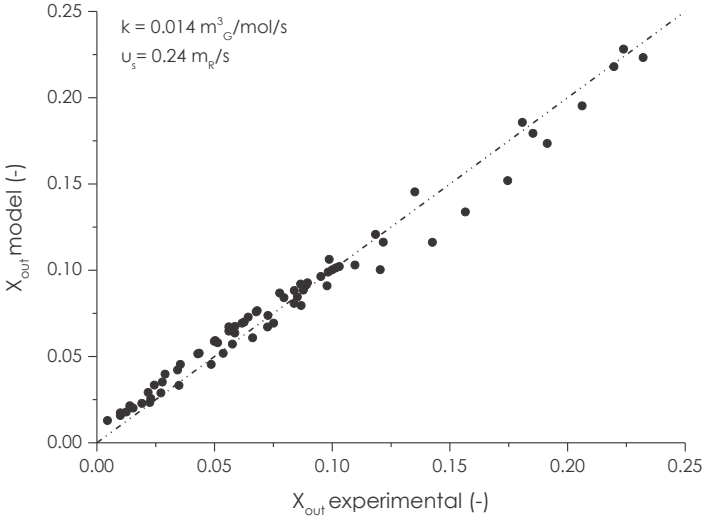

Figure 3: Parity plot of the measured and predicted outlet CO_2 fraction. Gas velocities were varied between 0.2 and 1 m/s. Solid fluxes were varied between 1 and 5 kg/m^2/s. The inlet CO_2 concentration was varied between 4 and 30 vol%.

4.0

Results and Discussion

4.1 | Variation of process parameters

The focus of the experimental work presented here is on the steady state performance of the lab-scale capture setup described in section 3. All reported data, i.e. values for temperatures, pressures and concentrations, are time-averaged values measured over a time interval of at least half an hour of experimental time. Table 7 shows the raw data and operating parameters for two continuous capture experiments, performed as duplo. Experiment 1 was part of a ten hour long continuous run in which the solid flux was varied. Experiment 2 was part of an eight hour long continuous run in which the gas velocity was varied. The experimental results show a good reproducibility. Even the pressure gradients and temperature gradient over the adsorber column are comparable between the two experiments. The difference in temperature between the gas entering the asdorber and the gas leaving the adsorber is only 3 K. This shows that heat effects are small in this reactor. More information can be found in Appendix C.

The heat demand of the desorber column is also reported in Table 7. In both experiments, tray one (top tray) and tray five (bottom tray) have a higher heat demand than the other trays. This is because a relatively large amount of heat is needed to heat the cold solids entering stage one and the cold fluidization gas on stage five. The higher desorber heat demand in experiment 1 can be explained by the slightly higher temperatures on each stage in experiment 1. As explained, in a small lab scale set-up, a large fraction of the heat added to the system is lost to the environment and this heat loss is a function of the temperature inside the desorber column.

In the experimental work performed, we have gathered over 300 hours of operating experience, the equivalence of approximately 350 adsorption/desorption cycles. Although the regeneration conditions tested here were relatively mild (90-120°C in N_2 in all experiments), it is important to note that we did not see any decrease in capacity of the sorbent material during the 300 hours of testing. The adsorption behavior of the fresh sorbent particles was compared to that of the used sorbent particles in two separate adsorption measurement done in the TGA described in section 2. The shape of the adsorption curve as well as the equilibrium capacity of the used sorbent material was the same as that of the fresh sorbent particles. Comparison

of the particle size distribution of the sorbent material before and after the testing runs showed no sign of attrition.
As mentioned in the introduction, the focus here is mainly on the measurement of the performance of the adsorber column. Still, under continuous operation the performance of the adsorber is closely linked to the performance of the desorber. The adsorber cannot operate in steady state without the stable operation and a constant degree of sorbent regeneration.
In TGA experiments we found that at 100°C and in N_2 the sorbent particles can be fully regenerated within 5 minutes of regeneration time. In the multistage fluid bed residence times are estimated to be much longer, over 30 minutes. Hence, it seems reasonable to assume that in all continuous experiments the sorbent particles are fully regenerated in the desorber.
On a process scale it is essential to regenerate the sorbent particles in a pure CO_2 environment [2]. Therefore we have also tried to estimate experimentally the time required to regenerate these sorbent particles in a CO_2 atmosphere. After an initial desorption step to desorber any pre-adsorbed CO_2 and H_2O, the sorbent particles were saturated with CO_2 at 40°C and at a CO_2 partial pressure of 0.8 bar in the TGA apparatus. Subsequently, the sorbent particles were heated up to 150°C resulting in the desorption of the adsorbed CO_2. This experiment was done twice; first with a heating rate of 1 K/min and then with a heating rate of 20 K/min. The CO_2 capacity of the sorbent material was calculated from the weight change during desorption. In both experiments, the sorbent particles were completely regenerated at 150°C. Moreover, it was found that the degree of regeneration was only a function of temperature in these experiments and not a function of heating rate. This implies that for heating rates between 1-20 K/min, the degree of desorption is equilibrium limited and not limited by the desorption reaction rate. In the desorber, sorbent residence times do not have to be much longer that 5 minutes to ensure full sorbent regeneration as long as the sorbent particles have attained the desired regeneration temperature before leaving the desorber column. The specific configuration of the TGA did not allow for tests with even higher CO_2 partial pressures or higher heating rates. The TGA results are presented in Appendix C.

Table 7: Raw data and calculated parameters obtained from two continuous capture experiments done under the same conditions.

Adsorber conditions	Exp1	Exp2	Unit
Adsorber mass flux (S)	3.2	3.2	kg/m²/s
Feed N_2	9.2	9.2	L/min
Feed CO_2	1.2	1.2	L/min
Total feed adsorber	10.4	10.4	L/min
Superficial gas velocity (u_G)	0.51	0.51	m/s
Inlet CO_2 concentration (X_{in})	11.2	11.2	vol%
Adsorber feed pressure	1.12	1.11	bara
Adsorber outlet pressure	1.09	1.09	bara
Outlet temperature solids	42.2	40.6	°C
Adsorber gas feed temperature	25.1	25.4	°C
Adsorber gas outlet temperature	28.4	28.1	°C
Outlet CO_2 concentration (X_{out})	4.99	5.03	vol%
CO_2 captured	27.9	27.7	mmol/min
Performance parameters			
Capture efficiency (E)	58.2	57.9	%
Productivity (P)	1.05	1.05	mol/m³/s
Adsorbent loading (Δq)	0.43	0.43	mol/kg
Circulation rate (CR)	1.36	1.35	kg/mol fed
Heat demand desorber			
Power stage 1	206	173	W
Power stage 2	77	86	W
Power stage 3	59	63	W
Power stage 4	57	48	W
Power stage 5	152	156	W
Cumulative power	551	526	W
Temperature stage 1	95	90	°C
Temperature stage 2	98	95	°C
Temperature stage 3	99	97	°C
Temperature stage 4	99	98	°C
Temperature stage 5	99	99	°C

It should be noted that the length of the adsorber column of the lab-scale capture set-up limits the columns performance. The length of the reactor is only 1.3 meters, which is roughly a factor 10 shorter than an industrial scale MEA scrubber. As a result, in its current configuration, it is not possible to achieve high capture efficiencies, high productivities and high working capacities all at the same time. Instead the reactor model will be used for a design and sizing study for a full-scale adsorber column.

The process parameters we have focused on here include the solid circulation rate, the CO_2 concentration at the inlet of the adsorber and the inlet gas velocity. In post-combustion capture, the inlet CO_2 concentration depends on the type and configuration of the power plant from which the CO_2 containing gas originates. For the capture process, the inlet CO_2 concentration is given parameter. The effect of the CO_2 inlet concentration on the column performance was tested here just to validate the reactor model.
The solid circulation rate was varied here to validate the simplified way of describing column hydrodynamics. However, an increase in the solid circulation rate results in a decrease in the sorbent working capacity since more solids are circulated to capture the same amount of CO_2. Since the working capacity has a large impact on the heat demand of the process, we aim to operate the process at a minimum solid circulation rate.

In the following six figures, data is presented for experiments done at different solid circulation rates, CO_2 concentrations and the inlet gas velocities and compared to model results. The lines plotted in these graphs represent the model results. The measured data are represented by data points in these graphs.

Figure 4 shows a plot of the adsorber productivity as function of the solid flux. The graph shows the productivity for three different experimental runs. In each run the CO_2 inlet concentrations was changed; from 3.8 vol% in the first run to 14.9 vol% and 26.8 vol% in the second and third run, respectively. This graph summarizes over 20 hours of steady state experimental time. The productivity represents the amount of CO_2 captured per m^3 of reactor volume per second. Increasing the solid flux linearly increases the productivity of the adsorber column which is due to an increase in the amount of solids present in the column, β, which also increases linearly with an increase in solid flux. The amount of particles inside the adsorber directly relates to the amount of amine groups available for reaction and thus an increase in the solid holdup is expected to improve the column productivity.

At a solid flux of 4.5 kg/m^2/s the column productivities are considerable; up to 2.4 mol/m^3/s at a capture efficiency of 55% and a gas velocity of 0.5 m/s. Comparing the experimental results (data points) with the modelled data (lines) in Figure 4, we can see that the model describes the effect of both the solid flux and the inlet CO_2 concentration on the adsorber performance adequately. It should be noted that the hydrodynamics of the adsorber column are described by only one, very simple, equation (namely equation 4), and the effect of for example the gas velocity on the solid holdup is not included in the model presented here. For this small lab-scale set-up and at the chosen gas velocity range this simplified model seems to suffice however. Deviations between model predictions and the experimental results might be caused by temperature effects in the adsorber column. Temperature effects are expected to be stronger at high column productivities as the heat released in the adsorber increases linearly with the column productivity. These temperature effects influence gas residence times as well as the equilibrium CO_2 adsorption capacity.

Figure 5 shows the column productivity as function of the inlet CO_2 fraction in the gas. In total this plot summarizes over 10 hours of continuous operation. In addition to the experiments performed with different mixtures of N_2 and CO_2, also several experiments were performed using pure CO_2 as adsorber inlet gas (Xin = 100%). In these experiments the inlet gas velocity through the column was kept constant and only the ratio of N_2 over CO_2 was changed. In the pure CO_2 adsorption measurements the initial gas velocity was the same as in the experiments with N_2/CO_2 mixtures.
These measurements were done in order to exclude mass transfer limitations in an attempt to verify the kinetic rate equation used in the reactor model. To do so we would need to measure the uptake rate as a function of the sorbent CO_2 loading. This data can be extracted from column productivity measurements at different sorbent working capacities. However, in these pure CO_2 measurements we found that the sorbent particles are saturated with CO_2 within around six seconds and the design of the set-up did not allow for the systematic variation of the sorbent residence time.

The data shown in Figure 5 shows a linear relation between the CO_2 feed concentration and the column productivity at a constant solid flux i.e. a constant β. A higher inlet CO_2 concentration increases the driving force for the uptake of CO_2 and this will result in a higher column productivity. A linear increase of the productivity with the inlet concentration points towards an external mass transfer limited process or reaction rate limited process with

a first order dependence on the CO_2 concentration.
However, external mass transfer is much faster than the uptake rates measured in the lab-scale set-up. Based on the kinetic rate equation we expect productivities of around 2.3 mol/m_R^3/s (Xin = 20 vol%, η = 1, β = 0. 9%, q_e = 2.4 mol/kg, ρ_s = 880 kg/m^3, k = 0.014 m_G^3/mol_{CO2}/s) whereas for a fully externally limited process we expect productivities of around 93 mol/m_R^3/s (Xin = 20 vol%, k_G = 0.14 m/s, β = 0. 9%, C* = 0). Clearly, the productivities we measured in the experimental work do not match with the productivities we would expect for an external mass transfer limited process. Therefore, we conclude that the linear relation between the CO_2 feed concentration and the column productivity, as shown in Figure 5, can only be the result of process limited by a kinetics with a first order dependence on the gas phase CO_2 concentration.

The pure CO_2 measurement shown in Figure 5 seems to deviate from this linear behavior. The reason is that the sorbent particles have attained their equilibrium CO_2 capacity well before they leave the adsorber column. At the column outlet the sorbent particles have adsorbed around 2.8 mol of CO_2 per kg of sorbent. Saturated sorbent particles do not adsorb more CO_2 and hence they are inactive during part of their stay in the adsorber column so lowering the productivity. The solid residence time in the adsorber is roughly 5-6 seconds (L = 1.3 m and u_s = 0.24 m/s). This means that without mass transfer resistances (i.e. in pure CO_2) the sorbent particles can be saturated with CO_2 in less than 6 seconds.

Figure 5 shows three lines calculated by the reactor model. Each line is calculated using a different value for the intrinsic reaction rate, k. As mentioned the value for k that gave the best fit to the experimental data was 0.014 m_G^3/mol/s. The two other lines represent the lines for a 'k' twice as large and half this 'best fit' value. Looking at Figure 5, clearly a much lower value for k results in an underestimation of the columns performance. A higher value for k overestimates the columns performance.

Figure 6 shows the results for pure CO_2 experiments done at higher solid fluxes but at the same inlet gas velocity. Also at these higher solid fluxes the model calculated productivities match with the values calculated from experimental results. Again also at these higher solid fluxes the particles are fully saturated with CO_2 at the outlet of the adsorber column.

The working capacity is calculated directly from the column productivity and the solid circulation rate. The working capacity of the sorbent particles is not a strong function of the gas velocity or the solid flux through the column. In Appendix C data is included supporting this statement.

Figure 7 shows a plot of the working capacity as function of the CO_2 inlet concentration. The pure CO_2 measurements done at different solid fluxes are shown as well. As mentioned, in pure CO_2 the sorbent particles are saturated with CO_2 in around 6 seconds. We see that for all the pure CO_2 measurements the sorbents achieve the same working capacity, i.e. achieve their maximum CO_2 capacity. At CO_2 concentrations relevant for post-combustion CO_2 capture (11 vol%) the working capacity of the sorbent, in this capture facility, is only 0.47 mol/kg which is only 20% of the sorbent equilibrium capacity under these conditions (q_e = 2.3 mol/kg, 40˚C and 11 vol% at 1 bar total pressure). Higher working capacities at this inlet concentration can be achieved by increasing the length of the adsorber reactor, thereby creating longer sorbent residences times.

Figure 8 show the capture efficiency as function of the superficial gas velocity through the column. Higher gas velocities result in higher CO_2 feed rates. The CO_2 uptake rate in the column is however not a function of the gas velocity. This is in line with the conclusion drawn earlier; the uptake rate is not limited by external mass transfer. As a consequence, the amount of CO_2 captured in the column remains largely unchanged over the velocity range tested here. Hence, it is the fraction of inflowing CO_2 captured that is decreasing with an increase in gas velocity. We clearly see that the model starts deviating from the measured data points at high solid fluxes and high gas velocities. We measure a higher capture efficiency under these conditions than the model predicts. It is very well possible that under these conditions the gas velocity is starting to have an impact on the solid holdup. A high gas velocity will result in an increase in the solid hold-up in the column and this will in turn improve the performance of the adsorber column. As mentioned before the hydrodynamics of the adsorber column are described by only one very simple equation, equation 4, and the effect of the gas velocity on the solid holdup is not included in the model presented here.

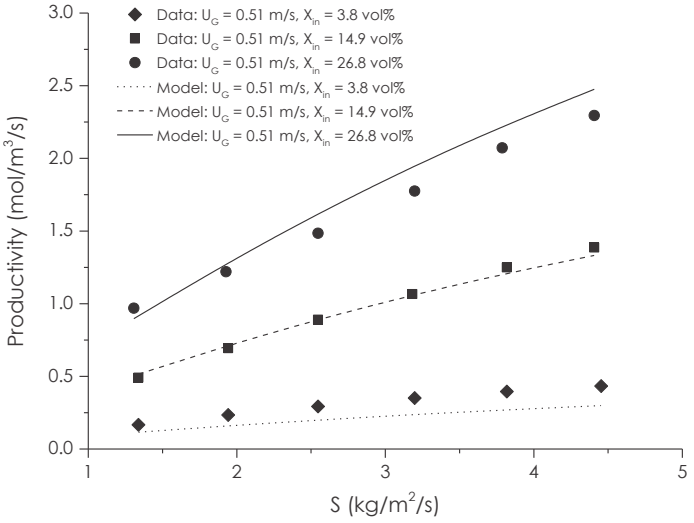

Figure 4: Plot of the column productivity as a function of the solid flux for three different CO_2 inlet concentrations. The gas velocity was 0.51 m/s. The inlet CO_2 fraction was 3.8 vol%, 14.9 vol% and 26.8 vol% respectively.

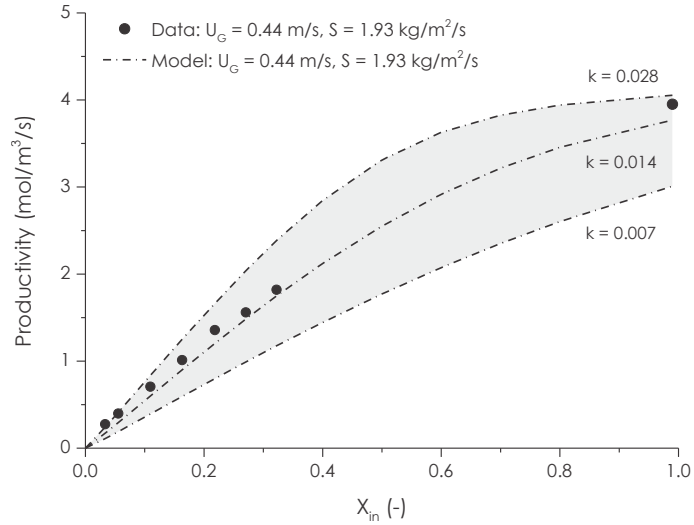

Figure 5: Plot of the column productivity as a function of the CO_2 inlet fraction. The gas velocity was 0.44 m/s. The solid flux was 1.93 kg/m^2/s.

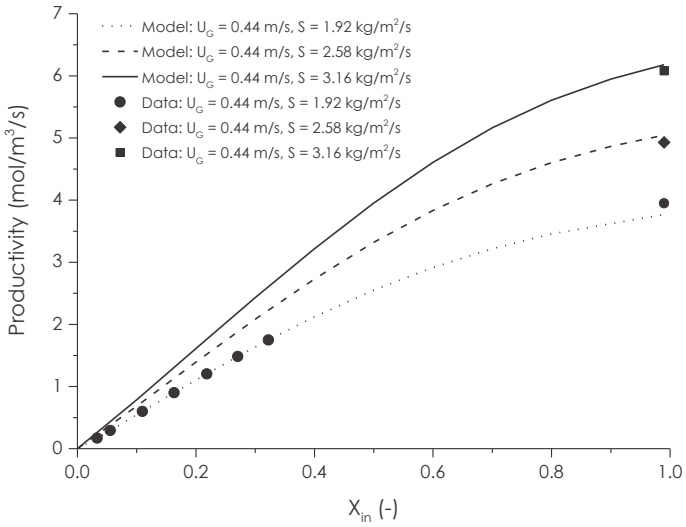

Figure 6: Plot of the column productivity as a function of the CO_2 inlet fraction. The gas velocity was 0.44 m/s.

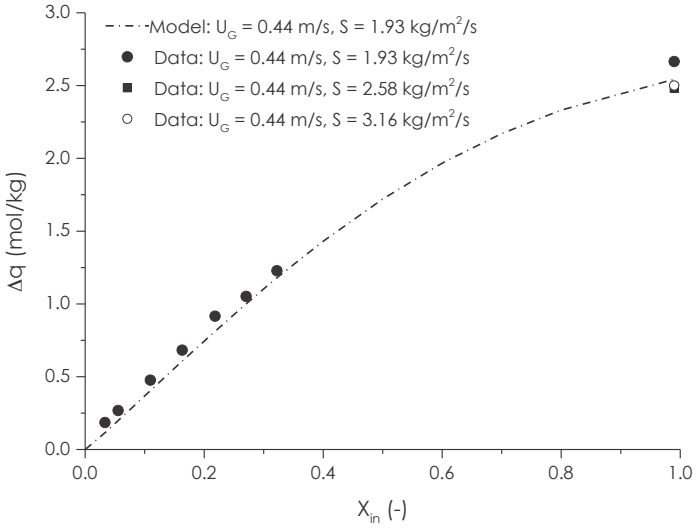

Figure 7: Plot of the sorbent working capacity as a function of the CO_2 inlet concentration. The gas velocity was 0.44 m/s.

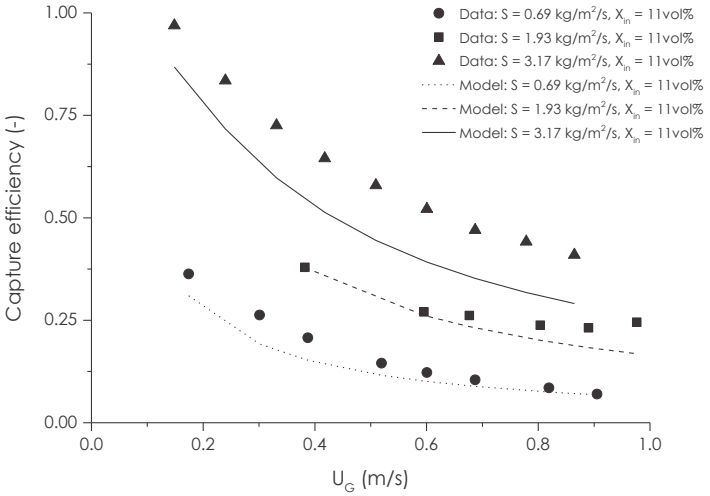

Figure 8: Plot of the capture efficiency as a function of the superficial gas velocity. The inlet concentration was 11 vol%.

4.2 | Energy demand

As mentioned in the introduction, the main cost driver in the conventional capture technology is the heat required for solvent regeneration. The net thermal energy demand of the MEA based process is around 4.2 GJ/tCO_2 or 185 kJ/mol [6]. A large part of this energy requirement is associated with heating of the aqueous amine solution from the absorption temperature to the desorption temperature and with the evaporation of solvent in the desorber column. Replacing H_2O as solvent by a solid support greatly reduces the energy required for CO_2 capture as; the evaporation of water is inhibited and the energy required for heating the sorbent up to the desorption temperature is much lower due to the lower heat capacity of solid supports, when compared to water. The heat demand of the desorber in the SAS based process will mainly be attributed to the heating of the solid particles and with the desorption of CO_2 i.e. the reaction heat. Estimates for the total heat demand of the process are presented in literature and are estimated at 1.9 GJ/tCO_2 [12, 13].

In the experimental study presented here we have tried to measure the heat demand of the process experimentally. The power demand of the trace heaters providing the heat to the desorber was monitored.
Since this is a small scale capture facility, a relatively large portion of the total heat demand of the system is associated with heat loss to the environment and with heating and of the cold fluidization gas. This was corrected for by measuring the heat required to keep the desorber column at a constant desorption temperature of 100°C without circulating the solids and without feeding CO_2. Subsequently, the heat demand of the desorber was measured for different solid circulation rates. In these experiments the adsorber column was operated with CO_2-free gas. Hence the additional heat required to keep the desorber at the set temperature was only associated with the sensible heat of the solids. Based on these measurements the heat capacity of the solids was estimated to be around 1700 J/kg/K. This is close to the value reported in literature for these type of particles of 1500 J/kg/K [14].

Figure 9 shows the heat demand of the desorber column plotted against the amount of CO_2 captured. In the experiments plotted in Figure 9 the inlet CO_2 concentration was varied resulting in an increase in the amount of CO_2 captured in the adsorber column. These experiments were presented earlier in Figure 5. The heat demand of the desorber increases with an increase in the amount of CO_2 that is captured; the more CO_2 is captured in

the adsorber, the higher the amount of heat required in the desorber. Although there is clearly scatter in the measured desorber heat demand, the slope of the plot represent the reaction heat. The slope of the line in Figure 9 is 62 kJ/mol. This values lies in the range typical for CO_2 adsorption by amine molecules; 40-80 kJ/mol [15, 16].

In Figure 10 we have plotted the total heat demand of the capture process plotted as a function of the working capacity of the sorbent material. The sorbent working capacity has a big impact on the heat demand of the process. The more CO_2 is captured per kilogram of sorbent material, the less sorbent has to be heated up per mole of CO_2 captured. Consequently the energy demand of the process will decrease with an increase in the working capacity. This is also visible in Figure 10. The heat demand of the lab scale facility is measured to be around 141 kJ/mol or 3.2 GJ/tCO_2 at a working capacity of 1.2 mol/kg. This heat demand includes both the sensible heat required to heat up the solid particles as well as the heat required to desorb the adsorbed CO_2. Increasing the working capacity further results in a decrease to around 72 kJ/mol or 1.64 GJ/tCO_2. These low energy demands were measured in experiments using pure CO_2 as adsorber gas. Again we would like to stress that there is scatter in the energy demand data. The energy demand can be measured with a higher accuracy in a larger scale reactor. It should be mentioned that there is no heat exchange included in this measured energy demand of the system.

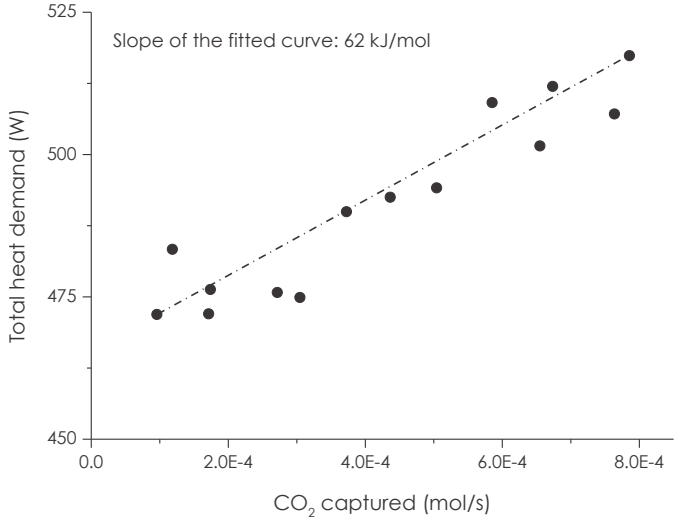

Figure 9: Plot of the desorber heat demand as a function of the amount of CO_2 captured.

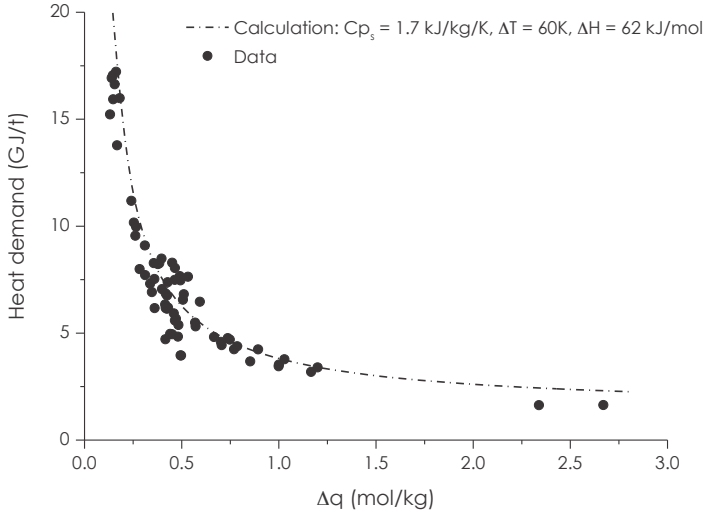

Figure 10: Plot of the desorber heat demand as a function of the operating capacity of the solids. The total heat demand was corrected for the heat lost to the environment. The calculation was based on the following equation:

$$\frac{\Delta H}{M_{w,CO_2}} + \frac{Cp_s \Delta T}{\Delta q \, M_{w,CO_2}}.$$

4.3 | Comparison to literature & column scale up

Table 8 shows the raw data and operating parameters of experimental data published in literature. The table does not only contain data measured for supported amine sorbents. It also includes data measured for a K_2CO_3 based sorbent [17] and data measured using CaO as sorbent material [18]. It should be noted that especially the work done by Arias et al. [18] involves a much larger reactor than the lab-scale facility used in this study. In all of the literature studies either a bubbling bed, a riser or a combination of both was applied as an adorber column.

The performance of the trickle flow reactor seems promising. High capture efficiencies, high working capacities and high productivities were achieved in separated experiments. The next step would be to scale up and increase the length of the adsorber column in order to achieve high capture efficiencies and high working capacities at the same time. To show the impact of reactor length on the adorber performance, the mathematical model was used to estimate the performance of an adsorber column with a length of 15 meters. The model results are shown in the last two columns of Table 8. In terms of capture efficiency and productivity this 15 meters long adsorber column has a similar performance as the scrubber in the MEA based process (see Table 4). The energy demand of the solid process is however expected to be much lower than the energy demand of the MEA based process. The productivity of trickle flow column can be improved. Especially the packing of the column needs to be re-designed and optimized in such a way that it gives higher solid holdups. This would directly translate into higher productivities of the adsorber column. The effect of an improved packing on the column productivity is shown in the last column of Table 8.

Table 8: Literature data on continuous CO_2 capture tests in a circulating system.

Researcher	Zhao, 2013	Veneman, 2012	Yi, 2007	Sjostrom, 2011	Arias, 2013	Veneman, 2015			Modelling full scale	
Source	[4]	[2]	[17]	[1]	[18]	This work			u_s= 0.24 m/s	u_s= 0.1 m/s
Sorbent type	PEI on SiO_2	PEI on SiO_2	K-based	Amine-based	CaO	Lewatit VP OC 1065			Lewatit VP OC 1065	
Adsorber										
Type	Fluid bed/riser	Fluid bed/riser	Fluid bed/riser	Riser	Riser	Trickle-flow			Trickle-flow	
Diameter (m)	0.05	0.04	0.025	0.0254	0.65	0.02	0.02	0.02	(4 x columns) 10	(6 x columns) 8
Height (m)	0.26	0.5	5.4	10.7	15	1.3	1.3	1.3	15	8
Gas flow (L/hr)	560.0	342	353	8500	4061608	1135	368	536	$1.9\ 10^9$	$1.9\ 10^9$
Velocity (m/s)	0.079	0.076	2.0	4.7	3.4	0.9	0.3	0.43	1.8	1.8
Temperature (°C)	45	40	80	25	680	30	30	30	30	30
Inlet concentration (%)	3.2	6.7	12	14	12.5	11.0	11.0	100	12.3	12.3
Outlet concentration (%)	0.5	2.1	6	11	n.s.	5.61	2.25	100	1.4	1.4
Pressure (bar)	1.1	1.1	1.1	1.1	1.1	1.1	1.1	1.1	1.1	1.1
Adsorber performance										
Moles CO_2 captured (mol/hr)	2.1	0.54	8.4	12.7	4860	2.7	1.4	6.4	$9.3\ 10^6$	$9.3\ 10^6$
Sorbent flux ($kg/m^2/s$)	0.42	0.53	21.0	10.0	5.5	4.1	1.9	4.1	4.9	4.9
Capture efficiency (-)	85%	56%	53%	24%	83%	52%	81%	21%	90%	90%
Productivity ($mol/m^3/s$)	1.2	0.2	0.9	0.7	0.3	1.6	0.9	4.0	0.6	1.1
Working capacity (mol/kg)	0.71	0.23	0.23	0.70	0.74	0.51	0.25	2.67	1.8	1.8
Energy demand (GJ/t)	-	-	-	-	-	5.38	10.16	1.64	2.5*	2.5*

* The process heat demand was calculated assuming a sorbent heat capacity of 1500 J/kg/K and a desorption temperature of 423 K. It was assumed 75% of the sensible heat can recovered through heat exchange. The reaction heat was assumed to be 87 kJ/mol.

5.0

Conclusion

The results obtained in the lab-scale capture facility show that a gas-solid trickle flow is a promising reactor concept for the post-combustion capture of CO_2 from simulated flue gas. The adsorber performance was measured over a wide range of experimental conditions in steady-state continuous operation. A set of experimental results was acquired which was used for model validation. The detailed reactor model was developed to interpret the experimental results and used for scale up purposes.

Based on the experimental work presented here we can conclude that:

- The sorbent material (Lewatit® VP OC 1065) showed to be thermally and mechanically stable under the tested conditions. The adsorption capacity and particle size remained unchanged after 300 hours of operation.
- The adsorption rate of CO_2 on Lewatit® VP OC 1065 was found to be linearly dependent on the CO_2 gas phase concentration.
- The developed mathematical model gave an adequate description of the experimental results. The effect of process parameters like gas velocity, solid flux and CO_2 inlet concentration can be described by the developed model. The adsorption reaction rate equation used in the mathematical model was assumed to be first order in the gas-phase CO_2 concentration and first order in the amount of free adsorption sites.
- Especially the solid hold-up has a large impact on the column productivity. The packing of the column needs to be re-designed and optimized in order to further improve the column productivities.
- Based on the measured desorber energy demand of the lab scale capture facility the reaction heat of the sorbent material was estimated to be 62 kJ/mol. In total the energy associated with heating of the sorbent particles and desorption was measured to be 72 kJ/mol at a working capacity of 2.7 mol/kg.

Acknowledgment

This research has been carried out in the context of the CATO-2-program. CATO-2 is the Dutch national research program on CO_2 Capture and Storage technology (CCS). The program is financially supported by the Dutch government (Ministry of Economic Affairs) and the CATO-2 consortium partners. The authors would also like to acknowledge Joram Boegborn and Antonio Salazar Castillo for their contribution to the experimental work. Benno Knaken, Johan Agterhorst and Karst van Bree are kindly acknowledged for the great work they did in the construction of the set-up.

References

1. Sjostrom, S., H. Krutka, T. Starns, and T. Campbell. Pilot test results of post-combustion CO_2 capture using solid sorbents. 2011.
2. Veneman, R., Z.S. Li, J.A. Hogendoorn, S.R.A. Kersten, and D.W.F. Brilman, Continuous CO_2 capture in a circulating fluidized bed using supported amine sorbents. Chemical Engineering Journal, 2012. 207: p. 18-26.
3. Zhao, W.Y., Z. Zhang, Z.S. Li, and N.S. Cai, Investigation of thermal stability and continuous CO_2 capture from flue gases with supported amine sorbent. Industrial & Engineering Chemistry Research, 2013. 52(5): p. 2084-2093.
4. Zhao, W.Y., Z. Zhang, Z.S. Li, and N.S. Cai, Continuous CO_2 Capture in Dual Fluidized Beds Using Silica Supported Amine. Ghgt-11, 2013. 37: p. 89-98.
5. Alesi, W.R. and J.R. Kitchin, Evaluation of a Primary Amine-Functionalized Ion-Exchange Resin for CO_2 Capture. Industrial & Engineering Chemistry Research, 2012. 51(19): p. 6907-6915.
6. Fisher, K.S., et al., Integrating MEA regeneration with CO_2 compression and peaking to reduce CO_2 capture costs, 2005.
7. Kiel, J.H.A., W. Prins, and W.P.M. Van Swaaij, Mass-Transfer between Gas and Particles in a Gas Solid Trickle Flow Reactor. Chemical Engineering Science, 1993. 48(1): p. 117-125.
8. Dudukovic, A.P., N.M. Nikacevic, D.L. Petrovic, and Z.J. Predojevic, Solids holdup and pressure drop in gas-flowing solids-fixed bed contactors. Industrial & engineering chemistry research, 2003. 42(12): p.

2530-2535.
9. Roes, A.W.M. and W.P.M. Van Swaaij, Hydrodynamic behavior of a gas-solid countercurrent packed-column at trickle flow. Chemical Engineering Journal and the Biochemical Engineering Journal, 1979. 17(2): p. 81-89.
10. Westerterp, K.R. and M. Kuczynski, Gas Solid Trickle Flow Hydrodynamics in a Packed-Column. Chemical Engineering Science, 1987. 42(7): p. 1539-1551.
11. Massman, W.J., A review of the molecular diffusivities of H_2O, CO_2, CH_4, CO, O_3, SO_2, NH_3, N_2O, NO, and NO_2 in air, O_2 and N_2 near STP. Atmospheric Environment, 1998. 32(6): p. 1111-1127.
12. Sjostrom, S. and H. Krutka, Evaluation of solid sorbents as a retrofit technology for CO_2 capture. Fuel, 2010. 89(6): p. 1298-1306.
13. Veneman, R., H. Kamphuis, and D.W.F. Brilman, Post-Combustion CO_2 capture using supported amine sorbents: A process integration study. Energy procedia, 2013. 37: p. 2100-2108.
14. Alesi Jr, W.R., M. Gray, and J.R. Kitchin, CO_2 adsorption on supported molecular amidine systems on activated carbon.
15. Gray, M.L., et al., Parametric study of solid amine sorbents for the capture of carbon dioxide. Energy & Fuels, 2009. 23: p. 4840-4844.
16. Li, W., et al., Steam-stripping for regeneration of supported amine-based CO_2 adsorbents. Chemsuschem, 2010. 3(8): p. 899-903.
17. Yi, C.K., S.H. Jo, Y. Seo, J.B. Lee, and C.K. Ryu, Continuous operation of the potassium-based dry sorbent CO_2 capture process with two fluidized-bed reactors. International Journal of Greenhouse Gas Control, 2007. 1(1): p. 31-36.
18. Arias, B., et al., Demonstration of steady state CO_2 capture in a 1.7 MWth calcium looping pilot. International Journal of Greenhouse Gas Control, 2013. 18: p. 237-245.

C.

Supporting experimental work

C.1 | Solid holdup measurements

The measured values for β are summarized in Table C.1. In the measured solid-flux range, β, was found to increases linearly with an increasing solid flux as expected based on equation 4 in Table 5. This indicates that under the tested conditions the solids velocity is constant. In work performed by Roes et al. [9], the solid velocity was also found to be constant for solid fluxes ranging from 1 to 6 kg/m^2/s and gas fluxes lower than 0.1 kg/m^2/s.

Table C.1: The measured solid holdup as a function of the solid flux for different.

β(%)		S (kg/m^2/s)		
		1.93	3.17	4.41
u_G (m/s)	0	0.83	1.29	1.75
	0.51	0.98	1.54	1.98
	0.87	1.06	1.53	2.21

C.2 | The adsorption rate equation

Figure C.1 shows the uptake rate of the sorbent particles at different gas phase CO_2 concentrations measured in a TGA apparatus. With this figure we want to show that: (1) the CO_2 uptake rate increases with an increase in the gas phase CO_2 concentration and (2) the CO_2 uptake rate decreases with an increase in the CO_2 loading of the sorbent particles. This implies that the reaction rate is at least a function of the CO_2 capacity, q, and that when q is equal to qe, the reaction rate must be zero. Figure C.2 shows a plot of the maximum uptake rate (i.e. the highest value in Figure C.1) as a function of the gas phase CO_2 concentration. In the reactor model we have assumed that the adsorption reaction rate was first order in the gas phase CO_2 concentration. The linear increase in the uptake rate with an increase in CO_2 concentration supports that assumption.

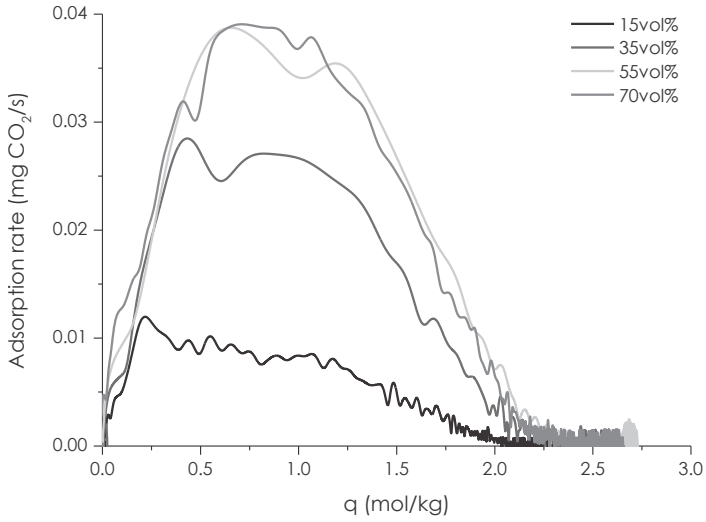

Figure C.1: Uptake rates plotted for Lewatit® VP OC 1065 as a function of the CO_2 loading of the solids particles. The gas phase CO_2 concentration was varied.

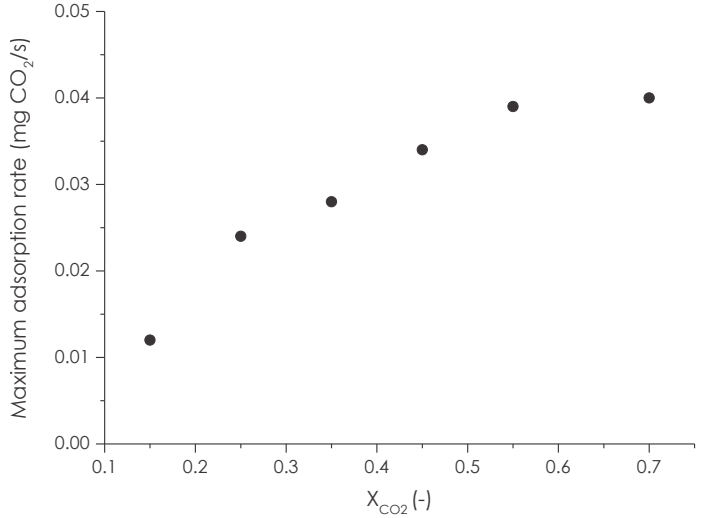

Figure C.2: Plot of the maximum uptake rate (i.e. the highest value in Figure C.2) as a function of the gas phase CO_2 concentration.

C.4. | Graphs showing the working capacity as a function of u_G and S

In Figure C.3, the working capacity is shown as function of the solid flux at different CO_2 inlet concentrations. At a high solid fluxes, a larger fraction of the incoming CO_2 is captured and so the average CO_2 concentration in the column is lower. This results in slower CO_2 uptake rates and thus a lower working capacities and lower column productivities. Figure C.4. shows the working capacity as a function of the gas velocity through the column for three different solid fluxes. We do not see a clear trend in Figure C.4.

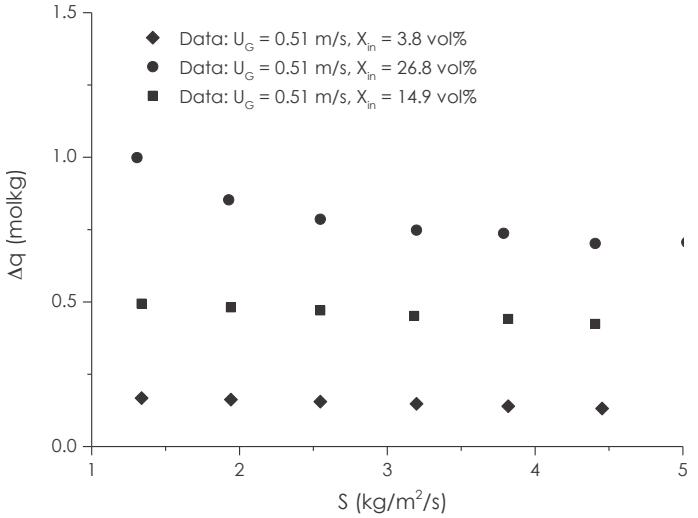

Figure C.3: Plot of the working capacity as a function of the solid flux at different CO_2 inlet concentrations.

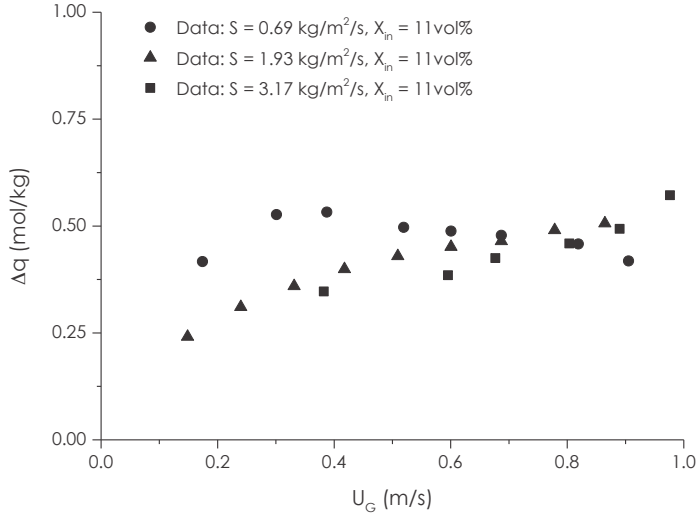

Figure C.4: Plot of the working capacity as a function of the gas velocity at three different solid fluxes.

C.5 | Effect of H_2O on CO_2 adsorption

In Chapter 3 we have shown that Lewatit® VP OC 1065 can adsorb much more H_2O than CO_2. The highest H_2O capacity observed was 12.5 mol/kg (at 95 %RH). The highest CO_2 capacity observed was 2.8 mol/kg (303 K, P_{CO2} = 81 kPa). We have concluded that the co-adsorption of H_2O in the adsorber column of the sorbent based process and the subsequent desorption of the co-adsorbed water in the desorber column could result in a significant increase in the heat demand of the process.

A kinetic selectivity of the sorbent material towards the adsorption of CO_2 could help to prevent the co-adsorption of large amounts of H_2O. In case the uptake rate of H_2O is much slower than the uptake rate of CO_2, the capture efficiency of H_2O will be lower than the capture efficiency of CO_2 thereby limiting the H_2O working capacity.

In the lab-scale capture facility, we have investigated this topic in more detail by feeding gas mixtures containing both CO_2 and H_2O to the adsorber column under continuous operation. The capture efficiencies for both CO_2 and H_2O at varying solid circulation rates are plotted in Figure C.5. Since we did not install a heater for the adsorber column, it is not possible in the current configuration to feed gas to the adsorber column with a dewpoint higher than 26˚C. This corresponds to a maximum concentration of 3.3 vol% H_2O at atmospheric pressure.

The measurements presented in Figure C.5 were performed using three different adsorber inlet gas compositions: (1) dry CO_2 containing gas (3.7 vol%), (2) humidified N_2 (3.3 vol% of H_2O) and (3) gas containing both CO_2 (3.7 vol%) and H_2O (3.3 vol%). The relative humidity of the gas entering the adsorber column is close to 100%. Based on isotherm data presented in Chapter 3 we know that under these conditions the equilibrium CO_2 capacity of the sorbent material is close to 2 mol/kg and the equilibrium H_2O capacity of the sorbent material is close to 13 mol/kg. This means that Lewatit® VP OC 1065 can adsorb far more H_2O than CO_2 under conditions relevant for post-combustion CO_2 capture.

Since the inlet H_2O concentration is similar to the inlet CO_2 concentration and the total flue gas flowrate is kept constant in all these experiments we can make a fare comparison between the CO_2 capture efficiency and the H_2O capture efficiency. We see that the H_2O capture efficiency is higher than the capture efficiency of CO_2. Already at low solid fluxes all H_2O pre-

sent in the the adsorber gas is adsorbed while still a relatively large fraction of CO_2 is present in the gas leaving the adsorber column. This leads to the conclusion that the adsorption of H_2O on Lewatit VP OC 1065 is faster than the adsorption of CO_2. Based on the difference in diffusion coefficients for CO_2 and H_2O we also expect H_2O to adsorb faster on the sorbent material. The diffusion coefficient of H_2O in air at 30˚C is 2.6 10^{-5} m^2/s. The diffusion coefficient of CO_2 in air at 30˚C is 1.6 10^{-5} m^2/s.

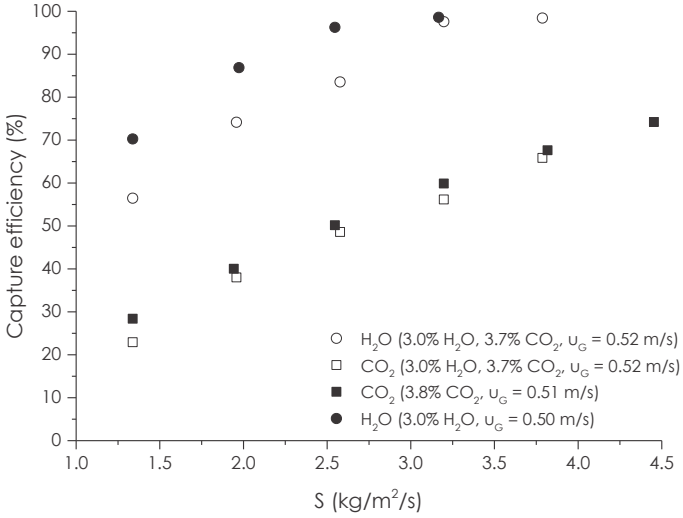

Figure C.5: A plot of the measured capture efficiency for different sorbent circulation rates.

C.6 | Desorption rate

We have tried to estimate experimentally the time required to regenerate these sorbent particles in a pure CO_2 atmosphere. The following TGA experiment was performed. After an initial desorption stage to desorber any pre-adsorbed CO_2 of H_2O, the sorbent particles were saturated with CO_2 at 40°C and at a CO_2 partial pressure of 0.8 bar in the TGA apparatus. Subsequently, the sorbent particles were heated up to 150°C resulting in the desorption of the adsorbed CO_2. This experiment was done twice; first with a heating rate of 1 K/min and then with a heating rate of 20 K/min. The CO_2 capacity of the sorbent material was calculated from the weight change during desorption. In both experiments, the sorbent particles were completely regenerated at 150°C. Moreover, it was found that the degree of regeneration was only a function of temperature in these experiments and not a function of heating rate. This implies that for heating rates between 1-20 K/min, the degree of desorption is equilibrium limited and not limited by the desorption reaction rate. In the desorber, sorbent residence times do not have to be much longer that 5 minutes to ensure full sorbent regeneration as long as the sorbent particles have attained the desired regeneration temperature before leaving the desorber column. This is an important finding for the design of the desorber column. The specific configuration of the TGA did not allow for tests with even higher CO_2 partial pressures or higher heating rates.

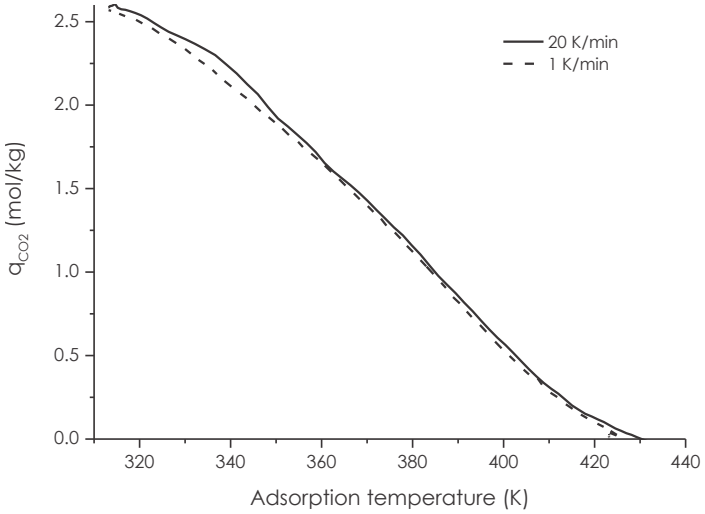

Figure C.6: A plot of the particle CO_2 loading during desorption as a function of the temperature. The particles were heated with 1 K/min and 20 K/min.

C.7 | Energy demand

Figure C.7 shows the heat demand of each of the five stages in the desorber column for three separate measurements. In the first measurement the heat demand of the desorber column was measured without solids being circulated. The desorber column was fluidized and kept at a constant temperature of 100˚C. Since there is no CO_2 capture or solid circulation, the heat generated by the heaters is used to compensate for the heat lost to the environment and to heat the incoming fluidization gas. A relatively large amount of heat is required to heat the incoming fluidization gas. This is reflected in the high heat demand of stage five, which is the bottom stage, compared to the other four stages. Also the top stage has a higher heat demand than the three other stages. Stage 1 is the top tray and hence is expected to lose more heat to the environment. Since this is a small scale capture facility a relatively large portion of the heat demand of the system is associated with heat loss to the environment and with heating and of the fluidization gas. The amount of heat lost to the environment was quantified by calculating the heat duty of the desorber without solid circulation (i.e. no CO_2 capture). In total a little over 400 W is required to keep the column at constant temperature.

In a second experiment, solids were circulated but no CO_2 was captured. N_2 was used adsorber feed gas. As in all capture experiments presented in this work the riser cooler was turned on. The cooling water temperature was set at 10˚C. From Figure C.7 we clearly see that circulating solids greatly increases the heat demand of top tray of the desorber column; it increases from 90 W to 220 W when the solids circulation is turned on. The heat duty of the other stages remains largely unchanged which indicates that the solids are already heated when leaving the first stage.
In a third experiment CO_2 was continuously captured in the adsorber column and the particles were regenerated at 100˚C. From Figure C.7, we can see that with CO_2 capture the heat demand on the first tray increases from 150 to 180 W. Now, next to the heating of the solid particles the particles are regenerated which requires heat. Also the heat demand of the second stage is slightly increased, most likely due to the regeneration of solid particles taking place at this stage.

Although in this small capture setup a relatively large amount of heat is lost to the environment, both the contribution to the heat demand by the circulation of solids as well as that for regenerating the sorbents could be identified.

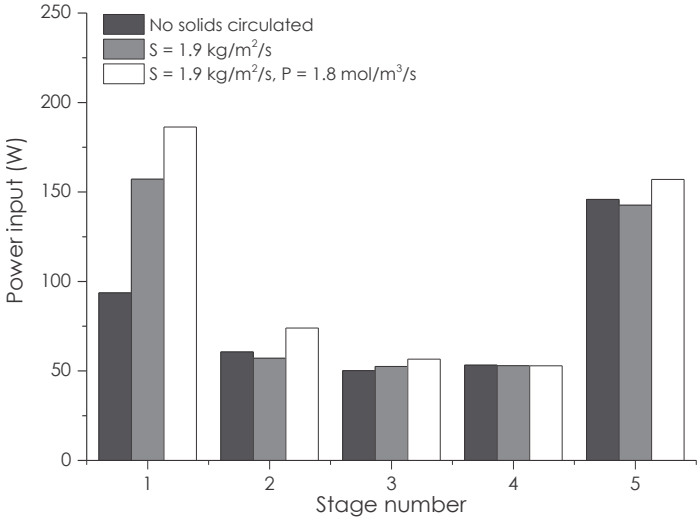

Figure C.7: Heat demand of the desorber column per stage. In the left column no solids are circulated and no CO_2 is captured. In the middle column solids are circulated but no CO_2 is captured. The right column shows the heat demand for a capture experiment.

Chapter 06

Techno-economic assessment of CO_2 capture using supported amine sorbents at a coal fired power plant

Abstract

This work focusses on the design and evaluation of the process technology required for adsorption-based post-combustion CO_2 capture using supported amine sorbents. This chapter presents a preliminary process design for a CO_2 capture facility at a 500 MWe coal-fired power plant and a techno-economic comparison of the performance of the novel capture process with the state of the art MEA based reference technology. In order to provide a good basis for comparison, we have also used the same cost model as used in the MEA based reference study.

Based on the techno-economic comparison we conclude that an adsorption-based capture process operated with Lewatit® VP OC 1065 sorbent particles has the potential to lower the capital investment and the utilities cost of the conventional amine scrubbing technology with 14% and 26%, respectively. The savings in operational cost are mainly the result of a lower heat demand of the supported amine based process compared to the MEA based system. In both systems, the captured CO_2 is released again by heating of the sorbent/solvent. However, due to the sorbent's lower heat capacity and higher CO_2 capacity, the sensible heat demand of the process is reduced. The lower capital costs are mainly the result of less expensive adsorption column compared the scrubber in the reference process. Overall this would bring down the cost of CO_2 avoided from $59 per tonne of CO_2 calculated for the MEA reference case to $43.5 per tonne.

Ultimately the cost of CO_2 avoided could potentially be reduced from $59 per tonne of CO_2 calculated for the MEA reference case to $37 per tonne of CO_2 when the working capacity is improved from 1.8 to 3.1 mol/kg and the sorbent degradation rate is improved from 2 kg/t to 0.5 kg/t.

1.0

Introduction

Application of carbon capture and storage (CCS) at fossil fuel burning plants is one of the methods to reduce the emission of CO_2 in the power sector. Currently however, CCS is considered too costly for large scale deployment as the installation of a capture facility at power plants could almost double the cost of the electricity produced by the power plant. Since capturing CO_2 is by far the most expensive step in the CCS chain, the development of a more cost effective capture technology is now the main objective of CO_2 capture research.

CO_2 capture using supported amine sorbents may offer a low-cost alternative to the conventional amine scrubbing technology. This process is anticipated to have lower operational costs as well as a lower capital investment than the conventional amine scrubbing technology. Application of this novel capture process could potentially bring the thermal energy requirement of the capture process down from around 2.7-4.3 GJ/tCO_2 for conventional amine scrubbing to around 1.9 GJ/tCO_2 [1] mainly due to the reductions in the sensible heat energy penalty of the CO_2 capture process described above.

The capital investment associated with the purchase of the absorber column makes up around 11% of the total CO_2 capture cost. In Chapter 4 it was found that the higher mass transfer rates in the adsorption column when compared to the mass transfer rates typical for MEA scrubbers allow for a more compact adsorber design In comparison with the conventional technology, next to the energy savings, also the column size of the scrubber can significantly be reduced by 50-70% when switching to a adsorption based process, bringing down the capture costs further.

Although both sorbent- and process development will have an essential role in realizing the envisioned cost savings, reports on process design remain rare [2] and the impact of process design on the economic performance of the capture system is not yet clear. Hence this Chapter presents a preliminary process design for a CO_2 capture facility at a 500 MWe coal-fired power plant and a techno-economic comparison of the performance of the novel capture process with the more established MEA technology. The aim here is to investigate the potential of the novel process, to study the effect of sorbent performance on the CO_2 capture costs and, finally, to calculate the resulting cost of low carbon electricity.

2.0

Design basis

The techno-economic performance of the novel sorbent based capture process is compared with the performance of a MEA-based capture facility, used as benchmark technology in this study. Studies on the techno-economic performance of a MEA-based capture facility for post-combustion capture are readily available [3-5]. The process evaluation study presented by Fisher et al. [3] will be used as a reference here. The CO_2 capture system is retrofitted to a 500 MWe coal-fired power plant and is designed to capture 90% of the emitted CO_2. The power plant general data is presented in Table 1. The same data was used as input for the MEA-based process evaluation study.

The process design will be based on the use of Lewatit® VP OC 1065 sorbent particles, studied in Chapter 2 and 3. The adsorber design is based on the work presented in Chapter 4. Although the system boundary of interest here does not specifically include CO_2 transport and storage systems, CO_2 compression is assumed to occur within the facility boundaries. A compressor is used to increase the pressure of the product gas from 0.1 MPa to 7.38 MPa [6]. A pump is used to boost the pressure of the liquefied CO_2 further up to 13.9 MPa.

Table 1: Base case definition [3].

General plant data	
Net plant power (MWe)	500
Flue gas flow rate (Nm^3/s)	535
Capture efficiency (%)	90
Flue gas pressure (kPa)	111.2
Temperature (K)	328
Flue gas molar composition (vol%)	
N_2+Ar	73.5
CO_2	12.3
H_2O	9.4
O_2	4.8

3.0

Process description

A scheme of the process flow sheet of the sorbent based capture process is shown in Figure 1. The process design is based on a trickle flow adsorber and a staged fluid bed desorber column. This adsorber type was selected in Chapter 4 as it provides counter current gas-solid contacting, and allows for high operating gas velocities while the adsorber pressure drop is relatively low. The staged fluid bed was selected as a suitable desorber as it combines good heat exchange characteristics with solid phase staging which is essential to keep the solid inventory in the desorber column to a minimum.

In the process evaluated here we assume the adsorber is operated at 30°C. This is below the dewpoint of the flue gas after the wet flue gas desulphurization scrubber. For regeneration, the sorbent is heated up to a temperature of 150°C. At these temperatures Lewatit® VP OC 1065 can be fully regenerated in a nearly pure CO_2 environment (See Chapter 5, Appendix C). Before entering the adsorber column, the flue gas passes through a flue gas blower to overcome the pressure drop through the adsorber column. In the adsorber, CO_2 is selectively picked up by the sorbent. The loaded sorbent, which contains the chemically bound CO_2 is then transported to the desorber column. For solids transportation both pneumatic transport and mechanical transport can be considered. In the cost calculations presented here a bucket elevator was assumed to facilitate the transportation of the solid material.

The 'colder' sorbent material coming from the adsorber is heated in the desorber column up to the desorption temperature. Part of the heat required to heat up the sorbent material is supplied by exchanging heat between the hot solids leaving and the cold solids entering the desorber in a 'lean/rich' solid-solid heat exchanger. The hot solids transfer heat to a thermo-oil, which is in turn heats the solids entering the desorber column. The desorption reaction heat and the remaining part of the sensible heat required in the process for heating the sorbent up to desorption temperatures will be supplied by low pressure steam extracted from the power plant steam cycle. The heat is supplied by flowing steam through heating tubes/plates.

The solids entering the adsorber column still have a temperature higher than the desired adsorption temperature. Additional cooling capacity is installed in the top of the adsorber to cool the solids further.
The extraction of steam results in a decrease in the gross power output of the power plant. Additionally, part of the produced electricity is used to operate electrical equipment like the flue gas blower and the CO_2 compressor in the capture plant causing the net power output of the power plant to decrease further. The reduced plant capacity was calculated in the same way as described by Fisher et al. [3].

After desorption of CO_2 the hot sorbent material leaves the desorber and passes through the heat exchanger, before it is recycled back to the adsorber column. In the staged fluid bed desorber, only a small amount of additional fluidization gas is required as the CO_2 released in the desorber itself will assist in the particle fluidization (self-fluidization) [2]. Hence, only a small product gas blower is required to recycle part of the CO_2 product gas as fluidization gas. Table 2 gives a summary of the process input parameters used in the economic evaluation of the process.

Table 2: Summary of process parameters assumed for the base case study.

Process parameters	MEA [3]	SAS
Heat exchange efficiency (-)[a]	84%	60%
Adsorber temperature (^{0}C)	40	30
Adsorber pressure (kPa)	111.6	111.6
Desorption temperature (^{0}C)	112.8	150
Desorber pressure (kPa)	192.3	100.0
Solvent/Sorbent make-up cost ($/t$CO_2$)	1.8	3
Solvent/Sorbent cost ($/t)	1250	3000
Solvent/Sorbent make-up rate (kg/tCO_2)	1.5	1
Absorption/Adsorption reaction heat (GJ/tCO_2)	1.9	2.0

a. The exchanger in the solvent based process has a 10 K temperature approach. The exchanger in the solid based process has a 24 K temperature approach.

In addition to the main capture plant process equipment, described above, there might be a need for flue gas conditioning upstream of the adsorber column. In the economic evaluation used as reference [3], costs associated with electrostatic precipitators (ESP), the flue gas desulphurization (FGD) unit and the selective catalytic reduction (SCR) unit are included in the overall cost calculations.
Here, we did not include costs associated with the drying of the flue gas upstream of the adsorber column nor with the cleaning of the CO_2 product stream leaving the desorber column.

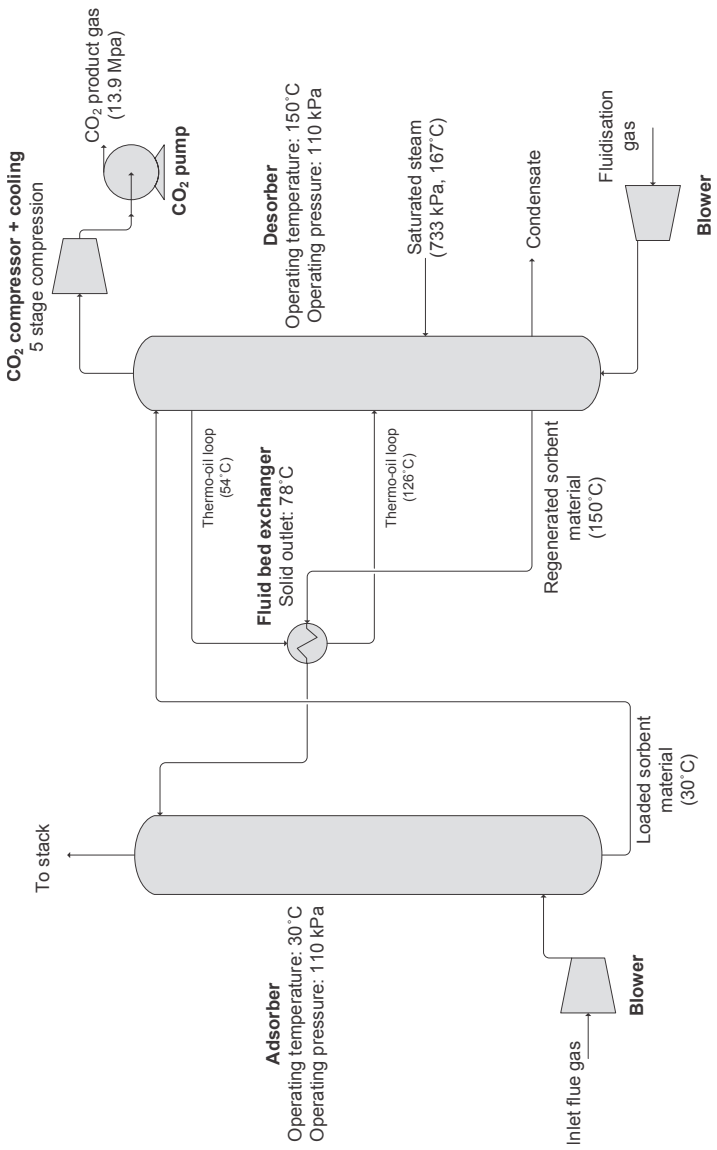

Figure 1: Schematic of the configuration of the SAS based capture process.

4.0

Methodology

The methodology followed consists of the following steps:

- Equipment sizing: Sizing of the GSTF adsorber column was based on the reactor model presented in Chapter 4. Sizing of the staged fluid bed desorber and the cross fluid bed heat exchanger was based on sizing methodology presented by Gupta et al. [7]. A detailed description of the design procedure of the adsorber and desorber column is provided in the Appendix D. Other equipment, like the flue gas blower, pumps and the CO_2 compressors, were sized to provide information on equipment cost and their use of utilities and consumables.
- Estimation of equipment cost: Based on the design calculations performed, costing methods presented by Peters et al. [8] were used to estimate the purchased equipment cost. Other cost elements included in the total capital investment are estimated as percentages of the delivered-equipment cost. A detailed description of the economic model used for the cost calculations is presented in Appendix D.
- Estimation of operational expenses: The costs associated with the operation of the CO_2 capture plant (variable operating costs) are calculated based on the required utilities. Other items included in the total operating cost are estimated as percentages of the delivered-equipment cost (see Appendix D).

Next, a comparison with the MEA benchmark CO_2 capture technology is made. Parameters such as the cost of CO_2 avoided, the productivity and the pressure drop are calculated and compared with values reported by Fisher et al. [3]. We have used the same cost model as used in the reference study, in order to provide a good basis for comparison. The accuracy of cost calculations similar to the ones presented in this study is reported to be ± 20-30% [8]. Considering the maturity of the MEA based process, cost estimation methods for this process are more established and more accurate than the preliminary cost estimation made here for the SAS. The cost data presented here for the SAS based process should therefore be considered as a rough indication of the potential of the this novel process.

Since here the assumed cost year basis is 2012, it is necessary to re-index the equipment and utility costs reported in the reference study to the year 2012. For this purpose, the Chemical Engineering Plant Cost Index was used [9]. Assumptions made in the economic evaluation presented here are summarized in Table 3.

Table 3: Assumptions made in economic analysis.

Assumptions	Value	Reference
Cost year basis	2012	-
Capacity factor (%)	85	[3]
Fixed charge factor (1/yr)	0.15	[3]

5.0

Process economics

In Table 4, the SAS-based capture process is compared to the MEA-based process on the following key performance indicators (i) productivity, (ii) pressure drop in view of electricity consumption for the flue gas blower and (iii) operating gas velocity in view of the footprint of the ab-/adsorber. The productivity of the capture system was defined as the amount of CO_2 captured per second per cubic meter of installed reactor volume. This productivity is a measure for the 'compactness' of the process and thus for CapEx; the higher the system productivity the lower the investment cost for the contacting devices to be applied. On basis of the sizing calculations performed, the GSTF adsorber column outperforms the MEA scrubber column in terms of productivity; the adsorber column is expected to be a factor two smaller than the MEA scrubber. This is mainly the result of higher mass transfer rates that can be achieved in GSTF reactors compared to scrubbing columns as discussed before in Chapter 4 of this thesis.

Moreover, the adsorber pressure drop was calculated to be 54 mbar for the adsorber column, which is significantly lower than the pressure drop of 103 mbar reported for the MEA scrubber. This might seem counterintuitive. However, the volume fraction of solids in the adsorber column is low (<6% of the adsorber volume) and the height of the column is smaller than the height of the MEA scrubber column.

Table 4: Adsorber design for capturing 90% of the CO_2 emitted by a 500 MWe coal fired power plant.

Process overall	MEA [3]	SAS
CO_2 captured (kg/s)	115	113
Solvent/sorbent working capacity (kmol/t)	0.94	1.8
Solvent/Sorbent flow rate (kg/s)	2739	1410
Thermal energy (GJ/tCO_2)	4.3	2.9
Electrical energy (GJ/tCO_2)	0.5	0.4
System productivity ($mol/m^3/s$)	0.4	0.6
Adsorber		
Column volume (m^3)	4712	2338
Productivity ($mol/m^3/s$)	0.56	1.1
Number of units	4	6
Dimensions (H x D)	15 x 10 m	8 x 8 m
Pressure drop (kPa)	10.3	5.5
Gas velocity (m/s)	1.8	1.8
Desorber		
Column volume (m^3)	1244	1911
Productivity ($mol/m^3/s$)	2.1	1.3
Number of units	4.0	1.0
Dimensions (H x D)	10 x 6 m	20 x 11 m
Heat exchanger		
Heat transfer coefficient ($W/m^2/K$)	511	155
Heat duty (MW)	563	152
Heat exchange area (m^2)	101136	40759
Temperature approach (K)	10	24
Cost per m^2 ($\$/m^2$)	148	171

5.1 | Capital cost

Table 5 shows the breakdown of the purchased equipment cost (PEC) for the SAS based capture facility and the MEA-based reference plant. Based on the cost calculations performed here, we conclude that, application of the SAS based capture process could potentially save ~29% of the cost of purchased equipment. This is mainly the result of the reduced cost of the adsorber column compared to the cost of the amine scrubber column. The cost for purchasing the scrubber in the MEA-based capture process was reported to be 21.9 million dollars [3]. The cost of the GSTF adsorber col-

umn was estimated at 10 million dollars. There are two main reasons for the lower cost of the adsorber compared to the scrubber. Firstly, the volume of the adsorber is a factor 2 smaller than the volume of the scrubber column. Secondly, the adsorber does not require an expensive structured packing since the porous support of the sorbent particles provides an open, accessible and large contact area for the contact between amine and CO_2.

Also the cost of the heat exchanger in the sorbent based process is lower than the cost of the heat exchanger in the MEA-based process. For both exchangers, the purchased costs are dominated by the price of heat exchange area. The required area is calculated from the duty, the averaged heat transfer coefficient and the average temperature difference between the hot and cold side of the exchanger. In Table 4 we see that the duty of the heat exchanger in the solid process is much lower than duty of the exchanger in the reference process. Also the average temperature difference between the hot and cold side of the exchanger is much higher. This is due the lower exchange efficiency; 84% in the MEA-based process compared to 60% in the SAS-based process. This translates into lower area requirement and hence lower exchanger costs for the solid heat exchanger.

In the solid process a thermo-oil is used to exchange heat between the hot solids leaving the desorber and the cold solids in the top stages of the desorber. This indirect way of exchanging heat limits the heat exchange efficiency. Also, additional heat exchange area is needed since the heat is first transferred from the hot solids to the thermo-oil in the exchanger and subsequently from the thermo-oil to the cold solids. The cost associated with the heat exchange area needed to transfer the heat from the thermo-oil to the cold particles is included in the desorber purchased cost.

The total capital requirement for the amine plant including CO_2 compression is 311 million dollars compared to 267 million dollars for the SAS plant. A detailed split-up of the total capital requirement is given in the Appendix D. The costs of the CO_2 compressor are not included in Table 5. The investment cost of the CO_2 compressor is estimated to be M$ 57.5 This value corresponds well with the compressor investment cost reported by Abu-Zahra et al. [4] of M$ 55.4 (corrected for inflation). Fisher et al [3]. reported the investment cost for the compressor to be M$ 43.3. The capital cost associated with the purchase of the CO_2 compressor is significant but not related to the capture technology comparison, which is the objective of this work.

Table 5: Breakdown of the purchased equipment (PEC) cost for a SAS based capture facility and a MEA-based capture facility in 2012 dollars.

PEC (M$)	MEA [3]	SAS
FG blower	2.7	7.0
Ab-/Adsorber	30.4[a]	10.0
Sorbent conveyor	-	1.5
Desorber	17.2[b]	17.8
Heat exchanger	15.0	7.0
Cooling system	10.5	10.5
Total purchased cost	75.8	53.7

a. Including cost of other equipment associated with the scrubber like the lean amine cooler, the rich amine pump and a filter for the rich amine solution.

b. Including cost of other equipment associated with the stripper like the reflux condenser, the reboiler and the reclaimer.

5.2 | Operating cost

Both CO_2 capture facilities require low pressure steam for the desorption of the captured CO_2 and electricity to operate electrical equipment like the CO_2 compressor. Figure 2 shows a split-up of the cost of utilities for both capture processes. The cost of steam and electricity used by the capture facility are normally not mentioned explicitly, as they are taken into account with the derating of the power plant. Here, we have chosen to also calculate the utilities cost to show how the utilities cost is distributed over the different unit operations. In these calculations we have assumed an electricity price of 14 $/GJ and a low pressure steam price of 7.4 $/GJ [8].

In the MEA scrubbing process in total around 38.9 dollars is spent per tonne of CO_2 captured on electricity, heating and cooling, compared to 28.9 dollars per tonne of CO_2 in the SAS based process. In both processes the utility costs are dominated by the cost associated with the heat demand of the process and the electrical energy required for compression of the CO_2 product stream, accounting in both cases for more than 80% of the total energy costs. The contribution of other electrical equipment, like pumps and blowers, to the total utility cost is only small. The cost for desorption of the captured CO_2 in de desorber column was estimated at 32.2 dollar per tonne for the MEA and 21.2 dollar per tonne for the SAS based process respectively. The net thermal energy input of the adsorption-based

capture process was calculated to be 2.9 GJ/tCO_2, including 2.0 GJ/tCO_2 for the reaction heat. The sensible heat energy penalty was estimated to be 2.2 GJ/tCO_2 of which 60% is exchanged in the solid-solid heat exchanger. This thermal energy penalty does not include efficiency losses or energy required for the desorption of any co-adsorbed water.

The net thermal energy input of the MEA-based capture process is reported to be 4.3 GJ/tCO_2 [3]. Based on the energy calculation done here, application of the SAS based capture process could save 33% of the thermal energy required in the MEA-based process. It should be noted here that values as low as 2.5 GJ/tCO_2 [10] are also reported for aqueous amine based capture systems. It should be noted that the 2.9 GJ/tCO_2 is calculated for the base case sorbent namely Lewatit® VP OC 1065 at a heat exchange efficiency of 60%.

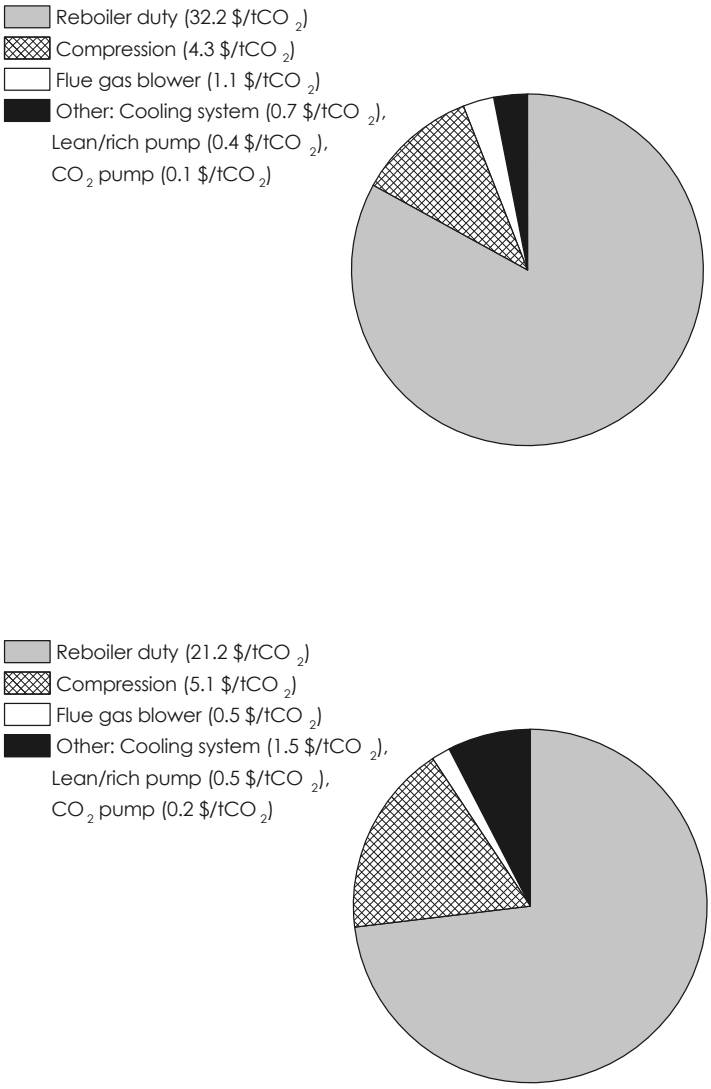

Figure 2: Split-up of the utilities cost for the MEA (top) and SAS (bottom).

5.3 | Cost of CO_2 avoided and cost of electricity (COE)

The installation of a capture facility at a power plant results in a decrease in the gross power output of the power plant as steam is extracted from the steam cycle for solvent/sorbent regeneration. Part of the produced electricity is used to operate electrical equipment like the flue gas blower and the CO_2 compressor in the capture plant, causing the net power output of the power plant to decrease further. The derated plant capacity was calculated in the same way as described by Fisher et al. [3]. The steam used for sorbent regeneration is taken from the power plant at a pressure of 944.6 kPa and is first used to drive the compressor train with a steam turbine. However, the expansion of the steam (to 733.3 kPa) is not enough to drive the compressors and additional compression energy is supplied by an electric motor using electricity produced by the power plant. Table 6 shows the effect of CO_2 capture on the power output of the pulverized coal plant for both the MEA-based capture facility and the SAS based capture facility.

As discussed above, the installation of a MEA capture facility at a power plant results in a decrease in the gross power output of the power plant as steam is extracted from the steam cycle for solvent regeneration. The main part of this heat is associated with heating of the aqueous amine solution from the absorption temperature to the desorption temperature and with the evaporation of solvent in the desorber column. The MEA plant considered here requires 4.3 GJ of heat per ton of CO_2 captured. To capture 90% of the CO_2 the MEA plant requires 492 MW of heat for solvent regeneration. The SAS based facility requires 'only' 324 MW. Due to this lower thermal energy requirement of the SAS-based process, the loss in gross power is less than when a solvent based process is installed.

The SAS-based capture facility at the pulverized coal plant is 25% more energy efficient than a MEA-based capture facility. These savings in energy results in savings in costs; the cost of CO_2 avoided are reduced from 59 dollars per tonne to 44 dollars per tonne. These cost savings are the result of a reduction in cost of utilities from 39 to 29 dollar per tonne of CO_2 captured and a slight reduction in capital cost from 15.4 to 14 dollar per tonne.

Table 6: Summary of the technical and economical results for the base case.

Plant data	No capture	MEA [3]	SAS
Gross power (MWe)	500.0	353.8	403.8
Net power (MWe)	453.0	282.5	326.9
Power plant auxiliaries (MWe) (including FGD. SCR)	47.0	47.0	47.0
Power output reduction (MWe)	-	170.5	127.1
Relative power output reduction (over ref. plant)	-	38%	28%
Capture plant capital requirement ($/t$CO_2$)	-	15.4	14.0
CO_2 emitted (kt/yr)	3428	337	337
CO_2 captured (kt/yr)	-	3029	3029
Emission rate (tCO_2/MWh)	1.02	0.16	0.14
CO_2 capture total electricity requirement (Gje/tCO_2)[a]	-	1.51	1.12
CO_2 capture heat requirement (Gj/tCO_2)[b]	-	4.28	2.90
Cost of CO_2 avoided ($/t$CO_2$)	-	59.3	43.5
Cost of electricity ($/MWh)	33.6	84.1	71.7

a. The power plant output reduction (GWe) divided by the amount of CO_2 captured (t/s).

b. The capture plant's steam demand (GWth) divided by the amount of CO_2 captured (t/s).

5.4 | Cost sensitivity analysis

Figure 3 shows the potential cost savings achieved by switching from the MEA based process to the SAS-based process estimated based on the cost model described in this Chapter.

We have considered several cases in Figure 3. Firstly, the cost savings were estimated for a process operated with the Lewatit® VP OC 1065 sorbent particles. This sorbent is already commercially available and serves as a benchmark here. Secondly, we have presented a column design for a 'second generation sorbent'. This sorbent material has a higher CO_2 working capacity than the benchmark sorbent (3.1 mol/kg instead of the 1.8 mol/kg for Lewatit® VP OC 1065). Lastly, a 'third generation' sorbent is considered. This sorbent has the same capacity as the 'second generation sorbent' but also has an uptake rate that is twice as high as the uprate rate of Lewatit®

VP OC 1065. In Chapter 4 an adsorber design was presented for these three cases. These column designs were incorporated in the economic evaluation presented here. For the Lewatit® VP OC 1065 sorbent particles we have evaluated the effect of a change in the heat exchange efficiency on the potential cost savings. From Figure 3 we see that exchanging more than 60% of the sensible heat will bring down the capture costs much further. The solid-solid heat exchanger has a heat duty that is much lower than that of the heat exchanger in the MEA based process. Especially at higher working capacities, the reaction heat, and not the sensible heat energy penalty, dominates the process' thermal energy demand. Hence the heat exchange efficiency does not have a large impact on cost. Due to the relatively low heat exchange rates, higher exchange efficiencies might even increase cost due the increasing capital cost of the exchanger.

For the 'second generation' particles we have evaluated the effect of the sorbent degradation rate on cost. The sorbent degradation rate is probably even more difficult to estimate than sorbent costs. A lower sorbent performance may be the result of chemical [11-17], mechanical or thermal degradation [18, 19]. However, it is still unclear what is the dominating degradation pathway or how fast these type of sorbents degrade under process conditions. The sorbent costs are estimated here, assuming that the support material is available at $ 2.5 per kg [20] and the amine is available at $ 1.5 per kg [21]. Sorbent preparation costs were estimated to account for 30% of the total sorbent costs. The sorbent make up rate was varied. As a reference, the solvent make-up cost in the MEA reference study were calculated assuming a make-up rate of 1.5 kg MEA per tonne of CO_2 captured and a MEA price of $ 1250 per tonne [21]. From Figure 3 we see that increasing the stability of the sorbent material has a large impact on the cost savings achieved. Regarding the sorbent stability we can conclude that the sorbent material should be capable of withstanding at least 7000 adsorption-regeneration cycles (2 kg/tonne degradation rate at a working capacity of 3.1 mol/kg) in order for the sorbent based process to be significantly cheaper than the MEA-based process. Currently however, most of the sorbent materials reported about in literature are tested for only a few (<50) adsorption-desorption cycles [22] and most of these stability test were not done under process conditions. Clearly, stability remains a critical issue and deserves special attention as well as the development of low cost sorbent materials. Based on the cost model used here, we conclude that the cost of CO_2 avoided could potentially be reduced from $59 per tonne of CO_2 calculated for the MEA reference case to $37 per tonne of CO_2 calculated for the sorbent-based process.

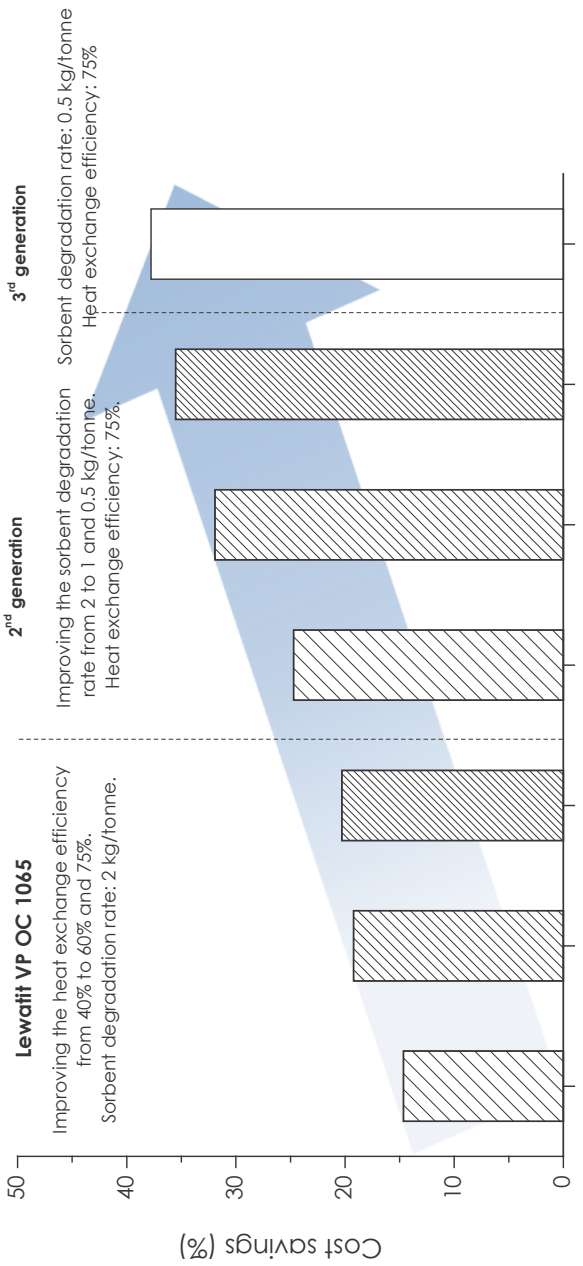

Figure 3: Potential cost savings achieved by switching to the SAS-based process. The cost savings are defined as:

$$1-\frac{\text{Cost of } CO_2 \text{ avoided}|_{SAS}}{\text{Cost of } CO_2 \text{ avoided}|_{MEA}} x100\%$$

6.0

Conclusion

In this work the feasibility of supported amine sorbents for post-combustion CO_2 capture applications in comparison to the conventional scrubbing technology is evaluated. A preliminary process design for a supported amine based CO_2 capture facility at a 500 MWe coal-fired power plant is presented and a techno-economic comparison is made between the novel sorbent based capture process and the MEA-based capture process.

Based on the techno-economic comparison we conclude that an adsorption-based capture process operated with Lewatit® VP OC 1065 sorbent particles has the potential to lower the capital investment and the utilities cost of the conventional amine scrubbing technology with 14% and 26%, respectively. The savings in operational cost are mainly the result of a lower heat demand of the supported amine based process compared to the MEA based system. In both systems, the captured CO_2 is released again by heating of the sorbent/solvent. However, due to the sorbent's lower heat capacity and higher CO_2 capacity, the sensible heat demand of the process is reduced. The lower capital costs are mainly the result of less expensive adsorption column compared the scrubber in the reference process. Overall this would bring down the cost of CO_2 avoided from $59 per tonne of CO_2 calculated for the MEA reference case to $43.5 per tonne.

Using the complete cost model, the impact of different process parameters on the cost savings was evaluated in a cost sensitivity analysis. Regarding the sorbent stability we can conclude that the sorbent material should be capable of withstanding at least 7000 adsorption-regeneration cycles in order for the sorbent based process to be significantly cheaper than the MEA-based process. We also conclude that exchanging around 60% of the sensible heat in a solid-solid heat exchanger is sufficient to achieve good process economics.

Ultimately the cost of CO_2 avoided could potentially be reduced from $59 per tonne of CO_2 calculated for the MEA reference case to $37 per tonne of CO_2 when the working capacity is improved from 1.8 to 3.1 mol/kg and the sorbent degradation rate is improved from 2 kg/t to 0.5 kg/t.

Acknowledgement

This research has been carried out in the context of the CATO-2-program. CATO-2 is the Dutch national research program on CO_2 Capture and Storage technology (CCS). The program is financially supported by the Dutch government (Ministry of Economic Affairs) and the CATO-2 consortium partners. The author would also like to thank Earl Goetheer (TNO), Marco Linders (TNO) and Cristina Sanchez Sanchez for their contribution to this work.

D.

Sizing and cost calculations

D.1 | Particle description

A Toth isotherm was adopted to model the equilibrium CO_2 capacity as a function of the CO_2 partial pressure and temperature. The adsorption isotherm was presented in Chapter 3 of this thesis. The CO_2 loading of the sorbent particles leaving the adsorber was calculated using the reactor model presented in Chapter 4. Regeneration of the sorbent in an almost pure CO_2 environment was investigated in Chapter 2 and Chapter 5. For Lewatit® VP OC 1065, we found that the sorbent can be completely regenerated at 150°C and we estimated, based on experimental data, that regeneration can be completed in less than 5 minutes.

D.2 | Blowers and Solid transportation

The blowers and the bucket lift conveyor were sized to provide information on equipment cost and their use of utilities and consumables. The duty and also the purchased equipment cost of the blowers and the bucket lift conveyor were calculated using equations presented by Peters et al. [8]. The discharge pressure (P2) of each blower is equal to the sum of the gas inlet pressure (P1) and the pressure drop over either the adsorber column, the heat exchanger or the desorber column.

Table D.1: Equations used for sizing and costing of blowers and solid transportation equipment.

Description	Equation	Source
Blower duty	$P_{BL}=\frac{P_{ad}}{\eta_{ad}}$	[8]
Blower adiabatic duty	$P_{ad}=m\,R'\,T_{in}\left(\frac{k}{k-1}\right)\left[\left(\frac{P_2}{P_1}\right)^{\frac{k-1}{k}}-1\right]$	[8]
Bucket lift duty	$P_{SL}=0.07\,F_s^{0.63}\,\Delta Z$	[8]
Purchased cost blowers (2002 US$)	$C_e=8000\,F+6000$	[8]
Purchased cost bucket lift (2002 US$)	$C_e=684\,F+7345$	[8]

The result of the calculations performed are summarized in Table D.2. The duty of the flue gas blower in the MEA process was reported to be 9200 kW. Based on the correlation above, for the same pressure drop (103 mbar) and capacity (690.5 kg/s) we calculate a blower duty of 8000 kW which is only 15% lower than the value reported by Fisher et al. [3].

Table D.2: Input and calculated duties and purchased cost of the blowers and solid transportation equipment used in the SAS process.

Parameter	Flue gas blower	Heat exchanger blower	Desorber blower
F (m^3/s)	576	32.6	32.2
m (kg/s)	678	35.6	40.3
M_w (g/mol)	29.2	29.2	44.0
k	1.40	1.37	1.37
T_{in} (K)	303	303	423
P_1 (Pa)	111000	111000	111000
P_2 (Pa)	116458	150123	150685
ΔP (Pa)	5458	39123	50685
P_{BL} (kW)	3921	1674	1871
C_e (2012 M$)	6.96	0.34	0.37

D.3 | CO_2 Compressor and pump

A compressor is used to raise the pressure of the CO_2 product gas from the desorber operating pressure (0.15 MPa) to 7.38 MPa ($P_{cut\text{-}off}$). Subsequently, a pump boosts the pressure further, up to the end pressure of 13.9 MPa. Here, the cut-off pressure is equal to the critical pressure at 40˚C (T = 313 K) [6]. The number of compression stages, N, is 5 [6]. The efficiency of the compressor and the pump were assumed to be 75%. In the reference study a different cut-off pressure was used; 8.61 MPa. The compression and pumping work were calculated based on equations proposed by McCollum et al. [6]. The total investment cost for the CO_2 compressor was calculated using a correlation proposed by Hendriks et al. [23]. The total investment cost of the pump was calculated based on a cost correlation McCollum et al. [6].

Table D.3: Equations used for sizing and costing of the CO_2 compressor and pump.

Description	Equation	Source
Duty of compressor (per stage)	$P_C=\left(\frac{m\ z\ R\ T_{in}}{M_w\ \eta}\right)\left(\frac{k}{k-1}\right)\left[(CR)^{\frac{k-1}{k}}-1\right]$	[6]
Compression ratio	$CR=\left[\frac{P_{cut\text{-}off}}{P_D}\right]^{\frac{1}{N}}$	[6]
Duty of pump	$P_P=\frac{m\ (P_{final}-P_{cut\text{-}off})}{\rho_L\ \eta}$	[6]
Investment cost compressor (2002 €)	$I_e=(10^5\ m^{-0.71}+1.1\ 10^6\ \ln(\frac{P_{cut\text{-}off}}{P_D})\ m^{-0.6})\ m$	[23]
Investment cost pump (2005 US$)	$I_e=1110\ P_P+70000$	[6]

Table D.4: Input and calculated duties and purchased cost of the compressor.

Parameter	Value
m (kg/s)	113
P_D (MPa)	0.1
$P_{cut\text{-}off}$ (MPa)	7.38
η	0.75
Mw (g/mol)	44
Tin (K)	313
CR	2.36
z (changes each stage)	0.995 / 0.985 / 0.970 / 0.935 / 0.845
k (changes each stage)	1.277 / 1.286 / 1.309 / 1.379 / 1.704
PC (MW)	8.39 / 8.32 / 8.24 / 8.09 / 7.78

The duty of the compressor was calculated to be equal to 40.8 MW. In the reference study a value of 35.0 MW was calculated. The difference is caused by a slightly higher efficiency (79.5%), a higher desorber pressure (192 kPa) and a higher cut-off pressure used in the calculation performed in the reference study. When the same input is used we calculate the compressor duty to be 34.1 MW which differs only 3% from the value calculated in the reference study.

Table D.5: Input and calculated duties and purchased cost of the pump.

Parameters	Value
ρ_L (kg/m^3)	630
η	0.75
P_P (MW)	1.56

The duty of the pump was calculated to be equal to 1.56 MW. The pump duty calculated in the reference study was 1.0 MW. Again, the main reason for this deviation is the higher cut-off pressure assumed in the reference study

D.4 | Adsorber pressure drop

Sizing of the adsorber column was based on the based on the reactor model presented in Chapter 4. The pressure drop calculations were based on a hydrodynamic model for trickle flow reactors presented by Dudukovic et al. [24].

Table D.6: Equations used in the sizing calculations.

Description	Equation	Source
Terminal velocity	$u_R = \sqrt{\frac{4\, d_p\, g\, (\rho_s - \rho)}{3\, \rho\, C_D}}$	[24]
Reynolds particle	$Re_p = \frac{u_R d_p \rho}{\mu}$	[24]
Drag coefficient	$C_D = \frac{24}{Re_p}\left(1+0.173\, Re_p^{0.6567}\right) + \frac{0.413}{1+16300\, Re_p^{-1.09}}$	[24]
Drag coefficient corr.	$C_D' = \frac{C_D}{\left(1-\sqrt{\frac{\beta}{\varepsilon}}\right)}$	[24]
Corrected packing voidage	$\varepsilon' = \varepsilon - \beta$	[24]
Packed bed contribution	$\left(\frac{\Delta P}{L}\right)_{PB} = \left[\frac{A_p(1-\varepsilon')}{Re_p} + B_p\right]\frac{u_G^2 \rho\, (1-\varepsilon')}{d_{eq}\varepsilon'^3}$	[24]
Flowing solids contribution	$\left(\frac{\Delta P}{L}\right)_{FS} = \frac{3}{4}\frac{C_D'\, \beta\, \rho\, (u_G - u_s)}{(\varepsilon-\beta) d_p}$	[24]
Pressure drop	$\frac{\Delta P}{L} = \left(\frac{\Delta P}{L}\right)_{PB} + \left(\frac{\Delta P}{L}\right)_{FS}$	[24]
Heat transfer coefficient	Value of 150 W/m²/K was assumed	[25]
Heat balance	$Q_A = Q_R + Q_S\,(1-\eta_{HX}) + Q_G$	
Reaction heat	$Q_R = m_{CO_2} \Delta H$	
Sensible heat	$Q_S = F_s\, Cp_s (T_D - T_A)$	
Heating/cooling of flue gas	$Q_G = F Cp_g (T_{FG} - T_A) M_w\, M_v$	
Purchased cost of vessel (2002 US$)[1]	$C_e = 3\, W + 70000$	[8]
Cost of column internals (in 2012 k€)	$C_e = 1.7515\, a_A^{0.7369}$	[26]

1.Wall thickness used calculate weight of the adsorber is 1.3 cm (calculated using ASME calculation procedure)

The pressure drop influences the duty of the flue gas blower and hence also the operating cost of the process. Based on our calculations we found that especially the packing has a large influence on system pressure drop as is also the case in the MEA process. It was found that the adsorber pressure drop per meter of packing was equal to 682 Pa. In the reference study the pressure drop per meter packing is reported to be 666 Pa. The lower overall pressure drop is hence the result of a shorter column length. At similar gas velocities as assumed here, pressure drops of 600-800 Pa per meter were measured by Large et al. [27] in a 2 meter high GSTF experimental set-up [27].

D.5 | Desorber and heat exchanger

Sizing of the multi-stage fluid bed desorber was based on a methodology presented by Kunii et al. [28]. The total sorbent hold-up was calculated as the product of the sorbent circulation rate and the estimated residence time required for desorption. It should be noted that inside the desorber 90 m^3 of CO_2 is released per second. This gas also helps to fluidize the particles inside the column

Table D.7: Equations used for sizing and costing of the desorber column.

Description	Equation	Source
Voidage at u_{mf}	Assumed a value of 0.5	
Minimum fluidization velocity	$u_{mf}= \frac{d_p^2(\rho_s- \rho)g\varepsilon_{mf}^3}{150\ \mu(1-\varepsilon_{mf})}$	[28]
Bed voidage	$\varepsilon_b= \delta+(1-\delta)\varepsilon_{mf}$	[28]
Bubble fraction	$\delta= \frac{u_0- u_{mf}}{u_b- u_{mf}}$	[28]
Bubble velocity	$u_b= \frac{5u_{mf}}{\varepsilon_{mf}}$	[28]
Volume of the bed	$V_B= \frac{F_s\tau_D}{(1-\varepsilon_b)\rho_s}$	
Operating gas velocity	$u_0=1.5\ u_{mf}$	
Heat exchange area desorber	$a_D=\frac{Q_D}{\alpha_D\ \Delta T_D}$	
Heat balance	$Q_D= Q_R+ Q_S$	
Volume occupied by heat exchange tubes	$V_H= a_D a'$	
Volume freeboard	$V_{TDH}=0.3\ V_B$	
Column volume	$V_D= V_B+ V_H+V_{TDH}$	
Pressure drop	$\Delta P= \frac{F_s\tau_D g}{0.25\ \pi\ D^2}$	
Purchased cost of vessel (in 2002 US$)	$C_e=11194\ V_D^{0.5531}$	[8]
Cost of column internals (in 2012 k€)	$C_e=1.7515\ a_D^{0.7369}$	[26]

Table D.8: Additional equations for the heat exchanger.

Description	Equation	Source
Heat balance	$Q_{HX}=Q_s\ \eta_{HX}$	
Heat exchange area exchanger	$a_{HX}=\frac{Q_{HX}}{\alpha_{HX}\ \Delta T_{HX}}$	
Volume of the bed	$V_B=\frac{a_{HX}}{a''}$	
Volume freeboard	$V_{TDH}=0.3\ V_B$	
Column volume	$V_{HX}=V_B+V_{TDH}$	
Pressure drop	$\Delta P=\frac{V_B(1-\varepsilon_b)\rho_s g}{D^2}$	
Purchased cost of vessel (in 2002 US$)	$C_e=11194\ V_{HX}^{0.5531}$	[8]
Cost of column internals (in 2012 k€)	$C_e=1.7515\ a_{HX}^{0.7369}$	[26]

The cost of the heat exchange area dominate the purchased cost of both the heat exchanger and the desorber column. The duty of the lean/rich exchanger in the solvent process is 563 MW while the solid/solid exchanger has a duty of only 152 MW. This translates into lower exchanger cost for the solid case.

Table D.9: Summary of heat exchanger design.

Properties	SAS (this work)	MEA (Fisher et al. [3])
Heat transfer coefficient (W/m/K)	150	511
Heat duty (MW)	152	563
Temperature approach (K)	24	9
Amount of area (m^2)	40759	101136
Purchased cost exchanger (2012 M$)	7.0	15.0
Cost per square meter area (US$ m^2)	171	148

In the desorber, the overall bed-to-wall heat transfer coefficient was calculated to be 155 W/m^2/K [28]. The steam was assumed to have a temperature of 440 K which is the temperature of saturated steam at 733 kPa. The heat required inside the desorber column was 477 MW. Part of this heat is supplied by exchanging heat with the hot solids leaving the desorber column. The average temperature difference between the solids and the steam is 17 K in the base case. Hence we can calculate that around 163272 m^2 of heat exchange area is required. In the MEA case around 31000 m^2 is required to supply the 500 MW of heat required for solvent regeneration.

D.6 | Cost indexing

Factors used for correcting for inflations.

Table D.10: CEPCI index.

Cost year	Index
2002	395.8
2005	468.2
2007	525.4
2012	596.2

D.7 | Purchased equipment cost

Based sizing described above the purchased equipment costs were calculated. A breakdown of the purchased equipment cost is given in the table below.

Table D.11: Breakdown of the purchased equipment cost.

Unit	PEC (M$)
Flue gas blower	7.0
Adsorber	10.0
Conveyor	1.5
Heat exchanger (including blower)	7.0
Desorber	17.1
Desorber blower	0.4
CO_2 compressor[1]	57.5
CO_2 pump	2.7
Cooling system[2]	10.5
Total (excluding the compressor)	53.7

1. Compressor investment cost 2. Adopted from MEA case

D.8 | Calculation of the capital expenditure

Table D.12: Breakdown of the total capital requirement.

Capital expenditure	Factor used	MEA (M$)	SAS (M$)
Purchased equipment cost (PEC)	75.8	53.7	
Purchased equipment installation (% of PEC)	18.00	13.6	9.7
Instrumentation and controls (% of PEC)	8.00	6.0	4.3
Piping (% of PEC)	20.00	15.2	10.7
Electrical systems (% of PEC)	10.00	7.6	5.4
Buildings (% of PEC)	18.00	13.6	9.7
Yard improvements (% of PEC)	6.00	4.6	3.2
Service facilities (% of PEC)	24.00	18.2	12.9
Total installed capital		154.6	109.5
Compressor investment cost (pump included)		43.3	60.2
Total process plant cost (PPC)		197.9	169.7
Engineering and home office (% of PPC)	6.00	11.9	10.2
Project contingency (% of PPC)	30.00	59.4	50.9

Process contingency (% of PPC)	5.00	9.9	8.5
Total plant cost (TPC)	-	279.0	239.3
Interest and inflation (% of PPC)	10.00	19.8	17.0
Total plant investment (TPI)		298.8	256.2
Royalty fees (% of PPC)	0.500	1.0	0.9
Start-up			
Component 1 (% of TPI)	2.00	6.0	5.1
Component 2	30 days of variable O&M	0.7	0.8
Spare parts (% of TPC)	0.50	1.4	1.2
Working capital	30 days of fixed O&M	0.7	0.6
Land (% of TPI)	1.00	3.0	2.6
Total capital requirement (TCR)		311.4	267.3

D.9 | Calculation of the operating expenditure

The costs associated with the operation of the CO_2 capture plant are summarized below. The sorbent make-up costs are calculated as the product of the sorbent cost and the sorbent degradation rate.

Table D.13: Breakdown of the operating cost.

Cost item	Factor	MEA (M$/yr)	SAS (M$/yr)
Maintenance (% of TPC)	2.2	6.1	4.7
Maintenance allocated to labor	12	0.7	0.6
Administration	30% of total labor cost	0.2	0.2
Operating labor	1 operator full time	0.8	0.8
Fixed O&M	-	7.9	6.3
Solid waste disposal	-	0.04	0.1
Sorbent make-up cost	-	6.0	9.3
Water cost	-	2.0	-
Variable O&M	-	8.0	9.4

D.10 | Calculation of the cost of CO_2 avoided and levelized cost of electricity (COE)

The capture facility requires steam and electricity to operate. These utilities are taken into account with the derating of the power plant. The derated plant capacity was calculated in the same way as described by Fisher et al. [3]. The cost of CO_2 avoided and the levelized cost of electricity were calculated using equation provided by Metz et al. [29].

List of symbols

P_{BL}	Actual power of blower (kW)	
P_{ad}	Adiabatic power (kW)	
η_{ad}	Adiabatic blower efficiency (-)	0.72
m	Mass flow rate of incoming gas (kg/s)	
R'	Specific gas constant (J/kg/K)	
T_{in}	Temperature of incoming gas (blower design) (K)	
k	Heat capacity ratio (-)	
P_1	Inlet pressure (Pa)	
P_2	Discharge pressure (Pa)	
P_{SL}	Power for solid transportation (kW)	
ΔZ	Height of vertical solid transportation (m)	24
C_e	Purchased cost	
F	Volumetric flow of incoming gas (m^3/s)	
P_C	Power of the compressor (kW)	
z	Compressibility factor	
R	Gas constant (J/mol/K)	
M_v	Molar volume of the gas (mol/m^3)	41
η	Efficiency of compressor/pump (-)	0.75
CR	Compression ratio (-)	
$P_{cut\text{-}off}$	Cut-off pressure (Pa)	$7.38\ 10^6$
P_D	Operating pressure of desorber (Pa)	$0.1\ 10^6$
N	Number of compression stages	5
P_P	Power of the pump (kW)	
P_{final}	Pump outlet pressure (Pa)	$13.9\ 10^6$
ρ_L	CO_2 liquid density (kg/m^3)	
u_R	Terminal velocity ($m\ s^{-1}$)	
d_p	Particle diameter (m)	$0.7\ 10^{-4}$
g	Gravitational constant (m/s^2)	9.81
ρ_s	Solid density (kg/m^3)	880
ρ	Gas density (kg/m^3)	1.1

Re_P	Particle Reynolds number	
μ	Gas viscosity (Pa s)	$1.6\ 10^{-5}$
C_D	Drag coefficient (-)	
β	Solid holdup (-)	
ε	Packing voidage	0.85
ε'	Corrected packing voidage	
A_p	Packing parameter	78
B_p	Packing parameter	0.97
u_G	Gas velocity adsorber (m/s)	1.8
u_s	Solid velocity (m/s)	0.1
d_{eq}	Packing equivalent diameter (m)	0.02
Q_A	Heat produced in the adsorber (W)	
Q_G	Sensible heat of the gas (W)	
Q_R	Reaction heat (W)	
Q_S	Sensible heat of the solids (W)	
η_{HX}	Heat exchange efficiency (base case) (-)	0.6
m_{CO2}	CO_2 captured (mol s^{-1})	2625
ΔH	Reaction heat (J mol^{-1})	$86.7\ 10^3$
F_s	Solid circulation rate (kg s^{-1})	
Cp_s	Solid heat capacity (J kg^{-1} K^{-1})	1500
T_D	Temperature desorber (K)	423
T_A	Temperature adsorber (K)	303
Cp_G	Gas heat capacity (J/kg/K)	1000
T_{FG}	Temperature of the flue gas (K)	
M_w	Gas molecular weight (kg $kmol^{-1}$)	0.29
W	Weight of adsorber vessel (kg)	
a_A	Required heat exchange area adsorber (m^2)	
u_{mf}	Minimum fluidization velocity (m/s)	0.34
ε_{mf}	Voidage at minimum fluidization (-)	0.5
δ	Bubble fraction (-)	
ε_b	Bed voidage (-)	
u_b	Bubble velocity	
u_0	Operating velocity desorber	

Q_D	Heat produced in the desorber (W)	
a_D	Required heat exchange area desorber (m^2)	
V_b	Volume of fluid bed (m^3)	
τ_D	Residence time in the desorber (s)	300
L/D	Aspect ratio (-)	1.5
Q_D	Heat demand desorber (W)	
α_D	Heat exchange coefficient desorber ($W/m^2/K$)	155
ΔT_D	Temperature difference between the steam extracted from the power plant and the desorber average temperature (K)	17
V_H	Volume occupied by heat exchange tubes (m^3)	
a'	Volume occupied by heat exchange area (m^3/m^2)	1/267
a"	Amount of heat exchange area per unit volume reactor (m^2/m^3)	87
V_{TDH}	Volume of freeboard (m^3)	
V_D	Desorber volume (m^3)	
Q_{HX}	Duty heat exchanger (W)	
α_{HX}	Heat exchange coefficient heat exchanger ($W/m^2/K$)	155
a_{HX}	Required heat exchange area exchanger (m^2)	
ΔT_{HX}	Heat exchanger temperature approach (K)	
V_{HX}	Exchanger volume (m3)	

References

1. Sjostrom, S. and H. Krutka, Evaluation of solid sorbents as a retrofit technology for CO_2 capture. Fuel, 2010. 89(6): p. 1298-1306.
2. Yang, W.C. and J. Hoffman, Exploratory design study on reactor configurations for carbon dioxide capture from conventional power plants employing regenerable solid sorbents. Industrial and Engineering Chemistry Research, 2009. 48(1): p. 341-351.
3. Fisher, K.S., et al., Integrating MEA regeneration with CO_2 compression and peaking to reduce CO_2 capture costs, 2005.
4. Abu-Zahra, M.R.M., J.P.M. Niederer, P.H.M. Feron, and G.F. Versteeg, CO_2 capture from power plants. Part II. A parametric study of the economical performance based on mono-ethanolamine. International journal of greenhouse gas control, 2007. 1(2): p. 135-142.
5. Abu-Zahra, M.R.M., L.H.J. Schneiders, J.P.M. Niederer, P.H.M. Feron, and G.F. Versteeg, CO_2 capture from power plants. Part I. A parametric study of the technical performance based on monoethanolamine. International journal of greenhouse gas control, 2007. 1(1): p. 37-46.
6. McCollum, D.L. and J.M. Ogden, Techno-Economic Models for Carbon Dioxide Compression, Transport, and Storage & Correlations for Estimating Carbon Dioxide Density and Viscosity, 2006, Institute of Transportation Studies, University of California.
7. Gupta, C.K. and D. Sathiyamoorthy, Fluid bed technology in materials processing. 1999, Boca Raton, Fla.: CRC Press. 498 p.
8. Peters, M.S., K.D. Timmerhaus, and R.E. West, Plant design and economics for chemical engineers. 5th ed. McGraw-Hill chemical engineering series. 2003, New York: McGraw-Hill. xvii, 988 p.
9. IHS Global Insight, I., Economic Indicators, in Chemical Engineering Magazine2012.
10. Rochelle, G., et al., Aqueous piperazine as the new standard for CO_2 capture technology. Chemical Engineering Journal, 2011. 171(3): p. 725-733.
11. Sayari, A. and Y. Belmabkhout, Stabilization of amine-containing CO_2 adsorbents: Dramatic effect of water vapor. Journal of the American Chemical Society, 2010. 132(18): p. 6312-6314.
12. Sayari, A., A. Heydari-Gorji, and Y. Yang, CO_2-induced degradation of amine-containing adsorbents: Reaction products and pathways. Journal of the American Chemical Society, 2012. 134(33): p. 13834-13842.
13. Sayari, A., Y. Belmabkhout, and E. Da'na, CO_2 deactivation of supported

amines: Does the nature of amine matter? Langmuir, 2012. 28(9): p. 4241-4247.
14. Drage, T.C., A. Arenillas, K.M. Smith, and C.E. Snape, Thermal stability of polyethylenimine based carbon dioxide adsorbents and its influence on selection of regeneration strategies. Microporous and mesoporous materials, 2008. 116(1-3): p. 504-512.
15. Heydari-Gorji, A. and A. Sayari, Thermal, oxidative, and CO_2-induced degradation of supported polyethylenimine adsorbents. Industrial & Engineering Chemistry Research, 2012. 51(19): p. 6887-6894.
16. Heydari-Gorji, A., Y. Belmabkhout, and A. Sayari, Degradation of amine-supported CO_2 adsorbents in the presence of oxygen-containing gases. Microporous and Mesoporous Materials, 2011. 145(1-3): p. 146-149.
17. Khatri, R.A., S.S.C. Chuang, Y. Soong, and M. Gray, Thermal and chemical stability of regenerable solid amine sorbent for CO_2 capture. Energy & Fuels, 2006. 20(4): p. 1514-1520.
18. S. Choi, J.H.D., C. W. Jones, Adsorbent Materials for Carbon Dioxide Capture from Large Anthropogenic Point Sources. ChemSusChem, 2009. 2(9): p. 796-854.
19. Zhao, W.Y., Z. Zhang, Z.S. Li, and N.S. Cai, Investigation of thermal stability and continuous CO_2 capture from flue gases with supported amine sorbent. Industrial & engineering chemistry research, 2013. 52(5): p. 2084-2093.
20. Abanades, J.C., E.S. Rubin, and E.J. Anthony, Sorbent cost and performance in CO_2 capture systems. Industrial & Engineering Chemistry Research, 2004. 43(13): p. 3462-3466.
21. Rao, A.B. and E.S. Rubin, A technical, economic, and environmental assessment of amine-based CO_2 capture technology for power plant greenhouse gas control. Environmental Science & Technology, 2002. 36(20): p. 4467-4475.
22. Samanta, A., A. Zhao, G.K.H. Shimizu, P. Sarkar, and R. Gupta, Post-combustion CO_2 capture using solid sorbents: A review. Industrial and Engineering Chemistry Research, 2012. 51(4): p. 1438-1463.
23. Hendriks, C. and W. Graus, Global carbon dioxide storage potential and costs, in EEP-02001, TNO and EcoFys, Editors. 2004.
24. Dudukovic, A.P., N.M. Nikacevic, D.L. Petrovic, and Z.J. Predojevic, Solids holdup and pressure drop in gas-flowing solids-fixed bed contactors. Industrial & engineering chemistry research, 2003. 42(12): p. 2530-2535.
25. Cheng, Y., C.N. Wu, J.X. Zhu, F. Wei, and Y. Jin, Downer reactor: From fundamental study to industrial application. Powder Technology, 2008.

183(3): p. 364-384.
26. Towler, G.P. and R.K. Sinnott, Chemical engineering design : principles, practice, and economics of plant and process design. 2nd ed. 2013, Boston, MA: Butterworth-Heinemann. xvi, 1303 p.
27. Large, J.F., M. Naud, P. Guigon, and M.A. Bergougnou, Hydrodynamics of the raining packed-bed gas-solids heat exchanger. The Chemical Engineering Journal, 1981. 22(2): p. 95-100.
28. Kunii, D.o. and O. Levenspiel, Fluidization engineering. 2nd ed. Butterworth-Heinemann series in chemical engineering. 1991, Boston: Butterworth-Heinemann. xxvii, 491 p.
29. Metz, B., O. Davidson, H.d. Coninck, M. Loos, and L. Meyer, IPCC special report on carbon dioxide capture and storage. Other Information: IEACR LIB 700. 2005. Medium: X; Size: 440; 23.3 MB pages.

Chapter 07

Summary and Outlook

Summary

This thesis deals with the development of a new supported amine based CO_2 capture process in order to reduce the costs for CO_2 capture at power plants.
Application of carbon capture and storage (CCS) at fossil fuel burning plants is, among other alternatives, a technically feasible method to significantly reduce the global anthropogenic emission of CO_2. However, current cost estimates show that using the current state-of-art technology in carbon capture and storage at power plants would result in an increase in the cost of electricity by 35-80% mainly due to high cost of CO_2 capture. This increase in cost of electricity is a major hurdle in the deployment of CCS and the development of a more cost effective capture technology is now a main objective of CO_2 capture research.

Applying a process using supported amine adsorbents (SAS) may offer a low-cost alternative to the conventional capture process. This research aims to develop a new capture process with a lower energy demand than the conventional process. The idea is to replace the liquid solvent by a solid sorbent i.e. applying an adsorption based capture process instead of an absorption based process. Switching from an aqueous solvent to a solid sorbent could reduce the energy required for CO_2 capture, as the energy required for heating a sorbent is (in general and at similar CO_2 capacities per unit of mass) much lower than the energy required for heating the aqueous amine solutions currently used. This is due to the lower heat capacity of solids compared to water. Moreover, the evaporation of solvent is not an issue in the novel process. These envisioned savings in energy would significantly reduce the CO_2 capture costs.

The work presented in this thesis focusses on the preparation and optimization of sorbent materials as well as the selection, design, modelling and experimental validation of process concepts. In addition a techno-economic evaluation of the developed process is presented. In this chapter we have summarized but also tried to reflect on the work presented in this thesis.

A detailed literature overview on sorbent based post-combustion CO_2 capture is provided in Chapter 1. Especially supported amine sorbents were identified as a promising class of CO_2 sorbents and the experimental work focused on testing and evaluating these materials. Energy calculations, pre-

sented in Chapter 1 of this thesis, show that supported amine sorbents have indeed the potential to significantly reduce the amount of energy required to capture CO_2. The conventional process requires around 3-4 GJ of heat per ton of CO_2 captured for solvent regeneration, while these supported amine sorbents require 1.5 to 2 GJ per ton of captured CO_2. This shows there is a clear incentive for further development and more detailed evaluation of these supported amine sorbents. The above mentioned energy analysis also revealed that we should aim to develop a sorbent with a cyclic capacity of at least 1.5 mol of CO_2 per kg of sorbent to end up with a process that is competitive on energy efficiency with the conventional technique. This sets a clear target for the sorbent development related activities performed in Chapter 2.

Impregnated sorbent materials were prepared by physical impregnation of silica and polymer based support materials with different types of amine molecules, resulting in sorbents with CO_2 capacities in the range of 1.5 to 3.8 mol/kg at conditions relevant for post-combustion CO_2 capture. The CO_2 capacity of the impregnated sorbents was significantly improved by tuning the amine loading and the pore volume of the support. However, exposing the impregnated sorbent materials to temperatures above 130˚C led to sorbent degradation as a result of (1) the loss of active amine material due to evaporation and (2) the undesired formation of urea. Whereas the impregnated sorbent material Diaion® HP-2MG (38wt%) showed the highest CO_2 capacity (3.8 mol/kg), the commercial sorbent Lewatit® VP OC 1065 was found to be a good candidate sorbent for its excellent thermal stability. Using the selected sorbent(s) we can potentially reduce the thermal energy requirement for CO_2 capture from 3-4 GJ/t to an estimated 2.2 GJ/t.

Since flue gas contains large amounts of water, we focused in Chapter 3 on the capture of CO_2 and H_2O from gas mixtures containing CO_2, H_2O and N_2, using Lewatit® VP OC 1065 as sorbent. Both CO_2 and H_2O were found to adsorb on the amine active sites present on the pore surface of the sorbent material. However, whereas the interaction between CO_2 and the amine groups is chemical, the adsorption behavior of H_2O on Lewatit® VP OC 1065 shows the characteristics of physical multilayer adsorption. The difference in interaction is also clearly reflected in the differences in the adsorption heat (ΔH_{H2O} = 43 kJ/mol, ΔH_{CO2} = 70-80 kJ/mol) and differences in the final capacity. The highest capacity observed for H_2O was 12.5 mol/kg (at a relative humidity (RH) of 95%). The highest CO_2 capacity observed was 2.8 mol/kg (303K, P_{CO2} = 81 kPa). Due to the high H_2O capac-

ity, the sorbent material can adsorb practically all water in the flue gas that enters the adsorber column. This increases the total energy demand of the sorbent based post-combustion capture process with 40%. To prevent the co-adsorption of large quantities of water, several options were analyzed using the adsorption isotherms obtained for CO_2 and H_2O. Lowering the dew point of the flue gas upstream of the adsorber was identified as the most viable option. In this way, a large part of the water is removed from the flue gas before it is contacted with the sorbent particles. This reduces the adsorption of H_2O in the adsorber column.

Whereas Chapter 2 and 3 were mainly focused on gathering equilibrium adsorption data, in Chapter 4 and Chapter 5 we aimed to select and design a suitable process around these sorbent particles and validated the process concept experimentally. The process selection and design was based on extensive particle and reactor modelling. The reactor model developed in this chapter was validated based on the experimental data presented in Chapter 5. We concluded that heat transfer, at a particle level, is fast enough to limit temperature differences inside the particle and between the gas and the particles to less than 5 K. The uptake rate of CO_2 was found to be determined by combination of external mass transfer, pore diffusion and reaction kinetics with particle effectiveness factors ranging from 60-70%.

We have based the reactor selection procedure on a list of desired process characteristics; a reactor 'wish' list. We would like a process with a high productivity (>0.6 mol/m^3/s), an adsorber that allows for high gas velocities (1-2 m/s) but still has a low pressure drop (<210 mbar) and we would like to make optimal use of the sorbents' CO_2 capacity. The productivity of the capture system is here defined as the amount of CO_2 captured per second per cubic meter of installed reactor volume.

In the experimental work presented in Chapter 5 we found that the rate of adsorption of the sorbent particles is a strong function of the gas phase CO_2 concentration. Consequently, these sorbent particles would perform best in a counter-currently operated adsorber column, as this would maximize the driving force for CO_2 capture and hence maximize the uptake rate. We argue that especially a gas-solid trickle flow reactor would perform well as a CO_2 adsorber column. Next to counter current G-S contacting, it allows for high gas velocities equal or higher than the gas velocities applied in a MEA scrubber without resulting in unacceptable pressure drops. For desorption in (almost) pure CO_2 atmosphere neither the desorber mass trans-

fer characteristics nor the choice of G-S contacting flow pattern will significantly influence the performance of the column. Here, good heat exchange characteristics and solid phase segregation is key and either a staged fluid bed or a cross-flow fluid bed are suitable reactor types. Solid phase segregation provides a better defined sorbent residence time and minimizes the sorbent inventory.

A lab scale continuous capture unit was designed and constructed. Lewatit® VP OC 1065 was applied in this continuous lab-scale CO_2 capture facility, consisting of a trickle flow adsorber and a multi-stage fluid bed desorber. The experimental work presented in Chapter 5 summarizes over 300 hours of operating experience with this facility. This is equivalent to approximately 350 adsorption/desorption cycles. The main focus here was on the performance of the adsorber column. We have measured the effect of process parameters like gas velocity, solid flux and CO_2 inlet concentration on adsorber performance in terms of the capture efficiency, productivity and working capacity. Typically around 5 kg of sorbent was circulated per hour.

The performance of the trickle flow adsorber was found to be adequately described by a 1-D plug-flow model. The experimental results combined with the modeling work showed that a gas-solid trickle flow reactor is indeed a suitable adsorber for the post-combustion capture of CO_2. The model was used to design a full scale adsorber unit to capture 90% of the CO_2 emitted by a 500 MWe coal fired power plant. The trickle flow adsorber is expected to outperform the scrubber in the conventional MEA based process in terms of productivity; 1.1 compared to 0.6 mol/m^3/s in the MEA based process.

Finally, the energy demand for CO_2 capture using this lab scale capture facility was measured. Based on the measured desorber energy demand, the reaction heat of the sorbent material was estimated to be 62 kJ/mol. In total, the energy associated with heating of the sorbent particles and desorption was 141 kJ/mol or 3.2 GJ/t at a working capacity of 1.2 mol/kg. With an increase in working capacity to 2.7 mol/kg, this energy demand is reduced to 1.6 GJ/t. This heat demand was measured under low desorption temperatures (100°C) and using N_2 as sweeping gas.

In Chapter 6 the feasibility of supported amine sorbents for post-combustion CO_2 capture applications in comparison to the conventional scrubbing technology is evaluated. This chapter presents a preliminary process design for a CO_2 capture facility at a 500 MWe coal-fired power plant and a techno-

economic comparison of the performance of the novel capture process with the state of the art MEA scrubbing technology.
Based on the techno-economic comparison we conclude that an adsorption-based capture process operated with Lewatit® VP OC 1065 sorbent particles has the potential to lower the capital investment with 14% and the utilities cost of the conventional amine scrubbing technology with 26%. The savings in operational cost are mainly the result of a lower heat demand of the supported amine based process compared to the MEA based system. In both systems, the captured CO_2 is released again by heating of the sorbent/solvent. However, due to the sorbent's lower heat capacity and higher CO_2 capacity, the sensible heat demand of the process is reduced. The lower capital costs are mainly the result of less expensive adsorption column compared the scrubber in the reference process. Overall this would bring down the cost of CO_2 avoided from $59 per tonne of CO_2, as calculated for the MEA reference case, to $43.5 per tonne of CO_2 avoided for the sorbents case.

The cost of CO_2 avoided could potentially be further reduced from the current $59 per tonne of CO_2 calculated for the MEA reference case to $37 per tonne of CO_2 when the capacity and the stability of the sorbent material are improved. As the cost estimates for the capture processes are done with the same methodology for both the MEA and the sorbents process, the anticipated benefits of the sorbent process are considered to be realistic and hence, there clearly is clearly scope to further develop this technology.

Outlook

In this thesis we have shown that supported amine based adsorption is a competitive process to capture CO_2 from flue gas. We have gathered equilibrium adsorption data, investigated the speed of the adsorption process and combined this knowledge into a reactor model that is now ready for more elaborate column design studies. In this process, we have learned that these sorbents possess high enough CO_2 working capacities to reduce the energy required for capturing CO_2 and high enough CO_2 uptake rates to reduce the size of the adsorber column. We have made clear steps towards scale-up as well. The experimental work presented in Chapter 2 of this thesis initially focused on testing several milligrams of sorbent material in TGA measurements, subsequently we continued with the testing of several grams of sorbent material in fixed-bed measurements in Chapter 3 and finally tested the use of several kilograms of sorbent material in Chapter 5. The concept was even taken to the tonne scale in a collaboration between the University of Twente and the Tsinghua University [1]. Still, in our view, before taking this CO_2 separation technology to the pilot scale, a few issues remain that need to be investigated further.

In this thesis, regeneration of the sorbent in an almost pure CO_2 environment was investigated in Chapter 2 and Chapter 5. For Lewatit® VP OC 1065, we found that the sorbent can be completely regenerated at 150°C and we estimated based on experimental data that regeneration can be completed in less than 5 minutes. Still, in Chapter 2 we found that at temperatures around 150°C the sorbent loses part of its capacity as a result of urea formation. This CO_2 induced degradation appears to be the leading degradation mechanism. Water/steam helps to suppress the formation of urea. This would allow for deep regeneration of the sorbent material at high temperatures. Future research should focus on answering the following questions: Can the addition of steam in the regeneration step completely prevent this CO_2 induced degradation and how much steam would be required to do so?

If the answer to the first question is a 'yes' and the answer to the second question is 'less than 20 vol% of H_2O in the regeneration gas (see Chapter 3 for more information)' we see no other (major) issues that need to be solved before taking the process to the pilot scale.

Looking a little further ahead, on a pilot scale, the main concerns would be related to solid handling and in particular the mechanical stability of the sorbent material. In the experimental work we have performed in Chapter 5 we have gathered over 300 hours of operating experience. Comparison of the particle size distribution of the sorbent material, before and after testing, showed no sign of attrition. Still, the mechanical degradation rate on a process scale will depend both on the type of support material as well as on the type of sorbent transportation equipment used. Therefore, dedicated attrition tests in pilot scale equipment are needed to further strengthen the confidence in this solid sorbent based system.

Switching from the more mature and commercially available MEA based process for post-combustion CO_2 capture to a SAS based process is estimated to result in a cost reduction of 15-40% for the CO_2 capture and compression process. Whereas the sorbent based process appears technically feasible and ready for scale up, some more work is needed to develop a sorbent that can be produced commercially against a competitive sorbent price (similar to amine solvents). The way forward would then be to investigate the process on a pilot scale, thereby optimizing the solids handling components (valves, heat exchangers) at a relevant scale and subsequently evaluate the process economics in more detail.

References

1. *Zhao, W., et al. Post-combustion CO_2 Capture demonstration using supported amine sorbents: Design and evaluation of 200 kWth pilot. in Energy Procedia. 2014*

Samenvatting

Dit proefschrift beschrijft de ontwikkeling en evaluatie van een nieuw proces om op een efficiëntere manier CO_2 af te vangen die door energiecentrales als rookgas wordt uitgestoten.
Momenteel is de energiesector verantwoordelijk voor 30 tot 40% van de totale wereldwijde antropogene uitstoot van CO_2 in de atmosfeer en dus kan het afvangen van CO_2 geproduceerd door energiecentrales de mondiale uitstoot van CO_2 significant verlagen. De kosten voor CO_2-afvangst op basis van de conventionele technologieën zijn echter hoog en dit heeft tot gevolg dat de elektriciteitsprijzen met 35-80% zullen stijgen wanneer energiecentrales worden uitgerust met een conventionele CO_2-afvangstinstallatie. Deze hoge kosten belemmeren de implementatie van 'CO_2 Afvangst, Transport en Opslag' (CATO). Daarom richt het onderzoek naar CO_2-afvangst zich vooral op het ontwikkelen van een nieuwe technologie om goedkoper CO_2 af te vangen.

Het conventionele proces voor het afvangen van CO_2 maakt gebruik waterige amineoplossingen (ook wel solvents, typisch 30% MonoEthanolAmine (MEA) in water) om CO_2 in te absorberen. In dit proces is veel warmte nodig voor het opwarmen van het solvent voor de regeneratie. Dit brengt hoge operationele kosten met zich mee. De warmtevraag van het proces is vooral zo hoog door de hoge soortelijke warmte van het solvent. Door van een vloeibaar 'solvent' over te stappen naar een vast 'adsorbent', kan het energieverbruik flink worden verlaagd aangezien, in de regel, vaste stoffen een lagere soortelijk warmte hebben dan de waterige amineoplossingen die ingezet worden in conventionele processen. Hierdoor kost het veel minder energie om het 'adsorbent' op te warmen dan om het 'solvent' op te warmen. Verder kan, door te switchen van een absorptieproces naar een adsorptieproces, ook het verdampen van water in de desorptiekolom grotendeels worden voorkomen, wat de energiebehoefte van het proces verder reduceert.

Dit proefschrift beschrijft zowel de ontwikkeling als de verbetering van adsorbentia, als ook de selectie, het ontwerp en de experimentele validatie van het geselecteerde procesconcept. Het proefschrift wordt afgesloten met een technisch-economische evaluatie van het ontwikkelde proces.

Hoofdstuk 1 geeft een gedetailleerd overzicht van de huidige kennis op het gebied van zogeheten 'post-combustion'-CO_2-afvangst met behulp van adsorbentia. Uit de literatuurstudie kwam naar voren dat vooral amine-gebaseerde adsorptiedeeltjes veelbelovend zijn. Een eerste energieanalyse laat zien dat het toepassen van dit type adsorbent, de energie die nodig is voor het regeneratief afvangen van CO_2 significant kan verlagen. Het conventionele MEA-proces verbruikt tussen de 3 en 4 GJ per ton CO_2 aan warmte om het solvent te regenereren. Deze amine-gefunctionaliseerde adsorbtiematerialen verbruiken naar schatting slechts 1.5 tot 2 GJ per ton CO_2. Het adsorbent moet een minimale werkcapaciteit van tenminste 1.5 mol/kg hebben om deze energiebesparingen daadwerkelijk te realiseren.

In hoofdstuk 2 zijn verschillende adsorbentia ontwikkeld door poreus silica- en polymeermateriaal te impregneren met verschillende aminemoleculen. Met de geproduceerde adsorbentia zijn CO_2-werkcapaciteiten tussen de 1.5 en 3.8 mol/kg behaald onder rookgascondities tijdens adsorptie. De CO_2-capaciteit van de geïmpregneerde deeltjes kan significant verbeterd worden door het aminegehalte te optimaliseren en het porievolume van het dragermateriaal te vergroten. Uit experimenten bleek verder dat wanneer deze geïmpregneerde deeltjes blootgesteld worden aan temperaturen boven 130°C, de capaciteit van de deeltjes achteruit gaat. Dit is toe te schrijven aan het verdampen van geïmpregneerd amine en de vorming van ureum.

Daar waar de capaciteit van de geïmpregneerde deeltjes gebaseerd op het dragermateriaal Diaion® HP-2MG veruit het hoogst was (3.8 mol/kg bij een aminebelading van 38 wt%), bleek het commerciële adsorbent Lewatit® VP OC 1065 het meest stabiel bij hogere temperaturen. Met dit materiaal kan de energiebehoefte reeds worden teruggebracht van 3-4 GJ/t voor het conventionele MEA-proces, naar 2.2 GJ/t.

Aangezien rookgas, naast CO_2, ook veel H_2O bevat, is er in hoofdstuk 3 gekeken naar de co-adsorptie van CO_2 en H_2O. Lewatit® VP OC 1065 is als benchmark-adsorbent geselecteerd op basis van de goede thermische stabiliteit. De experimenten laten zien dat zowel H_2O als CO_2 adsorbeert aan de aminegroepen van het adsorptie materiaal. Echter, waar de interactie tussen CO_2 en de aminegroepen chemisch van aard is, is de interactie tussen H_2O en de aminegroepen meer fysisch van aard. De adsorptie van H_2O laat dezelfde karakteristieken zien als multilaag-adsorptie. Het verschil in adsorptiegedrag is duidelijk terug te zien in zowel het verschil in adsorp-

tiewarmte (ΔH_{H2O} = -43 kJ/mol, ΔH_{CO2} = -70-80 kJ/mol) als het verschil in adsorptiecapaciteit. De hoogste gemeten capaciteit voor H_2O was 12.5 mol/kg (bij een luchtvochtigheid van 95%). De hoogste capaciteit voor CO_2 was 2.8 mol/kg (303K, P_{CO2} = 81 kPa).
Door de hoge adsorptiecapaciteit voor water adsorbeert Lewatit® VP OC 1065 bijna al het water dat in rookgas aanwezig is. Dit zou kunnen resulteren in een 40% toename in de energiebehoefte van het proces. Er zijn verscheidene strategieën geanalyseerd om te voorkomen dat het adsorbent grote hoeveelheden H_2O adsorbeert onder de procescondities in de adsorber. Aan de hand van de gemeten adsorptie-isothermen voor CO_2 en H_2O bleek het verlagen van het dauwpunt van het rookgas, reeds voordat het gas de adsorber binnenkomt, de meest geschikte methode.

In hoofdstuk 2 en hoofdstuk 3, lag de focus op het verzamelen van informatie over het CO_2- en H_2O-adsorptie evenwicht. Hoofdstuk 4 en 5 richten zich vervolgens op de selectie en het ontwerp van het meest optimale proces en het experimenteel valideren van dit procesconcept op lab-schaal. Voor de processelectie en het procesontwerp is een gedetailleerd deeltjesmodel en een gedetailleerd reactormodel ontwikkeld. Het reactormodel is gevalideerd aan de hand van experimentele data in hoofdstuk 5. Uit de simulaties blijkt dat warmtetransport in en rond de adsorptiedeeltjes snel genoeg is om de warmte af te voeren die vrijkomt tijdens adsorptie. Verder is duidelijk geworden dat de CO_2-opnamesnelheid van de deeltjes wordt bepaald door een combinatie van poriediffusie en reactiekinetiek. De benuttingsgraad van de gebruikte deeltjes is 60-70%.

De reactorselectie is gebaseerd op een lijst van gewenste karakteristieken. We zouden graag een proces ontwerpen met een hoge productiviteit, een adsorber ontwerpen die hoge gassnelheden toestaat zonder dat daar een hoge drukval mee gepaard gaat en optimaal gebruik willen maken van de CO_2-capaciteit van de deeltjes in het proces. De productiviteit is hierbij gedefinieerd als het aantal molen CO_2 dat afgevangen wordt per volume-eenheid van de reactor per seconde.

Uit het experimentele werk in hoofdstuk 5 bleek dat de CO_2-opnamesnelheid sterk afhangt van de CO_2-concentratie in de gasfase. Daarom zouden deze deeltjes het best presteren in een tegenstroom contactapparaat omdat op deze manier de drijvende kracht voor de opname van CO_2 het hoogst is. Een ‘gas-solid trickle flow’-kolom (GSTF-kolom) zou derhalve een uitstekende keus zijn voor de adsorptie van CO_2. Dit reactortype heeft een

tegenstroomkarakter en het laat hoge gassnelheden toe zonder dat daar een hoge drukval mee gemoeid gaat. Omdat er in de desorber bijna alleen CO_2 aanwezig is in de gasfase, zijn de massatransport eigenschappen van de reactor en de manier waarop het gas in contact wordt gebracht met de deeltjes minder van belang voor de prestaties van de desorber. Wel is het belangrijk dat de desorber over goede warmtetransport eigenschappen beschikt en dat het mengen van deeltjes zoveel mogelijk beperkt wordt. Zowel een 'staged fluid bed' als een 'cross-flow fluid bed' zouden uitstekende keuzes zijn als reactor voor de desorptie van CO_2.

Er is een CO_2-afvangstinstallatie ontworpen en gebouwd, bestaande uit een GSTF-adsorber en een 'staged fluid bed' desorber om de potentie van deze nieuwe afvangsttechniek verder te onderzoeken. Als adsorbent is voor Lewatit® VP OC 1065-deeltjes gekozen. In totaal is er meer dan 300 operationele uren aan experimentele ervaring opgedaan met het gebouwde systeem. Dit is equivalent aan 350 adsorptie-desorptiecyclussen. Het experimentele werk richt zich vooral op de prestaties van de adsorberkolom waarbij het effect van de gassnelheid, de adsorbentcirculatie snelheid en de CO_2-concentratie in het rookgas op de afvangstefficiëntie, de productiviteit en de werkcapaciteit is gemeten. Typisch wordt 5 kg vast materiaal per uur tussen adsorber en desorber gecirculeerd. In de ontworpen en gebouwde installatie kan daarmee een CO_2 afvangst efficiëntie tot 81% van de voeding, een productiviteit tot 3.95 mol/m^3/s en een werkcapaciteit tot 2.7 mol/kg worden behaald.

De prestaties van de GSTF-adsorber is nauwkeurig te beschrijven met een 1-D propstroommodel. Aan de hand van het model is er een adsorber ontworpen die 90% van de CO_2 kan afvangen die uitgestoten wordt door een 500 MWe kolencentrale. Onze berekeningen tonen aan dat de GSTF-adsorber beter presteert dan een typische absorber in het huidige MEA-proces; we verwachten een productiviteit van 1.1 mol/m^3/s voor de adsorber, waar de absorber in het MEA-proces een productiviteit heeft van 0.6 mol/m^3/s.

De energiebehoefte van de afvangstinstallatie is ook gemeten. Op basis van de gemeten energievraag van de desorberkolom, is de adsorptiewarmte afgeschat op 62 kJ/mol. In totaal kost het afvangen van CO_2 in deze opstelling 141 kJ/mol ofwel 3.2 GJ/t bij een werkcapaciteit van 1.2 mol/kg. Wanneer de werkcapaciteit verhoogd wordt naar 2.7 mol/kg, zal de energiebehoefte van het systeem reduceren tot 1.6 GJ/t. Deze energiemetingen zijn

gedaan bij lage desorptietemperaturen (100°C) en er is stikstof gebruikt als fluïdisatiegas in de desorber.
In hoofdstuk 6 is de potentie van deze nieuwe afvangsttechniek (SAS) vergeleken met de conventionele MEA-gebaseerde technologie. Dit hoofdstuk omvat een procesontwerp voor een afvangstproces bij een 500 MWe kolencentrale, een techno-economische evaluatie van de nieuwe techniek en een vergelijking tussen de conventionele technologie en de nieuwe technologie.

Op basis van de techno-economische evaluatie kunnen we concluderen dat een adsorptieproces dat Lewatit® VP OC 1065 gebruikt als adsorptiemateriaal in potentie zowel lagere kapitaalkosten (14%) als lagere energiekosten (26%) heeft dan het conventionele proces. De lagere energiekosten zijn vooral te danken aan een lagere energiebehoefte van het nieuwe adsorptiesysteem tijdens regeneratie, vergeleken met de conventionele absorptiesystemen. In beide systemen wordt de afgevangen CO_2 weer vrij gemaakt door het sorbent/solvent te verwarmen. Maar door de lagere soortelijke warmte en hogere capaciteit van het adsorptiemateriaal is de voelbare warmte die nodig is in het hier ontwikkelde proces lager. De lagere kapitaalkosten zijn het gevolg van een goedkopere adsorberkolom vergeleken met de absorber benodigd in het conventionele proces. Het nieuwe proces zorgt in potentie voor een daling in de 'cost of CO_2 avoided' van $59 per ton CO_2 voor het MEA-proces naar $43.5 per ton CO_2 voor het SAS-proces. Wanneer de stabiliteit en de capaciteit van de adsorbent deeltjes in de toekomst verder verbeterd wordt, dalen de kosten verder naar $37 per ton CO_2. Er is dus voldoende potentie om deze nieuwe techniek verder door te ontwikkelen.

About the Author

Rens Veneman was born on the 21st of March 1986 in Haaksbergen, Overijssel, the Netherlands. He started his degree in Chemical Engineering at the University of Twente in 2004 and obtained his bachelor's degree in 2009. During these years, he was active in the Study Tour committee of C.T.S.G. Alembic. This committee was responsible for the organization of a three-week study tour through Mexico. After finishing his bachelor studies, he started with a master's in Chemical Engineering at the University of Twente in the Process Technology track. In 2009, he performed his four-month internship at Shell Global Solutions in Amsterdam. In 2011, he completed his master thesis entitled "Solid sorbents for post-combustion CO_2 capture" under the supervision of Ass. Prof. Dr. Z. Li, Dr. Ir. J.A. Hogendoorn and Dr. Ir. D.W.F. Brilman. Following his master degree graduation from the University of Twente, he began his PhD research under the supervision of Prof. Dr. S.R.A. Kersten and Dr. Ir. D.W.F. Brilman. During his PhD, he worked on the development of an adsorption based CO_2 capture process. The results of this research are described in this thesis. He has presented his work at multiple international conferences including ISCRE 22, GHGT 11 and GHGT 12. His contribution to the POWER-GEN conference was awarded a best paper award.

Publication list:

1. Veneman, R., Li, Z.S., Hogendoorn, J.A., Kersten, S.R.A., Brilman, D.W.F., Continuous CO_2 capture in a circulating fluidized bed using supported amine sorbents, Chemical Engineering Journal, 2012. 207–208, p. 18–26.
2. Brilman, D.W.F., Garcia Alba, L, Veneman, R., Capturing Atmospheric CO_2 for Microalgae Cultivation, 20th European Biomass Conference and Exhibition Proceedings (1BO.2.1), 2012, p. 77-84.
3. Veneman, R., Kamphuis, H., Brilman, D.W.F., Post-Combustion CO_2 capture using supported amine sorbents: A process integration study, Energy Procedia, 2013. 37, p. 2100-2108.
4. Brilman, D.W.F., Garcia Alba, L, Veneman, R., Capturing atmospheric CO_2 using supported amine sorbents for microalgae cultivation, Biomass and Bioenergy, 2013. 53, p. 39-47.
5. Brilman, D.W.F., Veneman, R., Capturing atmospheric CO_2 using supported amine sorbents, Energy Procedia, 2013. 37, p. 6070-6078.
6. Heesink, A.B.M., Veneman, R., Magneschi, G., Brilman, D.W.F., Cutting the cost of carbon capture, Power Engineering International, 2013. 21 (8), p. 52-61.
7. Brilman, D.W.F., Bos, M.J., Veneman, R., Method of preparing methanol and reactor for use in said method, 2015. WO 2015/030578 A1
8. Veneman, R., Zhao, W., Li, Z., Brilman, D.W.F., Kersten, S.R.A., Adsorption of H_2O and CO_2 on supported amine sorbents, Energy Procedia, 2014. 63, p. 2336-2345.
9. Buchholz, O.S., Van der Ham, A.G.J., Veneman, R., Brilman, D.W.F., Kersten, S.R.A., Power-to-Gas: Storing Surplus Electrical Energy. A Design Study. Energy Procedia, 2014. 63, p. 7993-8009.
10. Zhao, W., Veneman, R., Chen, D., Li, Z., Cai, N., Brilman, D.W.F., Post-Combustion CO_2 Capture Demonstration Using Supported Amine Sorbents: Design and Evaluation of 200 kWth Pilot, Energy Procedia, 2014. 63, p. 2374-2383.
11. Veneman, R., Frigka, N., Zhao, W., Li, Z., Cai, N., Kersten, S.R.A., Brilman, D.W.F., Adsorption of H_2O and CO_2 on supported amine sorbents, International Journal of Greenhouse Gas Control, 2015. 41,p.268-275.

In preparation:

12. Veneman, R., Goetheer, E.L.V., Linders, M., Brilman, D.W.F., Techno-Economic assessment of CO_2 capture using supported amine sorbents at a Coal fired power plant

13. Veneman, R., Hilbers, T., Brilman, D.W.F., Kersten, S.R.A., CO_2 capture in a continuous gassolid trickle flow reactor, submitted to Chemical Engineering Journal.

Other publications:

- Oral Presentation at NPS 11 (conference), Presentation title: Solid Sorbents for Post-Combustion CO_2 capture, 2011.
- Oral Presentation at ISCRE 22 (conference), Maastricht, Presentation title: CO_2 Capture in a CFB using supported amine sorbents, 2012.
- Oral Presentation at POWER-GEN Europe (conference), Vienna, Presentation title: Supported amine sorbents versus aqueous amine solutions for post-combustion CO_2 capture at pulverized coal and NGCC power plants, 2013. Award for best paper.
- Poster at the GHGT-12 (conference), Austin (Texas, United States), Adsorption of H_2O and CO_2 on supported amine sorbents.
- Poster at the GHGT-11 (conference), Kyoto (Japan), Post-Combustion CO_2 capture using supported amine sorbents: A process integration study

Acknowledgments

About four years ago, I decided to start a PhD in the TCCB group of Prof. Dr. Ir. W.P.M. van Swaaij. With my thesis completed, and looking back on the time that has passed, I am glad to say I have never regretted that decision. I have greatly enjoyed the technical aspects of my work but more importantly, the people I have met have made the past four years a truly amazing and a very happy period in my life. Hence, I would like to take the opportunity here to thank them for their contribution to my work and/or to my life.

Firstly, I would like to thank Zhenshan Li, Kees Hogendoorn, Wim Brilman, and Sascha Kersten for sharing with me their enthusiasm, their creativity and their endless stream of new ideas. The most important thing they have taught me during my Msc. Research, is how much fun it is to learn and discover new things and what it means to do research. I will be forever thankful for letting me experience that and that experience alone was reason enough for me to continue the research we had started during my master thesis in a PhD. Zhenshan, I have greatly enjoyed working with you, during my master research and during my stay in Beijing. I am most grateful to you for giving me the opportunity to come to China and collaborate with you and Wenying (my PhD brother at the Tsinghua University). Also I absolutely love your positive attitude towards research. No matter what happened or what went wrong, your reply was always: "I think no big problem. It's just small problem" even when I broke the glass riser tube of our continues set-up for the third time in one week. I have had an amazing time during my stay in China and I fell in love with your country for its people, its food and its amazing scenery. I will never forget that experience and I want to thank you again for that. Also I would like to thank Wenying for making my stay in China unforgettable. I am happy to call you my friend. You have taught me how to drink 'beijo' and to eat chicken brain. These are skills that are essential in life and I will never forget that. Kees, although we have not been working together during my PhD I want to thank you for everything you have taught me during my master research. You have taught me how to structure my research and to be critical towards my own work. Thanks again for your time and effort. Wim, I would like to thank you for making my PhD into a very beautiful experience. You are always interested and enthusiastic. Your door is always open for anyone who needs help even though this

takes up a lot of your time. This is highly appreciated by bachelor students, master students and PhD students including myself and it is thanks to that that I have never felt alone in my research. I have greatly enjoyed working together and am very thankful for the opportunities you gave me. Thanks to you I have had the opportunity to present my research in Japan and the USA. Especially our trip to Japan was a memorable one I think. Our stay in the Cubicle Hotel in Osaka was unforgettable!!!
I remember Sascha making fun of us for not being able to find a hotel with proper rooms and joking about you not fitting into these cubicles since you were twice the size of a typical Japanese guy. Looking back, I think it was the best way to experience Japanese culture. I hope you agree.
Sascha, I highly appreciate your clear and direct way of communication. Moreover, even though CO_2 capture is not your main research field, my thesis has greatly improved in quality through the thorough discussions we had on the modelling work and the experimental work. I want to thank you for giving me the opportunity to do my PhD in your SPT research group! I have had an amazing time. Although we didn't visit conferences together we did meet each other in Hyderabad for the wedding of Prasad. It is unfortunate I cannot share here the pictures of you in a traditional Indian wedding costume without an AC in the building and with an outside temperature of around 38°C. Clearly no temperatures for a Dutch Professor.

Furthermore, I would like to thank the rest of my committee members. It is a great honor to have you in my defense committee and I hope we have a nice and fruitful discussion on the 18th of September.

I would like to express my gratitude to the SPT-team: Benno, Erna, Karst, Yvonne, Johan, Louis, Boelo, Jean-Paul en Wim van Swaaij. It was a pleasure to work within this research group thanks to the open and warm people that work in it. Benno, Karst and Johan, thanks so much for teaching me how to approach practical challenges that you face while debugging a set-up and performing experiments. You guys are life-savers! Also, thank you for making the continuous set-up into a true piece of art.

I would also like to thank all the people involved in CATO-2. I felt very lucky for being part of the 'CATO family' for the past four years. The CATO-2 programme has offered me the chance to share my research with other experts in the field on CATO-days, it has offered me the opportunity to learn about all aspects of CCS from fellow PhDs and it has allowed me to broaden my network in the research field by organizing conferences and social activi-

ties. Especially the trip to the Eiffel was a memorable one. The beer consumed during that weekend almost cleared out the programme budget. Still, it was money well spent since after that weekend I think everyone gained around 30 new friends.

I would also like to thank all the students, post-docs, PhDs and visiting PhDs with whom I have shared blood, sweat and tears but especially beer. Lucia, Shushil, Ehsan, Sam, Carolien, Varsha, Cindy, Xiao Hua, Daniele, Lisette, Martin, Marek, Puskar, Qian, Sandra, Stevia, Aniek, Guus, Rebecca, Pavlina, Dimitris, Laura, Roel, Ferran, Can, Dragan, Prasad, Mariken, Elia, Roger, Diego, Jose, Nancy, Nick and Michael thank you so so much for destroying my liver. Also here I would like to make my official apology to Laura for sharing with you the meatballs I cooked together with Guus, Can, Roger and Dimitris that day during lunch. I really did not know you were not into eating insects. I have never seen someone so disgusted since. I would also like to thank Pavlina, Martin and Laura for their help in 'arranging' the extra bottle of Tequila we desperately needed at that Tequila borrel. It seemed like such a good idea at that time to drink more.

Special thanks of course to my paranymphs Maria and Stijn. We have shared most of our PhD lives together and I could not have wished for better friends and better paranymphs. I would like to mention here that both of you will graduate in the near future and I have a lot of pictures of you guys that are excellent material for a "stukje". This is not a threat. Just sayin'. Maria, I have a picture of you singing "When my baby goes to Rio" using a fake plant as a microphone. Stijn, I have a picture of your face when you realized that eating chicken in India is a serious risk. The research we were working on was not related at all. Stijn is making shitty oil from wood chips and Maria is doing the same (I think or at least something like that .... It's confidential). I am working on CO_2 capture. Although we did not work together much we spent a lot of time out side of work. Stijn we have travelled through India together and I will never forget the Long-Island-Ice-tea's we have shared! I had an amazing time! Maria, we visited the "oktoberfest" together in München. We drank beers that were bigger than you hehe. I was not sure if you were drinking the beer or drowning in it. Special thanks as well to Tatra Tea, Vodka, Absynth, Tequila and Benno's home-made liquor's (I don't know what is in them but they greatly enhanced the party mood). Thanks also to the students I have had the honor to supervise during my PhD: Tim, Bart, Michel, Ellsie, Avissa, Ole, Natalia, Joram, Tim, Bennoit, Jorge, Antonio, Tom and Martin.

Writing this acknowledgement also made me think about the friendship and love I found in my life. Kees, Myrthe, Ilse, Jan Welmer, Thomas, Anne, Clint, Marloes, Stan, Niels, Thijs, Laura, Ruud, Monica, Brecht, Chrissy, Pablo, Lenny, Nienke, Maarten, Remon, Anouk and Silke. I realized that most of you I have known now for more than ten years; some of you for more than 20 years. This means we share over 250 years' worth of friendship together and I feel very lucky and very proud to call you my friends. I hope you all know you have a large contribution to the happiness in my life and that you are all very special to me (I am not just saying this because I hope you take it easy on me during "mijn stukje" at the defense party). I would like to thank Stan, Marloes and Clint for keeping me alive during my PhD. Thank you for sharing so many dinners with me after work (Clint your cooking is amazing). Clint, Ruud, Anouk and Marloes thank you all so much for the wonderful time we had in Thailand. I have a lot of good memories from that trip. Ruud, it was awesome to do the diving course together. I am still sorry for destroying your phone, your cigarettes, your other phone, your wallet, your ribs, your head and for luring a stray dog into your bedroom. Stan, thank you for all the adventures we had in China. Together we experienced the full power of 'beijo'. We found out that the best way to make new friends is to find a karaoke bar in the middle of nowhere and then start singing Celine Dion's "My heart will go on". The duet you sang with the enormous Chinese guy was unforgettable. Thank you so much!! Thomas, my Sanders brother, thanks for always being you. We don't see each other that often but when we meet it feels very natural. I feel we share a weird kind of humor together that I like very much. Please come over soon to help Martin Drent win the Champions League. :) I wish you and Anne a lot of luck and happiness in your new home!

Thanks to Laura and Thijs for their support as well! Both of you are passionate about your work and that is a very beautiful thing to see. Thijs thanks for always being there for me and other people in the group of friends we have! You have a very big heart! Laura, you have done an amazing job in designing the layout of this thesis. You are precise, hardworking and you have an amazing eye for detail! Thank you so much for your help in making this into a book I can be proud of.

I want to thank Marije, Henk, Anette, Oma Grietjen, Sam, Renee, Gerrit, Nienke and Lenny for their love and hospitality in the past years. You are all amazing people and I am very grateful for the time we have shared to-

gether. You are an extraordinary family; you are open minded, positive and supportive and I will never forget that.
I would also like to thank Ans, Louis, Luke, Maureen and Boomer for a lot of beautiful memories. For Siem and me it felt like having a second family while growing up and I am very grateful for that.

Lastly, I would like to thank my family; Ma, Pa, Siem. Pa and ma: you have always supported me and motivated me to get the best out of myself but also allowed me to make my own choices and I would like to thank you both so much for that. You have done a great job raising Siem and me and we have enjoyed a wonderful childhood! You both recently retired and it feels very good to see you both so happy and enjoying your time together! I think you two make a very strong team and I wish you both a lot of happiness together! Siem although we have had very different interests as kids (you were into cars and motors, I was into soccer) we had a lot of fun together. Do you remember convincing all the neighborhood kids that the scratches you had from falling off your bike were caused by a tiger attack in the woods near our house? Or our scam: convincing the other kids that "stuivers" where worth more than "dubbeltjes" so that we could double our capital! Hehe. We still have a lot of fun together and I am proud to call you my brother!

I love you all very dearly.

Sincerely yours,

Rens Veneman

ISBN 9789036539265